GEOLOGICAL SETTING AND TECTONIC EVOLUTION OF ZUNGERU AND ITS ENVIRONS, PART OF SHEET 163 (ZUNGERU NW), NORTH CENTRALNIGERIA

BY

ABUBAKAR ENEYE ALIYU

DEPARTMENT OF GEOLOGY

AHMADU BELLO UNIVERSITY, ZARIA

NIGERIA

OCTOBER, 2016

BY

ABUBAKAR ENEYE ALIYU, B.Sc. (2011)

M.Sc./SCI/35496/2012-2013

A DISSERTATION SUBMITTED TO THE SCHOOL OF POSTGRADUATE STUDIES, AHMADU BELLO UNIVERSITY, ZARIAIN PARTIAL FULFILLMENT OF THE REQUIMENTS FOR THE AWARDOF AMASTERS DEGREE IN GEOLOGY

DEPARTMENT OF GEOLOGY
FACULTY OF SCIENCE
AHMADU BELLO UNIVERSITY, ZARIA
NIGERIA

OCTOBER, 2016

DECLARATION

I declare that this work (thesis) entitled "**GEOLOGICAL SETTING AND TECTONIC EVOLUTION OF ZUNGERU AND ITS ENVIRONS, PART OF SHEET 163 (ZUNGERU**

NW), NORTH CENTRAL NIGERIA"was carried out by mein the department of Geology, Ahmadu Bello University, Zaria; under the supervisionof Prof. U.A. Danbattaand Dr. A.AIbrahim.

The information derived from literatures has been duly acknowledged in the text and a list of references provided. No part of this work was previously presented from another degree or diploma at this or any other university.

Name of Student	Signature	Date

CERTIFICATION

This thesis entitled "**GEOLOGICAL SETTING AND TECTONIC EVOLUTION OF ZUNGERU AND ITS ENVIRONS, PART OF SHEET 163 (ZUNGERU NW), NORTH CENTRAL NIGERIA"** by ABUBAKAR ENEYE ALIYU, meets the regulations governing the

award of the Degree of Master of Science (Structural Geology)of theAhmaduBello University, and is approved for its contribution to knowledge and literary presentation.

Chairman, Supervisory Committee Prof. U.A. Danbatta	Signature	Date
Member, Supervisory Committee Dr. A.A Ibrahim	Signature	Date
Head of Department Dr. H. HamzaSignature	Date	
Dean, School of Postgraduate Studies Prof. K. BalaSignature	Date	

ACKNOWLEDGEMENT

My profound gratitude goes to Almighty Allah for seeing me through to the end of this work despite the many challenges.

I wish to thank my parents for training me up to this time, and also the entire members of the family for their love, care and support. May Allah reward them abundantly.

I sincerely acknowledge the efforts of my supervisors, Prof. U.A. Danbatta and Dr. A.A. Ibrahim, and also my colleagues, other academic and non-academic staff of the Departmentfor their meaningful suggestions, careful corrections, constructive criticisms and commitment in ensuring thatthis research work is successfully completed.

Special thanks go to Global Land Cover Facility (GLCF) Maryland, for providing remotely sensed satellite data and products free of charge. I would not have been able to carry out remote sensing analysis of my study area without these data.

Finally, I appreciate the assistance and cooperation given to me in and around Zungeru by the District Head and the members of the communityduring the course of my fieldwork exercise.

DEDICATION

This work is dedicated to my ever loving parents, MalamMuhammad R.Aliyu and MalamaKarietuAliyu.

ABSTRACT

Fold and Thrust (FAT) Belts are regions that have been documented in environments resulting from plate convergence, such as those formed at plate boundaries. The Nigerian Basement Complex has been described by previous workers to have evolved by plate tectonic processes involving continental collusions. The present study, therefore seeks to investigate the presence of a thrust belt within the NW segment of the Nigerian Basement Complex. The geological investigations of Zungeru and its environs was undertaken in orderinterpret its structural and tectonic evolution. Remote sensing analysis usingsatellite data (Landsat ETM imageries

anddigital elevation models)and field investigations which include thecollection of rock samples as well as structural data show that the study area comprise of gneiss, migmatite, quartzite, phyllite, schist, amphibolite and mylonite. The Kalangai-Zungeru-Ifewara (KZI) transcurrent fault observed, cut through the study area producing fault rocks like cataclasites, sheared gneisses and mylonites. Structural relationships wereinvestigated through: microstructural, strain and fracture analyses and also evaluation of fold interference patterns. These analyses show that themain planar structures encountered in the study area are foliations and cleavages, bedding surfaces, fold axial planes, fault planes, joints and veins. Linear features measured in the field include bedding-cleavage intersection lineations, mineral stretching lineations, and minor fold axes (hinge lines). Rose diagram plots and circle inventory analysis of joints show that the fractures have a dominant NNE-SSW, NE-SW and NW-SE trends with the highest density in granite gneiss outcrops and lowest in migmatites. En echelon veins found in the area are thought to be evidence of shearing as a result of displacement across faults or shear zones. Microscale deformation at the scale of individual grains was determined through microstructural analysis of photomicrographs of rocks that deformed through a range of ductile grain scale deformation mechanisms such as recrystalization, intra-crystalline deformation and twining. Oriented thin-sections of deformed rocks from the study area were examined in the laboratory in order to determine the degree of deformation, the stress direction and sense of shearing. At this scale, the sense of shear indicators include porphyroclasts, mica fish and asymmetric microfolds, defining a predominant dextral strike-slip movement. The dominant stress direction is E-W, consistent with the Pan-African crustal shortening. This research reveals that the rocks in the area were affected by two successive deformational phases (D_1 and $D_{2)}$, indicated by the presence cataclastic S_1 cleavages and NNE-SSW trending open to isoclinal F_2 folds. The alignment of lineaments and other major structures into NE-SW, NW-SE and N-S orientations imply that the D_2 deformation was a late stage Pan-African event that affected the basement rocks of the study area. Processing of satellite images, structural analysis,microtectonics, and petrographic studies revealsthat the area evolved through a transpressional deformation, which involves a component of strike-slip movement and a component of shortening. Thrust tectonics as an evidence of crustal shortening was observed within myloniteatthe bank of River Kaduna.

TABLE OF CONTENTS

Title page - - - - - - - - - - - i

Approval page - - - - - - - - - - - ii
Declaration - - - - - - - - - - - - iii
Certification - - - - - - - - - - - - iv
Acknowledgement - - - - - - - - - - - v
Dedication - - - - - - - - - - - - vi
Abstract - - - - - - - - - - - - vii
Table of Contents - - - - - - - - - - - viii
List of Tables - - - - - - - - - - - x
List of Figures - - - - - - - - - - - xi
List of Plate - - - - - - - - - - - xiv

1.0 GENERAL INTRODUCTION - - - - - - - - 1
1.1 Background - - - - - - - - - - - 1
1.2 Location and Accessibility - - - - - - - - - 2
1.3 Climate and Vegetation- - - - - - - - - - 2
1.4 Relief and Drainage - - - - - - - - - 3
1.5 Statement of Research Problem and Justification - - - - - 4
1.6 Aim and Objectives of the Study - - - - - - - 5
1.7 Scope of the Present work - - - - - - - - 6

2.0 REGIONAL GEOLOGY - - - - - - - - 7
2.1 The Nigerian Basement Complex - - - - - - - 7

2.2 The Migmatite-Gneiss Complex- - - - - - - - 7
2.3 The Metasediments - - - - - - - - - 9
2.4 The Older Granite Suites - - - - - - - 10
2.5 Geochronology and Tectonic Evolution - - - - - - 12
2.6 Metamorphism - - - - - - - - - 14
2.7 Structural Relationships and Evolution of the Schist Belts - - - 15

3.0 MATERIALS AND METHODS - - - - - - - 19
3.1 Preamble - - - - - - - - - - 19
3.2 Remote Sensing Methods - - - - - - - - 19
3.3 Field Investigations - - - - - - - - - 20
3.4 Laboratory Work - - - - - - - - - 20
3.4.1 Petrography - - - - - - - - - - 20
3.4.2 Strain Analysis - - - - - - - - - 21

4.0 RESULTS - - - - - - - - - - 23
4.1 Remote Sensing - - - - - - - - - 23
4.1.1 Preamble - - - - - - - - - - 23
4.1.2 Lithological Mapping - - - - - - - - 23
4.1.3 Lineament Analysis - - - - - - - - - 24
4.2 Field Geology and Petrography - - - - - - - 51

4.2.1 Preamble - - - - - - - - - - 51
4.2.2 Gneiss - - - - - - - - - - 51
4.2.3 Migmatite - - - - - - - - - - 58
4.2.4 Quartzite - - - - - - - - - - 60
4.2.5 Phyllites - - - - - - - - - - 62
4.2.6 Garnet Mica Schist - - - - - - - - - - 64
4.2.7 Amphibolites - - - - - - - - - - 66
4.2.8 Fault Rocks - - - - - - - - - - 67
4.3 Geologic Structures - - - - - - - - - - 68
4.3.1 Preamble - - - - - - - - - - 68
4.3.2 Folds - - - - - - - - - - - 70
4.3.3 Primary Foliations (S_0) and Cleavages - - - - - - 72
4.3.4 Lineations - - - - - - - - - - 72
4.3.5 Faults - - - - - - - - - - 74
4.3.6 Joints and Veins - - - - - - - - - - 74
4.4 Microtectonics - - - - - - - - - - 82
4.4.1 Intracrystalline Deformation - - - - - - - 82
4.4.2 Twinning - - - - - - - - - - 83
4.4.3 Dynamic Recrystallisation - - - - - - - - 85
4.4.4 Microfolding and Microfaulting - - - - - - - 85

4.4.5 Shear Zones and Sense of Shear - - - - - - - 87
4.5 Strain Analysis - - - - - - - - - 88

5.0 DISCUSSION - - - - - - - - - 90
5.1 General Geology - - - - - - - - - 90
5.2 Structural Geology - - - - - - - - - 92
5.2.1 Superimposition of Structures and Strain Patterns - - - - - 92
5.2.2 Microtectonics - - - - - - - - - 94
5.2.3 Strain Analysis - - - - - - - - - 95
5.3 Tectonic Evolution - - - - - - - - - 95

6.0 Summary, Conclusion and Recommendations - - - - - 100
6.1 Summary and Conclusion - - - - - - - 100
6.2 Recommendations - - - - - - - - - 101
6.3 Contribution to knowledge - - - - - - - - 101

REFERENCES - - - - - - - - - - 103

LIST OF TABLES

Table 2.1: Deformation and structural history established for the schist belts in NW Nigeria 18

Table 4.1: Modal compositions in percentage (%) of the rocks from the study area - - 53

Table 4.2: Circle-inventory for evaluating joint density in augen gneiss - - - 77

Table 4.3: Circle-inventory for evaluating joint density in quartzite - - - 78

Table 4.4: Circle-inventory for evaluating joint density in migmatite - - - 79

Table 4.5: Circle-inventory for evaluating joint density in granite gneiss - - - 80

Table 4.6: Phi and Rs values for samples cut parallel to foliation (XY) - - - 88

LIST OF FIGURES

Figure 1.1: Location map of the study area - - - - - - 3

Figure 2.1: Location of the Nigerian Basement Complex between the West African and Congo Cratons and in relation to Hoggar and Borborema Provinces - - - - 8

Figure 4.1: False colour composite image for bands 7, 4, 1 displayed in R.G.B - 25

Figure 4.2:False colour composite image for bands 7, 5, 4 displayed in R.G.B - - 26

Figure 4.3:False colour composite image for bands 1/3:5/7:3/5 displayed in R.G.B- 27

Figure 4.4: False colour composite image for bands 5/1, 5/7, 4 displayed in R.G.B - 28

Figure 4.5:Principal component analysis of bands 1, 2, 3 displayed in R.G.B - - 29

Figure 4.6: Principal component analysis of bands 4, 5, 6 displayed in R.G.B - - 30

Figure 4.7: SRTM DEM displaying elevation variation within the study area with the higher elevation in the Northern and southeastern portion and the lower elevation in the southwestern portion - - - - - - - - - - - 31

Figure 4.8: Shaded relief image derived from DEM with illumination direction (solar azimuth), 0^0 used in identifying lineaments in different reliefs and topography - - - - 32

Figure 4.9: Shaded relief image derived from DEM with illumination direction (solar azimuth), 45^0 used in identifying lineaments in different reliefs and topography - - - - 33

Figure 4.10: Shaded relief image derived from DEM with illumination direction (solar azimuth), 90^0, used in identifying lineaments in different reliefs and topography - - - 34

Figure 4.11: Shaded relief image derived from DEM with illumination direction (solar azimuth), 135^0, used in identifying lineaments in different reliefs and topography - - - 35

Figure 4.12: Shaded relief image derived from DEM with illumination direction (solar azimuth), 180^0, used in identifying lineaments in different reliefs and topography - - - 36

Figure 4.13: Shaded relief image derived from DEM with illumination direction (solar azimuth), 225^0, used in identifying lineaments in different reliefs and topography - - - 37

Figure 4.14: Shaded relief image derived from DEM with illumination direction (solar azimuth), 270^0, used in identifying lineaments in different reliefs and topography - - - 38

Figure 4.15: Shaded relief image derived from DEM with illumination direction (solar azimuth), 315^0, used in identifying lineaments in different reliefs and topography - - - 39

Figure 4.16: Shaded relief images derived by combining four other shaded relief images with azimuth directions 0^0,45^0,90^0 and 135^0 - - - - - - - 41

Figure 4.17: Shaded relief images derived by combining four other shaded relief images with azimuth directions 180^0, 225^0, 270^0 and 315^0 - - - - - - 42

Figure 4.18: Lineaments from combined shaded relief images with azimuth direction 0^0,45^0,90^0 and 135^0 showing two main directions trends, with the predominance of NNE-SSW lineaments over the NNW-SSE directions - - - - - - - - - - 43

Figure 4.19: Lineaments from combined shaded relief images with azimuth direction 180^0, 225^0, 270^0 and 315^0 showing two main directions trends, with the predominance of NNW-SSE lineaments over the NNE-SSW directions - - - - - - - - - 44

Figure 4.20: Buffered combined shaded relief image with azimuth directions 0^0, 45^0, 90^0, 135^0showing two main directions trends, with the predominance of NNE-SSW lineaments over the NNW-SSE directions - - - - - - - - - - 45

Figure 4.21: Buffered combined shaded relief image with azimuth directions 180^0, 225^0, 270^0, 315^0showing two main directions trends, with the predominance of NNW-SSE lineaments over the NNE-SSW directions - - - - - - - - - - 46

Figure 4.22: Level of coincidence for combined shaded relief images (0^0, 45^0, 90^0, 135^0) and (180^0, 225^0, 270^0, 315^0) showing the combination of lineaments from two shaded relief image to produce the general lineaments of the area - - - - - - - - - 47

Figure 4.23: Reclassified Level of coincidence for combined shaded relief images (0^0, 45^0, 90^0, 135^0) and (180^0, 225^0, 270^0, 315^0) displaying the all the lineaments found in the study area in black and white colours for easy digitizing - - - - - - - - - 48

Figure 4.24:Final lineament map for the study area showing three major trends, with the predominance of N-S lineaments over the NNW-SSE and NNE-SSW directions - - 49

Figure 4.25: Lineament density map for the study area showing a higher lineament density at the northern and eastern parts of the study area and a medium to low lineament density at the western part of the study area - - - - - - - - - - 50

Figure 4.26: Geological map and cross-section of the study area - - - - 52

Figure 4.27: (A) Stereonet projection of S_1 cataclastic foliations represented on a lower hemisphere Schmidt net. (B) Poles to cataclastic foliation, S_1(lineation data) plotted on contoured Schmidt net - - - - - - - - - - - 74

Figure 4.28: Rose diagram showing the dominant orientations of joint in augen gneiss - 77

Figure 4.29: Rose diagram showing the dominant orientations of joint in quartzite - - 78

Figure 4.30: Rose diagram showing the dominant orientations of joint in migmatite gneiss 79

Figure 4.31: Rose diagram showing the dominant orientations of joint in granite gneiss - 80

Figure 4.32: Locations of major structures in the Zungeru region manually extracted from Landsat images - - - - - - - - - - - - 81

Figure 4.33: Rose diagram generated from combined joints orientations in all the rocks in the study area - - - - - - - - - - - - 82

Figure 4.34: Fry plots for two dimensional strain analysis of samples cut parallel to foliation (XY) - - - - - - - - - - - - 89

Figure 4.35: Geological and lineaments map of the Zungeru area - - - - 97

Figure 4.36: Dominant direction of lineaments from final lineament map plotted on a rose diagram - - - - - - - - - - - - 98

Figure 4.37: A 3-D schematic diagram depicting the transpressional deformation pattern of the study area - - - - - - - - - - - - 99

LIST OF PLATES

Plate I: A photograph of augen gneiss showing feldspar mineral lineation around GarunGabas. Location: (9° 52' 21.1" N, 6° 06' 46.3" E) - - - - - - - 54

Plate II: Photomicrographs of augen gneiss. (A) View in XPL. (B) View in PPL. Qtz=quartz, Mus=muscovite, Bio=biotite, Opq=opaque mineral, Ort=orthoclase, Ept=epidote(Slide no: stn4) -55

Plate III: A photograph of banded gneiss north of Zungeru town. Location: (9° 49' 57.9" N, 6° 10' 25.2" E) - - - - - - - - - - - 56

Plate IV: Photomicrographs of Banded Gneiss. (A) View in XPL. (B) View in PPL. Qtz=quartz, Mus=muscovite, Bio=biotite, Opq=opaque mineral, Plag=plagioclase, Mcrn=microcline (Slide no: stn11) - - - - - - - - - - - - 56

Plate V: Photograph of a Granite Gneiss outcrop in Zungerutownwith a distinct quartz vein. . Location: (9° 48' 18.0" N, 6° 09' 31.5" E) - - - - - - - 57

Plate VI: Photomicrographs of Granite Gneiss. (A) View in XPL. (B) View in PPL. Qtz=quartz, Mus=muscovite, Bio=biotite, Ort=orthoclase, Mcrn=microcline (Slide no: stn24) - - 58

Plate VII: Photograph of a flat-lying Migmatite-Gneiss outcrop around DogonRuwa with light and dark bands. Location: (9° 46' 48.0" N, 6° 12' 1.6" E) - - - - - 59

Plate VIII: Photomicrographs of migmatite sample. (A) View in XPL. (B) View in PPL. Qtz=quartz, Bio=biotite, Ort=orthoclase, Opq=opaque mineral, Mus=muscovite, Plag=plagioclase (Slide no: stn9) - - - - - - - - - - - - 60

Plate IX: A photograph of a whitish massive exposure of quartzite outcrop in GarunGabas. Location: (9° 51' 25.5" N, 6° 07' 37.5" E) - - - - - - - 61

Plate X: Photomicrographs of Quartzite. (A) View in XPL. (B) View in PPL. Qtz=quart and Opq=opaque mineral (Slide no: stn2) - - - - - - - - 62

Plate XI: Photograph of phyllite with distint S_1 cleavage planes. Location: (9° 48' 18.8" N, 6° 09' 31.5" E) - - - - - - - - - - - - 63

Plate XII: Photomicrographs of Quartz-Muscovite-Phyllite. (A) View in XPL. (B) View in PPL. Qtz=quartz, Mus=muscovite, Bio=biotite, Gnt=garnet, Opq=opaque mineral (Slide no: stn25) - 64

Plate XIII: Outcrop of schist dipping to the west found around Tunganmai-jaki. Location: (9° 52' 45.4" N, 6° 10' 59.8" E) - - - - - - - - - 65

Plate XIV: Photomicrographs of garnet-mica schist. (A) View in XPL. (B) View in PPL. Qtz=quartz, Mus=muscovite, Plag=plagioclase, Bio=biotite, Gnt=garnet (Slide no: stn1) - - - 65

Plate XV: Photograph of an amphibolite outcrop east of Zungeru found along a fault zone. Location: (9° 47' 31.2" N, 6° 10' 21.7" E) - - - - - - - - - 66

Plate XVI: Photomicrographs of amphibolite. (A) View in XPL. (B) View in PPL. Qtz=quartz, Bio=biotite, Ort=orthoclase, Aug=augite, Opq=opaque mineral, Hbn=hornblende, Plag=plagioclase (Slide no: stn8) - - - - - - - - - - - 68

Plate XVII: Photograph showing mylonitic garnet mica schists dipping to the west and scattered chuncks of cataclasticquartzites all within a shear zone in the study area. Location: (9° 52' 18.3" N, 6° 07' E) - - - - - - - - - - - 69

Plate XVIII: Photograph showing sheared gneiss within a shear zone in the study area trending NNE-SSW and dipping to the west. Location: (9° 53' 26.9" N, 6° 07' 17.2" E) - - - - 70

Plate XIX: Photograph of mica schist with refolded F_2 “S-fold” oriented NNE depicting the right-limb of a major F_2 fold. Location: (9° 48' 18.0" N, 6° 09' 31.5" E) - - - - 71

Plate XX: Photograph of amphibolite outcropwith quartz vein forming almost N-S open to isoclinal F_2 fold. Location: (9° 47' 23.0" N, 6° 09' 9.0" E) - - - - - - 71

Plate XXI: Crenulation cleavages on mylonitic garnet mica schist showing S_1 and S_2 foliations. Location: (9° 52' 18.3" N, 6° 07' E) - - - - - - - - 73

Plate XXII: Photograph of L_1 intersection lineation on gneiss at Akusu. Location: (9° 49' 57.9" N, 6° 10' 25.2" E) - - - - - - - - - - - 73

Plate XXIII: (A) An outcrop scale strike-slip fault showing sinistral sense of shear. Location: (9° 52' 45.4" N, 6° 07' 5.6" E) - - - - - - - - - - 75

Plate XXIV: Outcrop scale orthogonal joint system on granite gneiss exposure. Location: (9° 48' 18.0" N, 6° 09' 31.5" E) - - - - - - - - - 76

Plate XXV: Photograph of gneiss with En echelon sigmoidal quartz veins defining a dextral shear zone. Location: (9° 47' 58.9" N, 6° 04' 55.7" E) - - - - - - 76

Plate XXVI: Photomicrograph of augen gneiss with undulose extinction in quartz. Grain boundaries are irregular due to grain boundary migration (Slide no: stn4) - - - - 83

Plate XXVII: Photomicrograph of augen gneiss with albite twinning and multiple twin planes in plagioclase (Slide no: stn4) - - - - - - - - - 84

Plate XXVIII: Photomicrograph of migmatite withalbite twinning and single twin plane in plagioclase (Slide no: stn10) - - - - - - - - - 84

Plate XXIX: Photomicrograph of augen gneiss withcross-hatched twinning in microcline(Slide no: stn4) - - - - - - - - - - - 85

Plate XXX: Photomicrograph of quartzite showing polycrystalline quartz with irregular grain boundaries formed in response to grain boundary migration (GBM) recrystallization (Slide no: stn2) - - - - - - - - - - - - 86

Plate XXXI: Differentiated crenulation cleavages in garnet mica schist with asymmetric microfolds(Slide no: stn1) - - - - - - - - - 87

Plate XXXII: (A) Photomicrograph of garnet mica schist showing σ-type K-feldspar porphyroclast with a weak stair-stepping (Slide no: stn1) - - - - - - - 87

Plate XXXII: (B) Photomicrograph of augen gneiss showing lenticular Muscovite mica fish. Both porphyroclasts exhibit a dextral shear sense (Slide no: stn4) - - - - - 88

Plate XXXIII: Photograph of quartzite and amphibolite in thrust relationship with one another at Kundu. (9° 49' 16.8" N, 6° 08' 56.3" E) - - - - - - 99

CHAPTER ONE

GENERAL INTRODUCTION

1.1 BACKGROUND

Nigeria is underlain by Precambrian Basement Complex rocks, anorogenic Younger Granites of Jurassic age, Cretaceous to Recent sediments and Tertiary to Recent volcanic rocks, with the basement rocks occupying about half of the land mass of the country (Black, 1980). Zungeru forms part of the Nigeria's Precambrian Basement Complex terrain which is a segment of theregional Dahomeyide fold belt (Affaton et al., 1991).Structural geology typically pertains to the observation,description and interpretation of structures that can bemapped in the field. It deals with how folds, faults and other deformation structures appear and form in the lithosphere. Structuresoccur in many different settings, ranging from features hundreds of kilometers long down to microscopic details and have experienced changes in stressand strain.Structural geology is an essential tool in unraveling the geologic history of any given area or region within the Earth, especially in mountain belts where original arrangements of rocks andgeologic contacts have been modified by deformational movements.

Geologic domains such as the Canadian Rockies, in which regional horizontal tectonic shortening of the upper-crust yields a distinctive suite of thrust faults, folds, and associated mesoscopic structures, are called Fold-thrust Belts or Fold-and-Thrust Belts.Fold and Thrust Belts are typical regions in most Orogenic belts controlled by compressional tectonics and have been documented in environments resulting from plate convergence such as those formed at plate collusion boundaries. Fold-and-thrust (FAT) belts have a worldwide distribution and occur in a variety of tectonic settings (Nemcok *et al*., 2005; Cooper, 2007).

Thrust tectonics (or contractional tectonics) is concerned with the structures formed, and the tectonic processes associated with the shortening and thickening of the crust or lithosphere. Therefore, this research falls within the realm of investigating the presence of a thrust belt within the Nigerian basement.

1.2 LOCATION AND ACCESSIBILITY OF THE STUDY AREA

The study area is located in and around Zungeru town in Niger State, North Central Nigeria. It lies withinLatitudes9° 45' and 10° 00' N and Longitudes 6° 00' and 6° 15' E, and formspart of Zungeru (Sheet 163NW) that underlies an approximate 770km^{2}in aerial extent (Fig. 1.1).

The towns and cities in the study area areKagara to the North, Kontagora to the North West, Minna to the North East and Bida to the South. It has a good network of roads linking it to all parts of the country. The major roads run through Tegina to the North, Wushishi and Bida to the South and Minna to the North East.It is also accessible by innumerable minor roads and footpaths and by Zungeru-Minna-Kano rail line from the North, and Zungeru-Lagos rail line from the South.

1.3 CLIMATE AND VEGETATION

Zungeru has a dry sub-humid climate that is classified as a Tropical Savanna with two seasons, a wet and dry season, and a tropical dry forest biozone. The wet season has a rainfall peak inSeptember. Temperature in the study area averages 28.2 °C. In a year, the average rainfall is 1222 mm. March is warmest monthin any year with an average temperature of 38.3 °C at noon. December is the coldest month with an average temperature of 18.9 °C at night. Zungeru has no distinct temperature seasons as the temperature is relatively constant during the year, sharply dropping at nights. December is on average the month with most sunshine.

Most of the land area is not cultivated, as the natural vegetation is still intact. The study area falls within the Guinea Savanna belt, characterized by soil which may be described as lateritic and suitable for growing of many savannah crops and cereals.

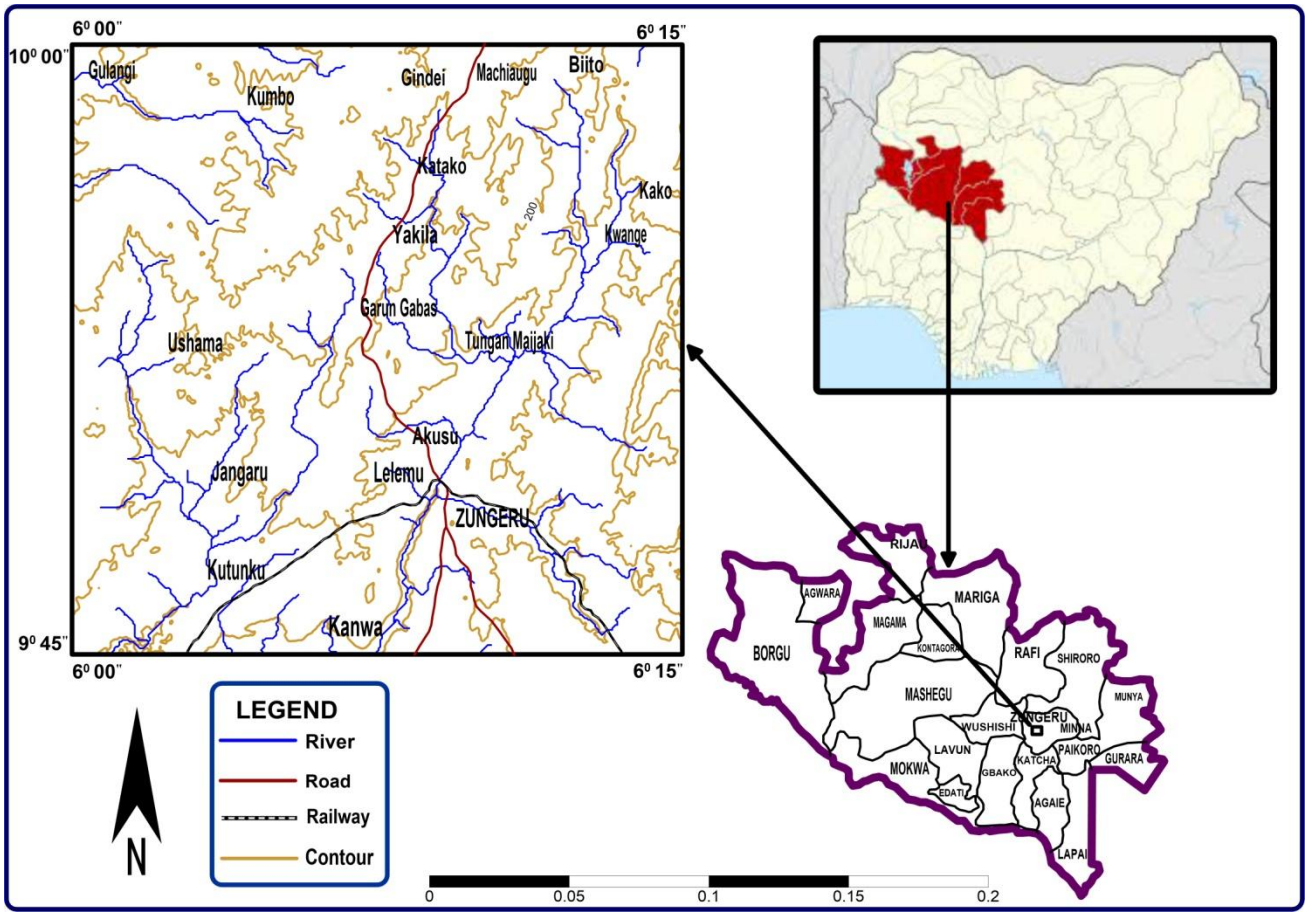


Figure 1.1: Location map of the study area

1.4 RELIEF AND DRAINAGE

Zungeru is a low-lying town located in a valley surrounded by highland which form the watershed for its river systems. The major rivers in the area include the River Kaduna and other smaller rivers such as Innamayi and Tausheta. Neighboring towns and villages are therefore on a higher elevation. Several rivers and streams drain the study area and many of these streams are seasonal, as they usually flow during the rainy season and are completely dry during the dry

season. The drainage patternis dendritic, and due to presence of numerous stream channels, the study area can be considered as well-drained.

1.5 STATEMENT OF RESEARCH PROBLEM AND JUSTIFICATION

Both the ensimatic and ensialic models of evolution have been proposed to explain the evolution of some of the schist belts of Nigeria (Ogezi, 1977; McCurry and Wright, 1977, Wright and Ogezi, 1977, Holt *et al*., 1978; Holt, 1982, Utke, 1987; Rahaman *et al*., 1988; Ajibade and Wright, 1989; Danbatta, 1991; Danbatta, 2008; Elueze, 1992).

Ajibade and Wright (1989) proposed that the Nigerian Basement Complex evolved as a result of closure of small oceans between a series of microcontinents due to the collision between the West African Craton and the Congo Craton. They proposed that the southern Pan-African domain in West Africa (the Togo-Benin-Nigeria Shield) is an aggregation or "mosaic" of island arcs, interarc basins and continental fragments.

According to Odeyemi *et al*. (1999) the Ifewara fault in the southwest and the Zungeru-Kalangai fault in the north and north central parts of Nigeria are by far the most prominent lineament systems in Nigeria. Suggestions on the nature, structure and origin of the Ifewara fault favour an overthrust relationship between the amphibolites and the rocks of the Effon Psammite formation (Hubbard, 1975), while Turner (1983) opined that the fault may represent a collisional suture zone.The 50km long belt of Zungeru mylonites is also associated with crustal convergence, located within the vicinity of large shear zones and itself represents a re-folded thrust zone (Ajibade, 1982; Ajibade et al., 1979).

Ball (1980) considered the KZI and AYI faults to be the result of a horizontal maximum stress axis oriented E-W, linked to the collusion at the West African Cratonic margin.

According to Onyedim and Ocan (2001), the Kalangai-Zungeru-Ifewara shear zone is contemporaneous with the emplacement of the mylonites at both Ifewara and Zungeru areas, thus suggesting that the mylonites might have been produced as a result of Pan-African shearing along the Ifewara-Zungeru fault. Field mapping and fracture data from an area located southeast ofOsu town near Ilesa, show that the Ifewara fault is a 3 to 5 km wide shear zone dominated by flat-lying mylonites, probably associated with some thrust tectonics (Affaton *et al*., 1991).

From these lines of information provided in the preceding paragraphs, it is clear that there are similarities between the processes of evolution of the Nigerian Basement and that of Fold-and-thrust (FAT) belts. The present study therefore seeks to answer the following questions: (i) is there a thrust belt within the present Zungeru study area?; (ii) if there is, what is the style of deformation that created it?; (iii) is it a thin-skinned or a thick-skinned deformation?

1.6 AIM AND OBJECTIVES OF THE STUDY

The aim of this research work is to investigate the tectonic evolution of the study area, with the following specific objectives:

(i) To map the study area on a scale of 1:50,000 and identify the lithological units.

(ii) To analyze the shear zones in the area by describing their orientation and style of deformation.

(iii) To determine the amount of strain in the rocks of the study area.

(iv) To determine the style of deformation and the structural geometry that affected the area.

(v) To describe those tectonic events that affected the area and determine the relative ages of fabric elements.

(vi) To carry out joint analysis by measuring the density of joints and shear fractures.

(vii) To update and produce geological and structural maps of the study area on the scale of 1:50,000.

1.7 SCOPE OF THE PRESENT WORK

The scope of the present work involves: (i) literature review of previous work; (ii) remote sensing interpretation; (iii) field mapping using traverse exposure method at the scale of 1:50,000; (iv) collection of representative rock samples for laboratory analyses, etc.The research focuses on mapping of the various lithologies found within the study area, determining their contact relationships and then analyzing their associated structures. These will help to determine whether or not the study area was affected by thrust tectonics and also provide additional structural evidences that are consistent withthe Pan-African crustal convergence.The overall structural analysis of the area will lead to detail description of the tectonic events that have affected the area over time. These analyses will include: microstructural analysis; strain analysis; analysis of fractures; and fold interference patterns.

CHAPTER TWO

REGIONAL GEOLOGY

2.1THE NIGERIAN BASEMENT COMPLEX

The Nigerian Pan-African Basement is part of an Upper Proterozoic to Lower Phanerozoic mobile belt situated between the West African and Congo Cratons(Fig. 2.1).The belt is interpreted to have evolved by plate tectonic processes which involved continental collision between two blocks, the passive continental margin of the West African Craton and the active continental margin (Pharusian belt) of the Tuareg Shield about 600 Ma (Burke and Dewey, 1972; Leblanc, 1981; Black *et al.*, 1979; Caby *et al.*, 1981; Ajibade *et al*., 1987; Garba, 2002). The Nigerian Basement Complex lies in the reactivated part of the belt (Ajibade *et al.*, 1987).

The lithology of the Basement Complex has been described by many workers such asOyawoye (1972); McCurry (1976); Woakes *et al.*(1987); Rahaman (1976; 1988); Garba (2003); Dada (2006, 2008); Baba *et al*.(2006) among others. The Nigerian Basement Complex is divided into three major lithological units that include:

i. Polymetamorphic Migmitite-Gneiss Complex.
ii. Metasediments
iii. Older Granite suite

2.2 THE MIGMATITE-GNEISS COMPLEX

The migmatite-gneiss complex is generally considered as the Basement Complex “Senso Stricto” (Rahamam, 1988; Dada, 2006). About half of the Nigerian Basement consists of the migmatite-gneiss complex (Kröner *et al*., 2001).It is a heterogeneous assemblage including migmatized gneisses, banded gneisses and a series of metamorphosed basic and ultrabasic rocks.

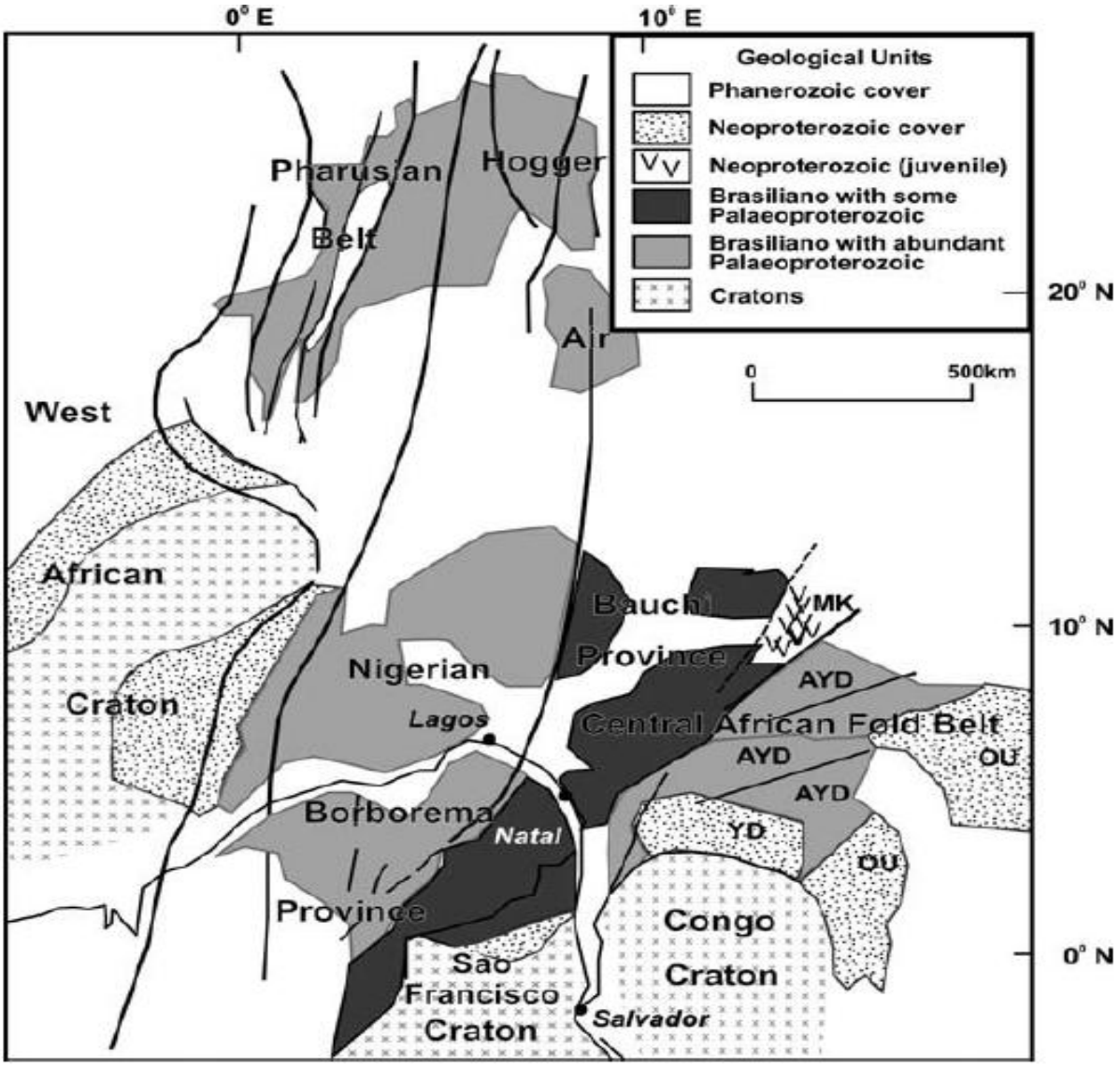


Figure 2.1: Location of the Nigerian Basement Complex between the West African and Congo Cratons and in relation to Hoggar and Borborema Provinces (adapted from Dada, 2008).

These rocks strongly resemble thetonali-tetrondhjemite-granodiorite(TTG) suites of Archean and Early Proterozoic terrains elsewhere in the world (Dada *et al*., 1993). Petrographic evidence indicates that Pan-African reworking led to recrystallization of many of the constituent minerals of the migmatite-gneiss complex during partial melting, and most display medium to upper amphibolites facies-metamorphism (Dada, 2008).

The gneisses of the migmatite-gneiss complex are interleaved with amphibolites that may be derived from Mg-rich rocks such as continental basalts (Caby *et al*., 1990; Dada,1999; Dada, 2008). However, there are no conclusive age and isotopic data to elucidate their origin (Dada, 2008). Oyawoye (1972) noted that the banded gneisses are possibly the oldest rocks in the country, older than granite gneiss that yielded aRb-Sr whole-rock isochron age of 2190±30 Ma. Ajibade (1988) distinguished the ancient migmatites in northern Nigeria from the Pan-African migmatites by their complex polyphase deformation and mylonitization.

Possibly because of their mixed and, therefore, complex nature, it has been difficult to define the protoliths of the banded gneisses (Kröner *et al*., 2001). Some authors suggested that they were metasediments derived from graywacke and shale (Freeth, 1971; Burke and Dewey, 1972), whereas others interpreted them as orthogneisses (Onyeagocha 1986; Ekwere and Ekwueme, 1991; Kröner *et al.,* 2001). However, most workers agree that migmatization occurred during upper amphibolite-facies regional metamorphism (Oyawoye, 1972; Onyeagocha and Ekwueme, 1990). There is also consensus that metamorphic segregation, partial melting, and injection of leucogranitic material contributed to the formation of the banded gneisses and migmatites (Kröner *et al*., 2001). According to (Dada, 1999; 2008), gneisses and amphibolites in Nigeria form a bimodal association who's petrological and geochemical characteristics indicate a primary igneous origin.

2.3 THE METASEDIMENTS

The metasediments are divided into "Ancient Metasediments" and "Newer Metasediments" (Oyawoye, 1972) or "Older Metasediments" and "Younger Metasediments" **(**McCurry, 1976).

The "Ancient Metasediments" (Oyawoye, 1972) or Older Metasediments (McCurry, 1976) are high grade metasedimentary remnants in the gneisses and migmatites and are believed to have

been formed about 2,500 Ma (McCurry, 1976). They consist of calc-silicate rocks, arkosic quartzite and high grade schist that occur as lensoid relics in the regional gneisses or as paleosomes of migmatites (Danbatta, 2008).

The "Newer Metasediments" (Oyawoye, (1972) or "Younger Metasediments" (McCurry, 1976) are low-grade sediment dominated schist groups and are composed mainly of pelitic and semi-pelitic schist, metaconglomerate, quartzite, calc-silicate rock, marble, mafic to ultramafic rocks, acid to intermediate volcanic rocks and rare banded iron formations (Danbatta, 2008). In the western half of the country, they occur as discontinuous north-south trending belts within the basement. There are twelve of such metasedimentary belts namely: Zungeru-Birnin Gwari, Kushaka, Malumfashi, Kazaure, Wonaka, Maru, Anka, Zuru, Toto, Iseyin-Oyan River, Ife-Ilesha and Igara-Kabba-Lokoja belts (Ajibade, 1976; Turner 1983; Danbatta, 1999; 2008).The metasediments are poorly represented in the eastern half of the country and this is attributed by Ajibade (1988) to the strong migmitization and assimilation effects on the sediments by the large volumes of the Pan-African rocks. However, few outcrops of some members of the metasediments particularly quartz schist, biotite schist and calc-silicate rocks occur in Gwoza and Ngoshe area in northeastern Nigeria (Nwabufo and Mbonu, 1988). Furthermore, outcrops of some members of the metaseiments were equally reported in the Oban Massif, Obudu Plateau and the adjoining Cameroon Republic (Ekwueme, 1990; 1991).

2.4THE OLDER GRANITE SUITES

The Older Granite suites comprise the syntectonic to late tectonic granitoids. They intrude both the migmatite-gneiss complex and the metasediments. The granitoids include rocks varying in composition from granite to tonalite and charnockites with smaller bodies of syenite, gabbro and pegmatite (Ajibade *et al.,* 1987). The granitoids have yielded radiometrics ages in the range of

750-500 Ma which lie within the Pan-African spectrum. These Pan-African granitoids are referred to as the Older Granites in Nigeria to distinguish them from the Mesozoic anorogenic granite ring- complexes (the Younger Granites).

Based on orogenic criteria, Truswell and Cope (1963) grouped the Older Granites into synkinematic and late-kinematic types. The synkinematic group is usually coarse grained, foliated bodies with gradational contact and containsxenolith of their country rocks, while the late-kinematic group is commonly fine grained, rarely foliated and have sharp contacts with the surrounding country rocks.

Jones and Hockey (1964) have, on the basis of field relationship, mineralogy and texture, recognized three phases of the Older Granite suite:

a. Early phase which comprises rocks of high colour index and relatively complex mineralogy. The phase comprises of closely intermingled gabbroic, doleritic and granitic rocks usually intruded by acid veins. They are of minor occurrence and do not form distinct topographic features and are usually found as xenoliths within the latter phase. Hockey *et al.* (1986) have described a number of doleritic xenoliths within coarse porphyritc granite in Lokoja-Auchi area.
b. Main phase includes the most dominant and extensive unit of the Older Granite suites. The rocks, predominantly medium grained biotite-hornblende granite and porphyritic biotite granite, are readily distinguished from others by their characteristic large subhedral pinkish to reddish (occasionally whitish) alkali feldspar set in a medium to fine grained groundmass of quartz, microcline, oligoclase, biotite and hornblende. In many cases the feldspar megacrysts are commonly aligned along with the biotite which imparts

a gneissose appearance to the rock. Rahaman (1976) equated this phase to the synkinematic type of Truswell and Cope (1963). The foliation is usually well developed at the margins of the rock bodies which indicate some degree of movement during emplacement. Rahaman (1988) pointed out that the activity of the fluid phase during the emplacement may also be important in determining the structural feature of the granite mass.

c. Late phase comprises of homogenous granite, as well as pegmatite and aplites dykes. Homogenous granites comprise of fine to medium grained biotite and biotite muscovite granites and granodiorite. Although the homogenous granites are generally equigranular in some varities the feldspar crystals locally develop to megacrystic size. The homogenous granites are second to the coarse porphyritic granites in abundance and topographic expression. The rocks of this phase generally lack foliation and are evidently instrusive.

In the northeast of Nigeria, Ferre *et al.* (1998) have described hypersthene-bearing monzogranitic and quartz-monzonitic rocks of Neoproterozoic age with ferro-potassic transalkaline and metaluminous characteristics which have affinity with within-plate or post-collisional granites. They assigned these rocks to the post-collisional stage of the Pan-African orogeny. In southeast Nigeria, Ukwang and Ekwueme (2009) have documented granitic rocks in Obudu Plateau with volcanic arc and syncollisional affinity emplaced with regard to the Pan-African orogeny.

2.5GEOCHRONOLOGY AND TECTONIC EVOLUTION

The Nigerian Basement evolved through polyphase tectono-metamorphic history, including Liberian (2700±200 Ma), Eburnean (2000±200 Ma) and Pan-African (600±150 Ma) events (Grant, 1970; Ajibade *et al.*, 1987; Dada 1998).

According to Dada *et al.* (1993)and Dada (1998), U-Pb zircon age of 2.4 to 2.5 Ga on grey gneisses from northern and southwestern Nigeria suggests distinct crustal initiation event with significant crustal growth at the Archean-Proterozoic boundary (Liberian). Ajibade *et al*. (1987) reviewed the nature of the early Proterozoic Eburnean event in Nigeria, which clearly indicates its importance and involvement in the evolution of the Nigerian Basement Complex. According to these authors, the Eburnean was probably accompanied by sedimentation, deformation, and metamorphismand syntectonic igneous activity.

The Pan-African event was related to the collision of Birrimean plate (comprising the present West African Craton) and the Dahomean (comprising the present day Nigeria-Benin Shield), as reported by Burke and Dewey (1972). The orogeny started with the opening of the Buem Ocean in Neoproterzoic time, its subsequent closure reactivated Dahomean while Birrimean remained stable.Many workers on the Nigerian Basement (McCurry, 1971; Rahaman ,1976); Cahen *et al*., 1984)are of the view that the Pan-African orogenic event was the latest, most pervasive and penetrative deformation episode, and that it completely obliterated earlier structures, primary fabrics and metamorphic assemblages of the complex.

On the other hand, Grant (1978), Mullan (1979), Ajibade (1988), Fitches *et al*. (1985), and Ekwueme (1987) are of the opinion that although it was pervasive, the Pan-African event did not completely homogenize the rocks of the basement, so that traces of earlier structures still remain within the complex. Many workers considered the Rb-Sr method to be unreliable in dating migmatitic rocks from which most ages older than Pan-African were obtained (Krönere*t al*., 2001). Ajibade and Wright (1989) argued that the Nigerian Basement is an aggregation of allochthonous terranes, which explains the relicts of Liberian andEburneanorogenic events, as well as the spread of radiometric ages within the Pan-African range (750±450 Ma).

Field evidence has for a very long time reveal the Nigerian Basement as an assemblage of contrasted terranes with a well-developed metasedimentary cover to the west and a largely vestigial crystalline terrain to the east (Oyawoye, 1972; McCurry, 1976; Rahaman, 1976; Fitches *et al.,* 1985; Ajibade *et al.,* 1987). It is a continuum between the Hoggar to the north (McCurry, 1976) and the Borborema Province to the south (Caby, 1989; Dada, 2008;Fig 2.1). Sutures have been proposed along two transcurrent fault zones, and in particular within the Ife–Ilesha schist belt, which has been interpreted as a back-arc marginal basin (Rahaman *et al*., 1988), and east-verging nappes (Caby and Boesse 2001; Dada, 2008). Structural studies by Black *et al*.(1994) and Ferre *et al*.(1996) have also strengthened the view on the contrasted nature of the Nigerian Basement. The presence of Archean crustal segments in the Nigerian as in Central Hoggar is compatible with an intracratonic setting (Dada 1998). Furthermore, the relict Archean ages strongly support the Continental collision model of Caby *et al.* (1981) and Caby (1989) that the region and the West African and Sao Luis Cratons must have been part of the same crustal province which was drifted apart, reunited and in part reworked in the Late Proterozoic (Dada *et al*., 1995, Dada and Rahaman 1995; Dada, 1998).

2.6METAMORPHISM

The Western part of the Nigerian Basement Complex generally experienced regional metamorphism but local thermal metamorphism occurred as a result of plutonic intrusion within some of the Schist Belts resulting in the formation of contact aureoles. Metamorphism reached the greenschist to middle amphibolite facie in the younger metasediments and upper amphibolite facie conditions in the crystalline rocks (McCurry, 1976; Ogezi, 1977; Ajibade, 1971 and Egbuniwe, 1982). A bimodal distribution of metamorphic facie exist between the greenschist to middle belt metamorphic facie of metasediments on one hand and upper amphibolite facie of the

crystalline rocks on the other hand (McCurry,1971). Evidence of mobility and plastic deformation in the latter indicates that metamorphic conditions in these rocks are similar to those described by Holland and Lambert (1969).

Grade of metamorphism varies from one place to another. In Zungeru area for example, Ajibade (1987) recognized a Barovian type of metamorphism with metamorphic grade ranging from greenschist facie to almadine amphibolite facie (staurolite-almadine-muscovite sub facie). There are also some indications of two periods of syntectonic metamorphism separated and followed by periods of static metamorphism (McCurry, 1971 and Danbatta, 1998).

Retrograde metamorphism occurred within shear/fractured zonesofchloritization of biotite, sericitization of feldspar and conversion of hornblende to biotite as a result of reduction in temperature and pressure (Ajibade, 1987; Egbuniwe, 1982 and Garba, 1992). Texturally, muscovite (or sericite) probably of regional metamorphism are lath-like and aligned within the schistocity, while the larger ones are tabular and overgrew the schistocity during contact metamorphism. Thermal metamorphism is recognized in the Anka and Maru Belts which results from the emplacement of Older Granites. This has formed a narrow contact aureole. In the pelitic, semi pelitic schist and psammites are indications of greenschist metamorphism (Egbuniwe, 1982). In the staurolite-garnet biotite bearing pellites, the presence of staurolite suggest lower amphibolite facie conditions (Winkler, 1974), while the first appearance of biotite and almadine garnet are respectively indications of middle-upper greenschist facie metamorphism (Miyashiro, 1973).

2.7 STRUCTURAL RELATIONSHIPS AND EVOLUTION OF THE SCHIST BELTS

In recent years, much attention has been given to the evolution of the metasediments (Annor, 1995; Adekoya, 1996; Olobaniyi, 1997; Annor, 1998; Danbatta, 1999; 2001; 2003; 2008). The

main points of contention that concern the evolution of the metasediments include the timing of formation of the basin of deposition, their age relationship, origin of the mafic and ultramafic rocks associated with some of them, and structural control. All the models proposed over the years for the evolution of the metasediments could be classified under ensialic and ensimatic processes.

According to those in favour of ensialic evolution process, crustal thinning in response to initial crustal extension and continental rifting at the cratonic margin about 1000 Ma ago, led to deposition of sediments in a graben-like structures floored by continental crust. The closure of the ocean at the West African cratonic margin led to deformation and metamorphism of the sediments and underlying basement resulting in the formation of the metasediments and reactivation of older basement during the Pan-African orogeny (Russ 1957; Oyawoye, 1964a; 1972; McCurry, 1971; 1976; Vaniman, 1976; Grant, 1978; Chukwu-Ike, 1978; Turner, 1983; Ajibade, 1976; Ajibade *et al*., 1987., Danbatta, 1999). Ensimatic models of evolution had also been proposed to explain the evolution of the metasediments (Ogezi, 1977; McCurry and Wright, 1977; Holt,*et al.*, 1978; Holt, 1982; Utke, 1987; Rahaman *et al*., 1988; Ajibade and Wright 1989; Danbatta, 1991; Elueze, 1992). Earlier proponents of this model attributed the formation of some metasediments (eg.Anka, Ife-Ilesha and Zuru metasedimentary belts) to the closure of some oceanic basins. They proposed that some marginal back-arc basin floored by oceanic material were first formed and in which some sediments were subsequently deposited. However, Holt (1982) observed that the Anka metavolcanic rocks have chemical characteristics of both island arcs and continental environments. He concluded that the metasediments were deposited in a retro-arc basin related to subduction processes along the margin of the West African Craton.

According to Utke (1987), these metasediments possibly represent additional microcontinents that were separated from pre-existing ones.

The schist belts are complexly deformed with earlier folds being refolded by later ones. Burke *et al.* (1976) made a detailed study of the structures in the Ibadan area and observed two major phases of deformation associated with the low-grade schists in the area. Rahman (1976) described an early tight to isoclinals folds with nearly flat lying axial surfaces in the Iseyin area, which are refolded by open folds with steep axial planes and nearly N-S axes. For the Igarra belt, a major open synform that refolds an earlier E-W fold was documented by Odeyemi (1988), as a major structural feature of the belt.

In Nigeria, structural studies of the metasedimentary belts have led to the proposition of two major phases of Pan-African deformation (McCurry 1971, 1976; Rahaman 1976, 1988). Phase one is characterized by isoclinals folds (F_1) with sub-horizontal S_1 axial schistocity plane and a dominant east-west mineral lineation (L_1) parallel to the folds' axis. Phase 2 is characterized by regional isoclinals folds (F_2) with sub-vertical axial planes and subhorizontal axes and an S_2 axial plane of shistocity. However, it is the second phase of deformation that is regionally most pervasive. It has left an N-S inprint not only in the schist belts but all over the Nigerian basement.

A comparison of structural events in the schist belts from NW Nigeria has indicated similar structural trends (Egbuniwe, 1982). There are similarities of the dominant deformations in all the belts, with the exception of the minor D_3 and D_4 events, which are not everywhere (Table 2.1).

Table 2.1: Deformation and structural history established for the schist belts in NW Nigeria (after Danbatta, 2008)

Belt/source of information Deformation events	Kazaure belt (Danbatta, 2002)	Malumfashi Belt (McCury, 1973)	Anka Belt (Holt, 1982)	SW of Zuru Belt (Danbatta, 1991)	Kushaka Belt (Grant, 1978)	Birnin Gwari (Ajibade, 1980)	Maru Belt (Egbuniwe, 1982)
D_4					Rare and relct minor folds. Local developme nt a strain0slip cleavage	Steeply dipping folds and kinks. Axial planes strike N-S/E-W	Steeply dipping kinks with E-W strike
D_3				Open folds with smooth profiles and sleep NNE-SSW axial planes dip	Open folds with NNE-SSW axial planes. Axes plunge north and south	Open folds NE-SW axial dip and rounded or angular crest.	Open to right Chevron folds and tight to isoclinals folds
D_2	Upright isoclinals folds with NNE-SSW axial planes. Cleavages developed	Tight Isoclinals D2 folds with N-S axial planes strike Cleavages developed	Steeply dipping, E-W striking bands.	Tight to isoclinals folds with moderate plunging axes, N-S cleavages developed.	Tight to isoclinals disharmon ic folds with steep axes. Axial planes strike N-S	Co-planar with D1 open to isoclinals large scale folds of S, schistocity. Axial planes strike NE-SW.	Open to isoclinals folds. Steeply dipping N-S striking cleavage
D_1	Relict recumbent isoclinals folds with N-S trending axial planes. Mostly obliterated.	Early ENE-WSW foliation mated to Dc folds. Largely obliterated.	Open to isoclinals upright folds with NNE-SSW axial planes and Axes.	Rare and obliterated minor folds with shallowly dipping E-W to ENE-WSW trends. S1 axial plane clevarage	Rare minor folds with E-W axial planes	Folding of cover rocks on NE-SW trending axial planes. Cataclastic deformation of basement cover contact. Cleavage well developed	Reflicts flatlying folds with N-S axes and S1 clevage. Folds obliterated by transportation

CHAPTER THREE

MATERIALS AND METHODS

3.1 PREAMBLE

The methodology adopted for this research work consists of remote sensing interpretation, field study and laboratory analyses. Satellite imageries such as digital elevation models (DEM) and Landsat ETM of the study area were used for reconnaissance survey before going to the field for ground truthing. The field study involved geological mapping of lithologies and structural features on a scale of 1:50,000 which was undertaken using a topographic base map, geologic hammer, compass-clinometer and GPS. Laboratory work involved sample preparation, petrographic and strain analyses. The petrographic study was undertaken at the Petrographic Laboratory, Department of Geology, Ahmadu Bello University, Zaria. The fry method or center-to-center technique for strain analysis was employed in order to calculate the strain in deformed rock samples in the study area.

3.2 REMOTE SENSING METHODS

Remote sensing analysis of the study area was carried out using Landsat ETM imageries and a digital elevation model. Six bands (1, 2, 3, 4, 5, and 7) and a digital elevation model were downloaded from Global land cover facility website (http://glcf.umd.edu/). Image processing was carried out using different softwares such as Erdas Imagine, Envi, Arc Gis, PCI-Geomatica, and Rock work. Image processing technique employed include false colour composite and principal component analysis (used to map lithological units), band rationing and lineament analysis. Lineaments for the study area were automatically generated and their dominant strike direction determined through rose diagrams.

3.3FIELD INVESTIGATIONS

Field investigationswere carried out in two (2) stages, first was a reconnaissance visit for five days, followed by the second field visit during which geological field mapping was undertaken on a scale of 1: 50,000 for two weeks. Fresh rock samples were collectedand the co-ordinates of every sampling point wererecorded with a Global Positioning System (GPS). Preliminary observation and identification of constituent minerals in the rock samples were carried out using magnifying lens. Field measurement of strikes and dip directions of planar and linear features was carried out usinga compass-clinometer. Other structural imprints like displacement of faults, dimension of veins and dykes were also recorded.

3.4 LABORATORY WORK

3.4.1 Petrography

Fresh representative rock samples were selected from the different rock types and thin sections were produced in the thin section laboratory of the Department of Geology, Ahmadu Bello University.

(i) A thin slice of rock or mineral specimen was cut using the diamond saw and trimmed to fit onto a glass microscope slide.

(ii) The rock slice was glued to the microscope slide with clear epoxy.

(iii) The slide with rock slice on its surfacewas mounted in a special holder and smoothened on a diamond slap until an appreciable reduction in the thickness of the rock slice was achieved. Finally, it was hand finished with 600 grit silicon carbide on a glass lap.

(iv)When a thickness of 0.03mm was reached, the section was ready for examination under the microscope. The thickness of the section is usually measured with a digital micrometer or

estimated by visual inspection. With experience, a good estimation can be made by visual examination of the section and final checking with a microscope.

(v) A cover slip is sometimes placed on the mount to protect the specimen.

The prepared slides were examined under the petrological microscope to identify the minerals and other features that hitherto were not seen in hand specimen.

3.4.2 Strain Analysis

The center-to-center technique (also called the fry method after its inventorFry, 1979), was used to calculate the strain in rocks that before deformation contained randomly scattered objects or particles, such as phenocrysts in deformed granitic rocks. During deformation, the centers of adjacent objects become closer in the directions in which the rock is being shortened and farther apart in the directions in which the rock is being lengthened.

Specifically, the Fry method is a graphical approach that uses the distribution of the centers of initially spherical strain markers to define a strain ellipse for the rock in question (Fry, 1979; Ramsay and Huber, 1983). A Fry plot is produced by plotting the location of strain-marker centers as a function of distance from every other strain-marker center. Practically, this can be done manually by plotting each grain center on a piece of tracing paper overlying a photomicrograph of grains; if the overlay is moved incrementally, and grain centers plotted again, the shape of a strain ellipse eventually appears.

The ellipse is in the form of a void in the center of the Fry plot, which defines the strain ellipse with an axial ratio (Rs). The orientation of the strain ellipse is measured using the rake of the long axis from the baseline (Φ) in the principle plane of strain. The Fry method is most effective with strongly anti-clustered, initially spherical strain markers of equal size that are strained

homogenously (Fry, 1979; Dunne *et al*. 1990; Crespi, 1986). The occurrence of such strain markers is not common in nature. To compensate for this problem, Erslev (1988) developed the normalized Fry method. This modification accounts for natural variations in the sizes and sphericity of strain markers. The normalized Fry method generates plots with greater definition of the central void.

In order to evaluate strain and associated structural and micro-structural changes in the area, seven (7) samples of deformed rocks were analyzed. Thin-sections from each deformed rock were prepared for strain analysis along the XY planes of the finite strain ellipsoid.

EllipseFit v.3.1.1strain software was used to analyze the photomicrographs obtained from the samples. This program creates elliptical outlines and calculates grain centers of individual grains.EllipseFit generates normalized Fry plots from digitized grain data in accordance with the methods outlined by Erslev (1988). EllipseFit software calculated the orientation and lengths of strain axes and plotted best-fit strain ellipses, removing the potential for error that arises from hand fitting.

CHAPTER FOUR

RESULTS

4.1 REMOTE SENSING

4.1.1 Preamble

Acquisitionof data by remote sensing is among thetechnological advancement that has beenrealized, and in geological aspect, thetechnique is normally used in acquiringEarth's surface geological data like; structural features, lithologies and lithological sequences, relative age of rock strata, typesof drainage, soil type, vegetation cover, etc(Drury 1993). This technique when usedtogether with field mapping, i.e ground truthing, makes geological mapping more effective and efficient.

4.1.2 Lithological Mapping

(a) False Colour Composite Technique

False colour composite techniques likethose used by Rowan *et al*. (1974), Raines*et al*. (1978) and Riley *et al*. (2006),represented in R: G: B were employed for lithological mapping of rocks. Landsat band ratio as well as R.G.B composite images played an important role in identifying different rock types in the study area. Band ratios are effective in reducing the effect of illumination derived from the sun, slope and shadows to a marked degree. The image processing band-ratio technique is applied by dividing the digital number (DN) values of one band by the corresponding DN values of another band and displaying the new DN values as grayscale image (Sabins, 1997).

(b) Principal Components Analysis (PCA)

Principal components analysis (PCA) allows redundant data to be compacted into fewer bands in order to reduce thedimensionality of the data. An important advantage of PCA is that most of the

information withinall the bands (represented by the variance) can be compressed into a much smaller number of bands with little lossof information (Gibson and Power, 2000). The bands of PCA data are non-correlated and independent, and are oftenmore interpretable than the source data (Jensen, 1996).

4.1.4 Lineament Analysis

The structural and tectonic framework of the Nigerian Basement Complex has been reported as comprising northeast – southwesterly and northwest – southeasterly lineaments superposed over a dominant north-southerly trend (Olasehinde et al., 1990), and NW-SE and NE-SW pair superposed on a N-S joint set (Annor et al., 1990; Annor and Freeth, 1985).

Lineaments in the Basement Complex have a widespread occurrence and are found as sheared rocks and zones, which form as dykes and ridges and also as straight channeled streams which exploits weak zones of the earth.

In the present study, Erdas Imagine Software was used to generate shaded relief images from Shuttle Radar Topography Mission Digital Elevation Model (SRTM DEM) (Fig. 4.7). The DEM indicates that the highest elevation is in the Northern part of the study area and in the extreme southeastern part, marked by yellowish colour. The lower elevations are found along the river channels and in the southwestern portion of the study area, as marked by bluish colour as shown in Fig. 4.7.

The method can enhance lineaments at different orientation by simulating topographic illumination under varied light direction. In order to identify linear topographic features from the DEM, eight shaded relief images were created.

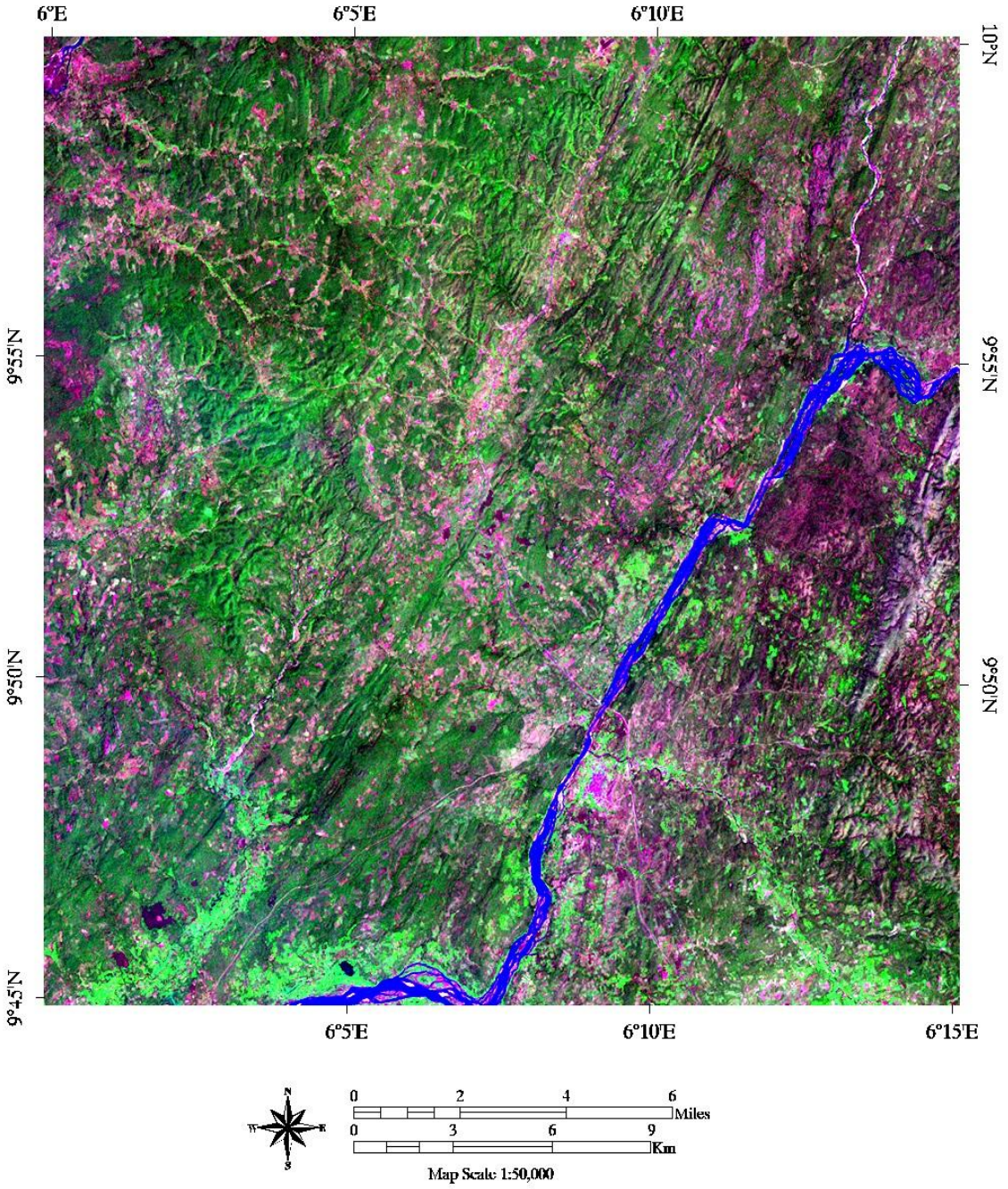


Figure 4.1: False colour composite image for bands 7, 4, 1 displayed in R.G.B. Note the dominance of green (vegetation) over the shades of red (gneiss, schist and amphibolite), and the blue colour delineating the drainage in the southeastern corner.

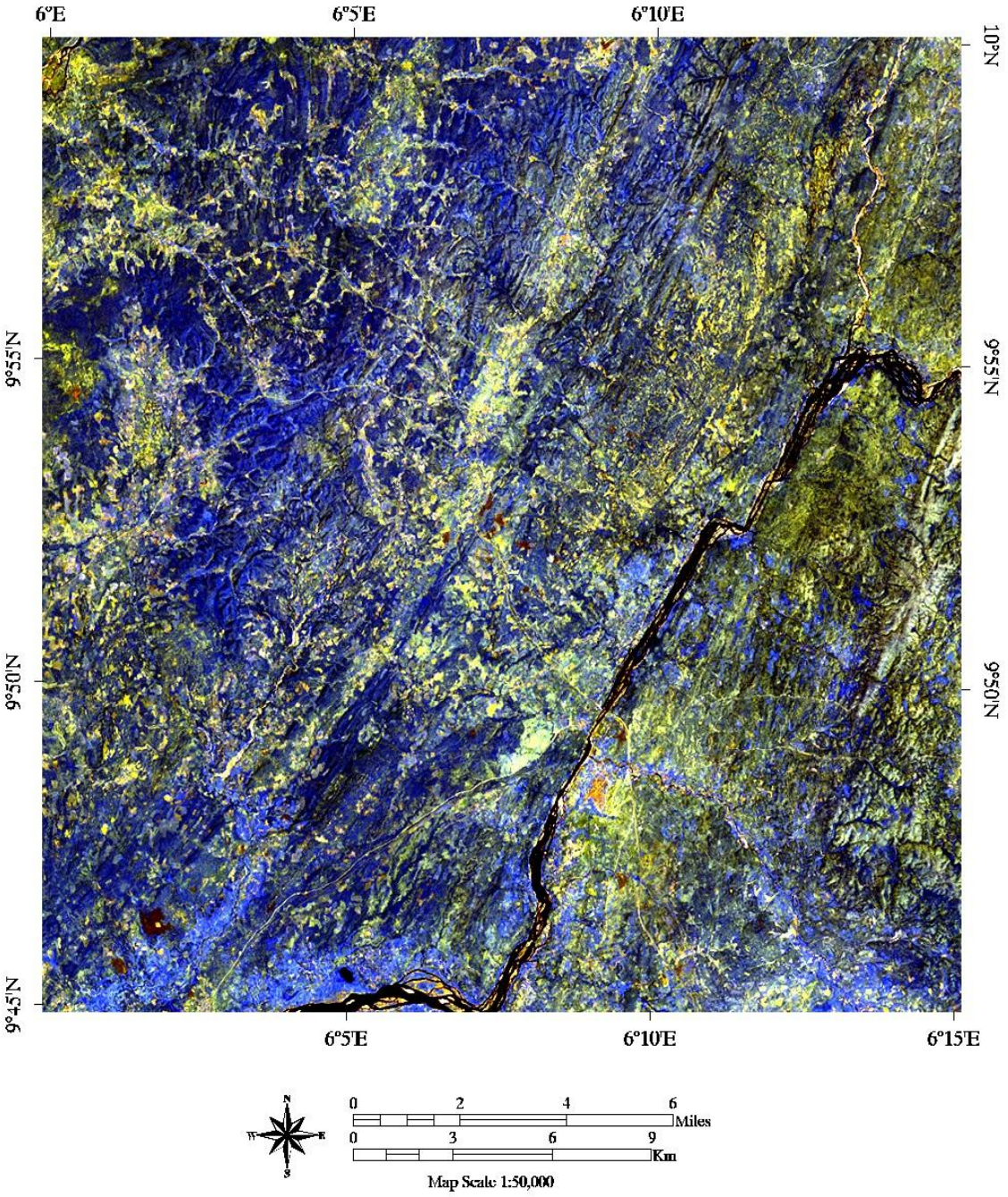


Figure 4.2:False colour composite image for bands 7, 5, 4 displayed in R.G.B. Note that the vegetation cover appears as blue, the drainage system as black, while areas covered by gneiss, amphibolites, migmatites and mylonites by yellow.

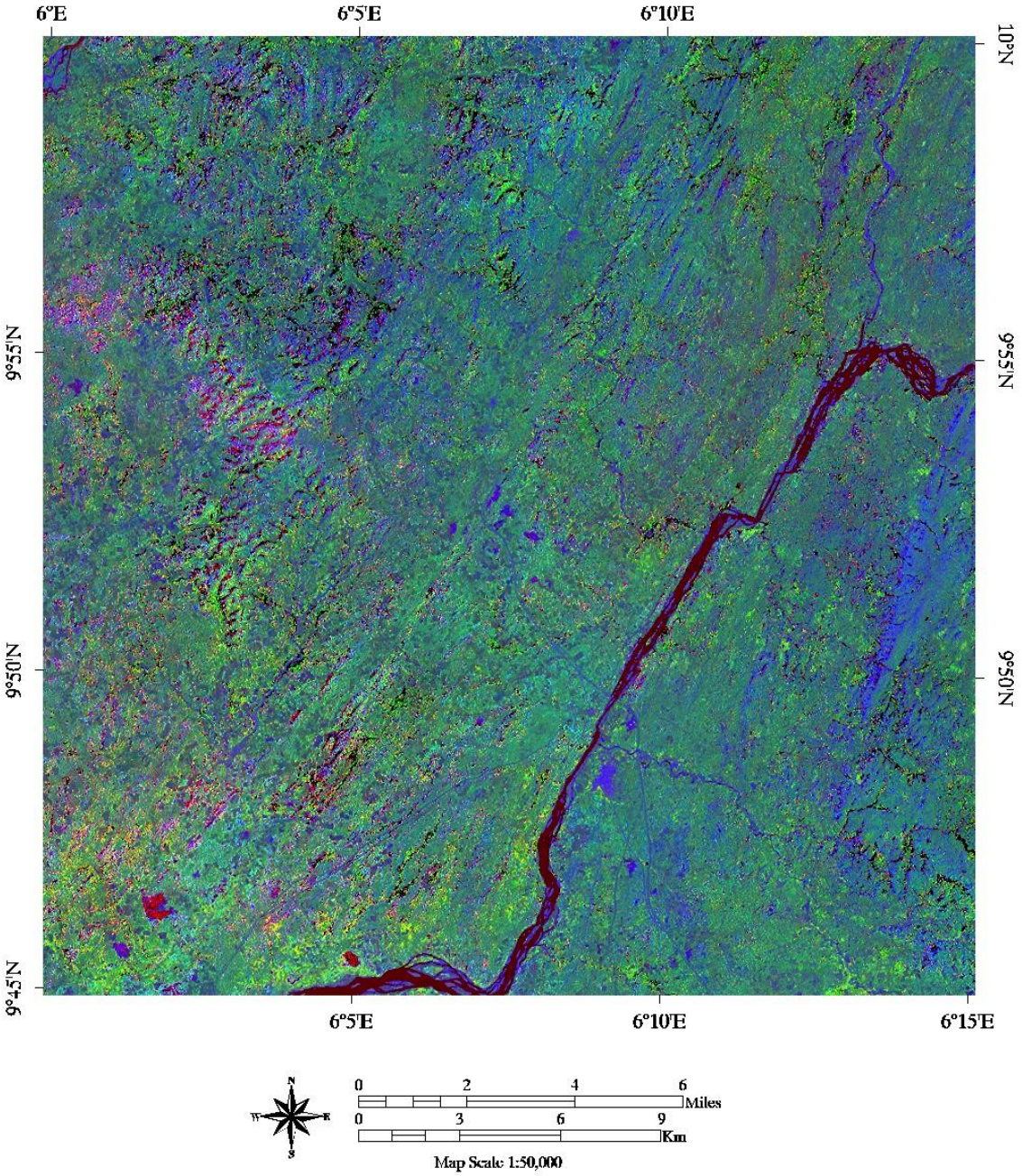


Figure 4.3:False colour composite image for bands 1/3:5/7:3/5 displayed in R.G.B. The greenish-yellow region shows area occupied by quartzites, while the bluish region delineates areas occupied by gneiss and amphibolites.

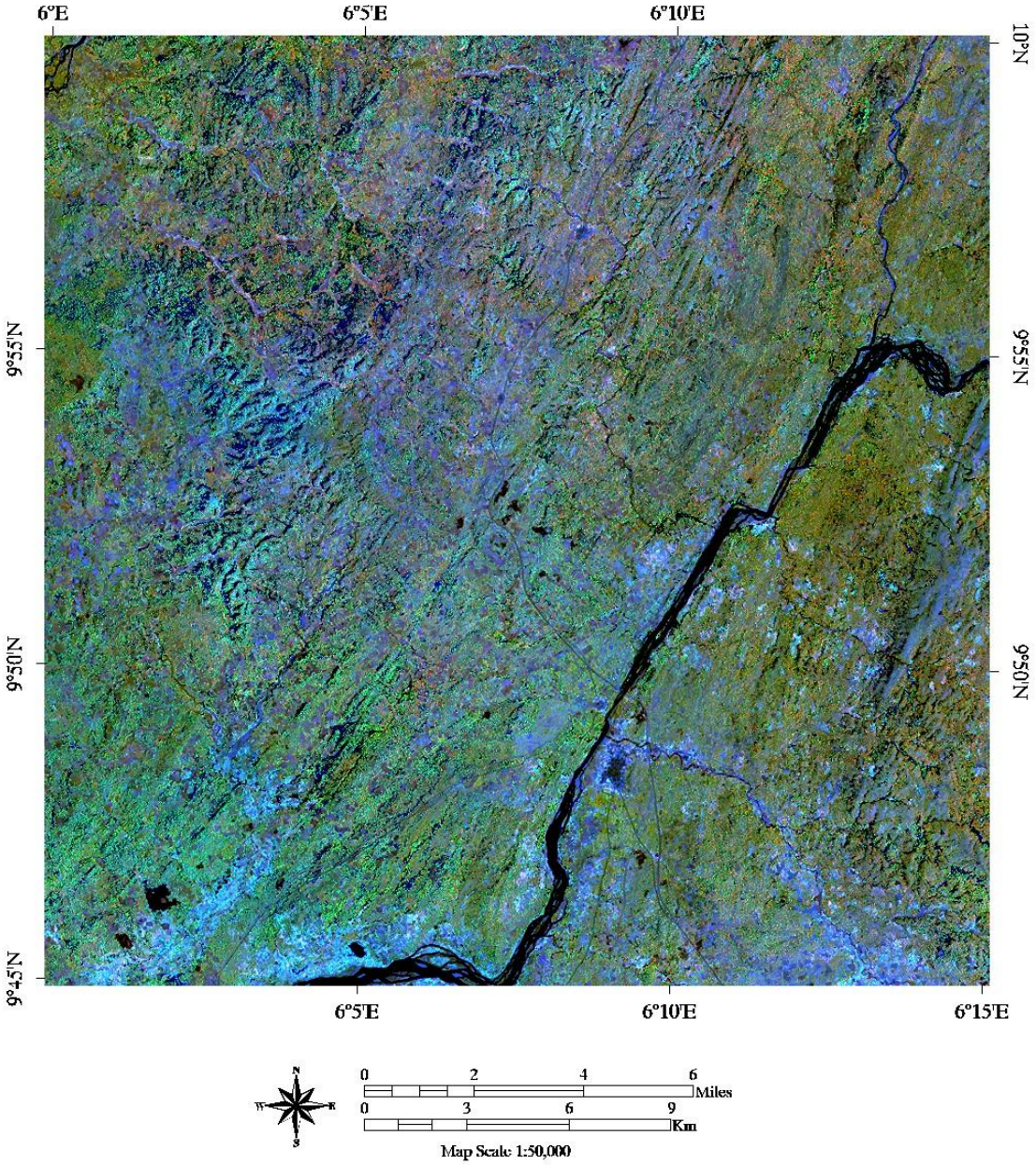


Figure 4.4: False colour composite image for bands 5/1, 5/7, 4 displayed in R.G.B. Note that the major water body in the southeastern portion of the area is displayed as black while areas occupied by gneisses and amphibolites are light purple

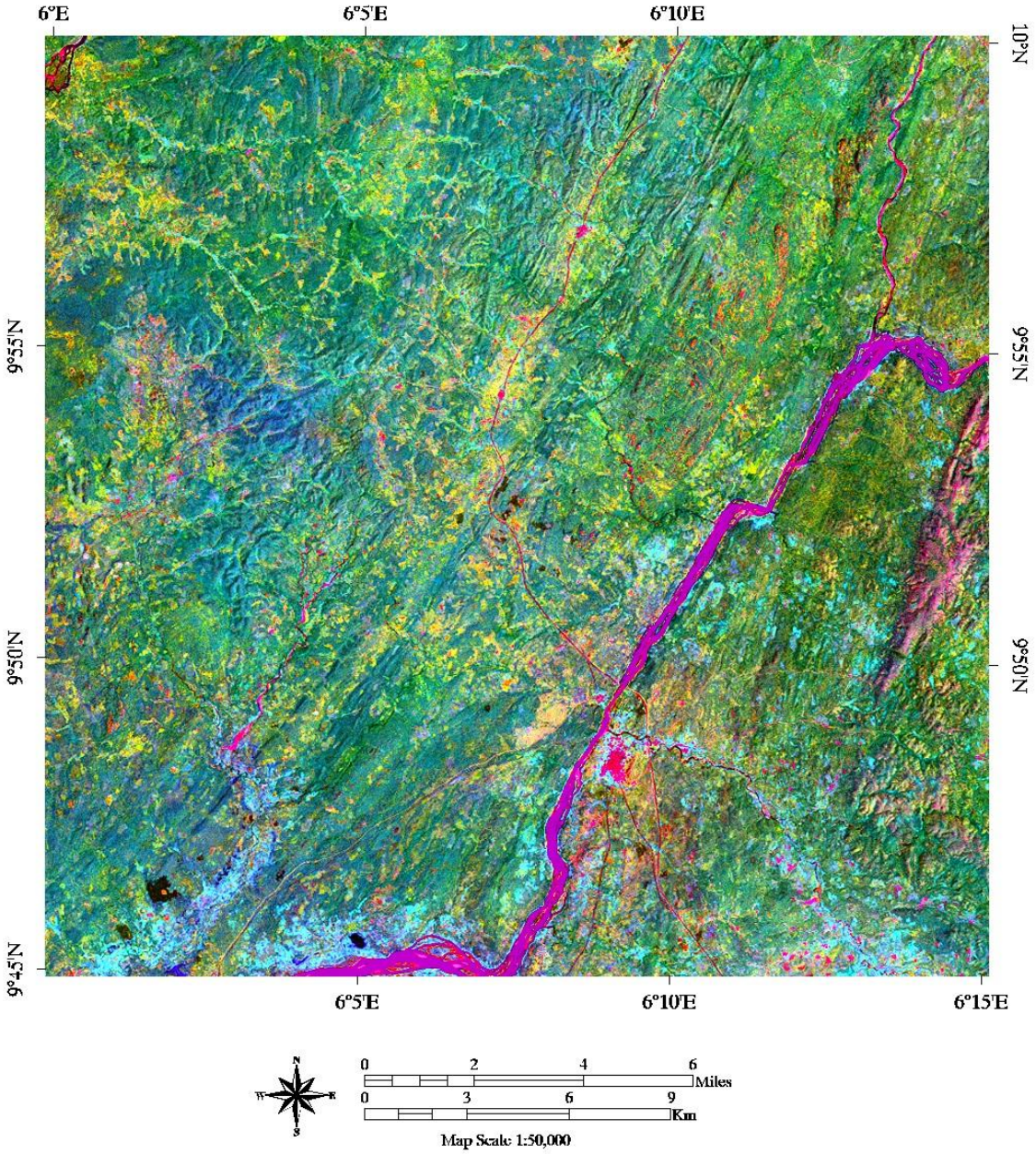


Figure 4.5:Principal component analysis of bands 1, 2, 3 displayed in R.G.B. Note that the major drainage system and an amphibolite region in the far eastern portion of the study area are indicated by purple colour.

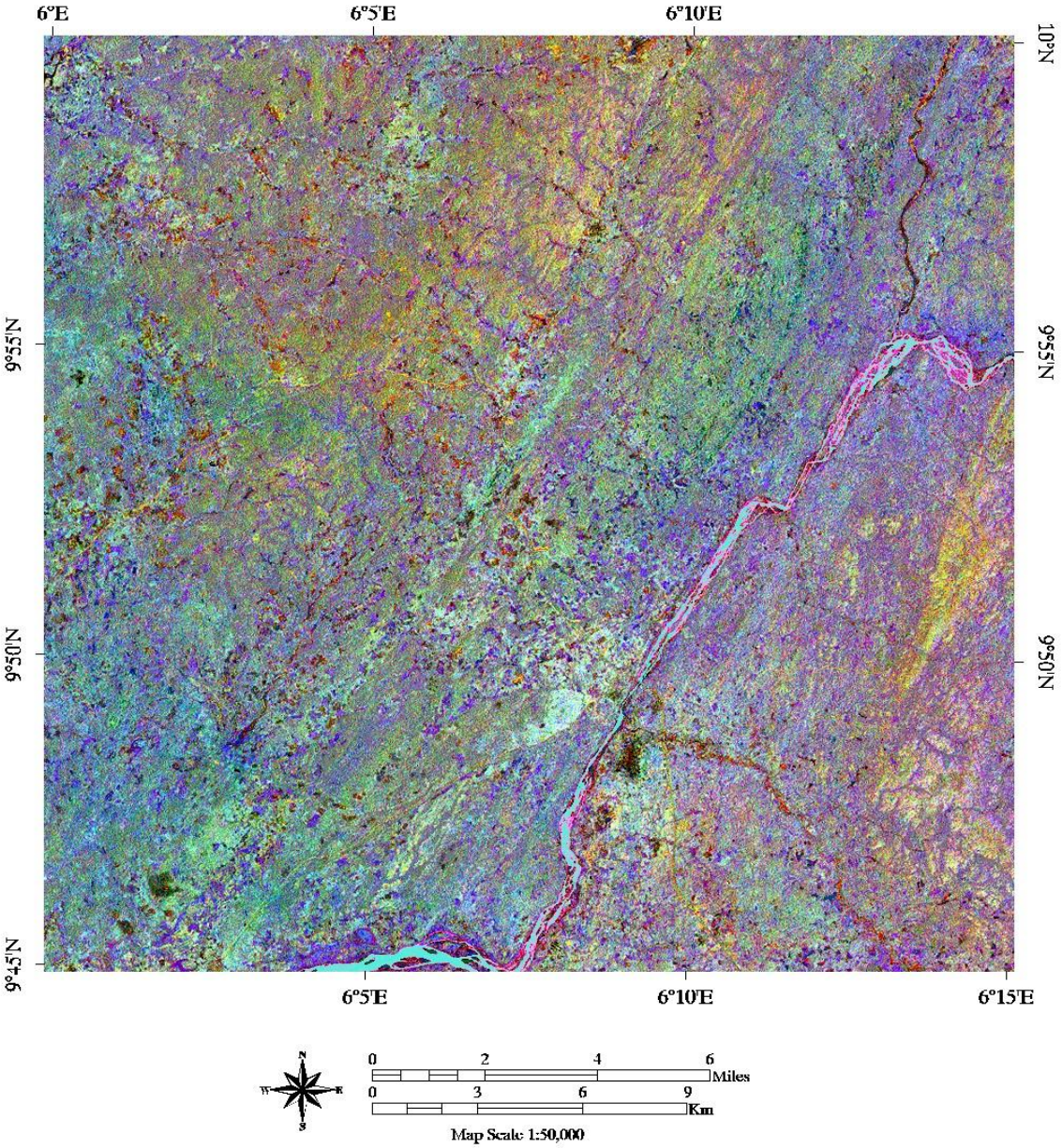


Figure 4.6: Principal component analysis of bands 4, 5, 6 displayed in R.G.B. Note that the different lithologies and drainage systems exhibit an almost uniform colour.

An ambient light setting of 0.2 and a solar elevation of 30^0 were used to ensure good contrast. Shaded relief images were created by varying the solar azimuth (sun angle) through the following contrasting illumination angles; 0^0, 45^0, 90^0, 135^0, 180^0, 225^0, 270^0 and 315^0 (Figures 4.8-4.15).

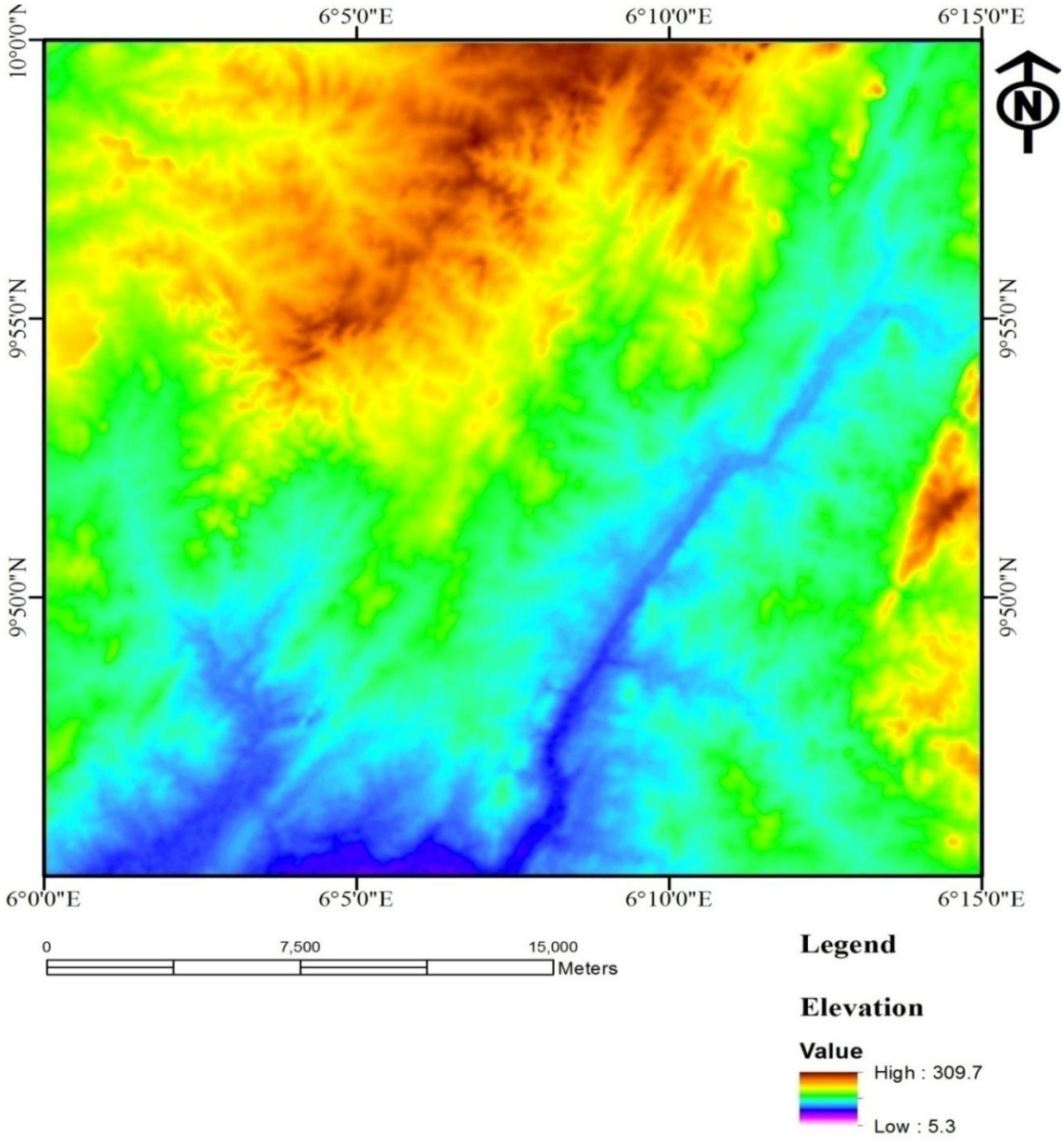


Figure 4.7: SRTM DEM displaying elevation variation within the study area with the higher elevation in the Northern and southeastern portion and the lower elevation in the southwestern portion.

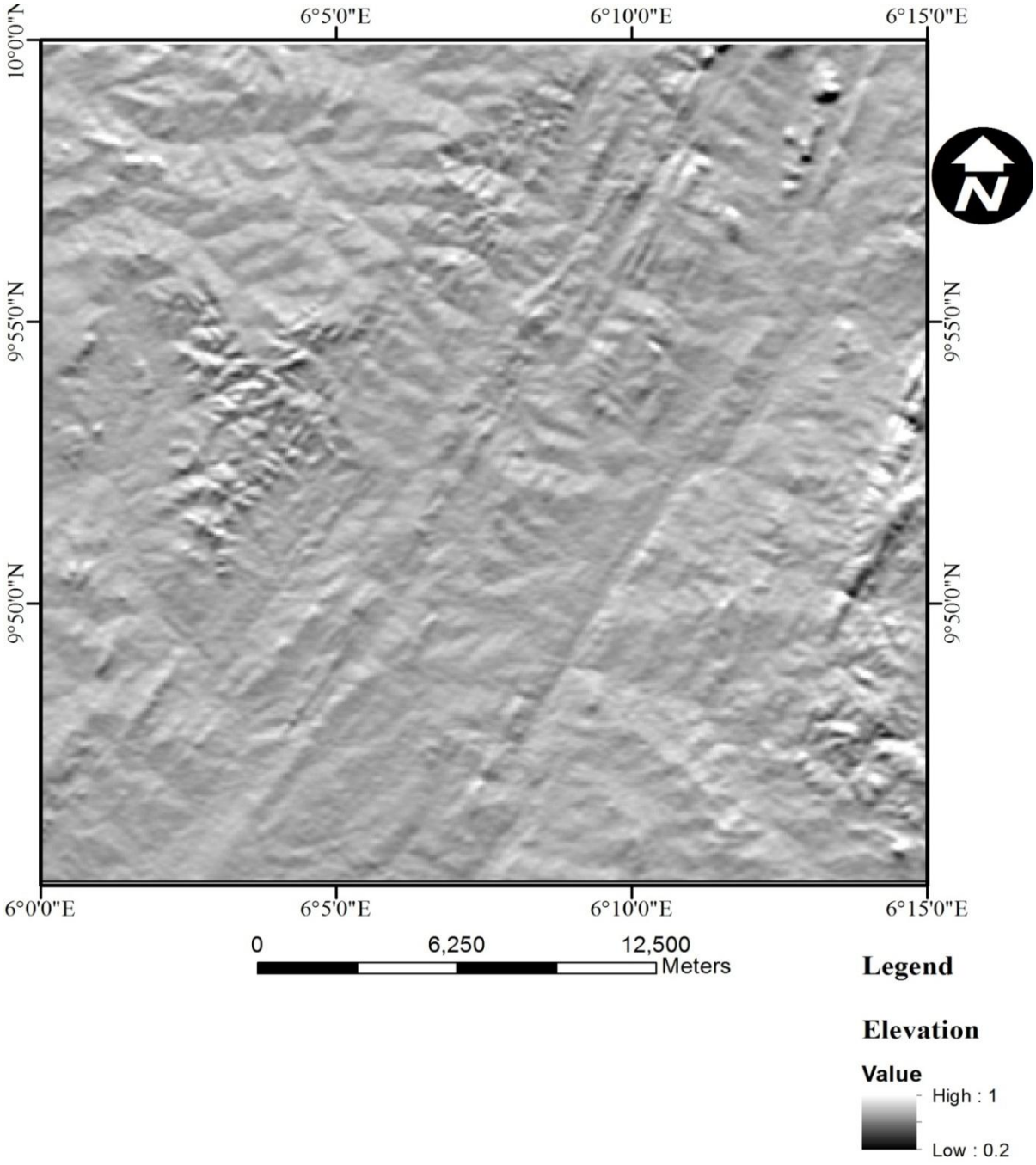


Figure 4.8: Shaded relief image derived from DEM with illumination direction (solar azimuth),0^0 used in identifying lineaments in different reliefs and topography.

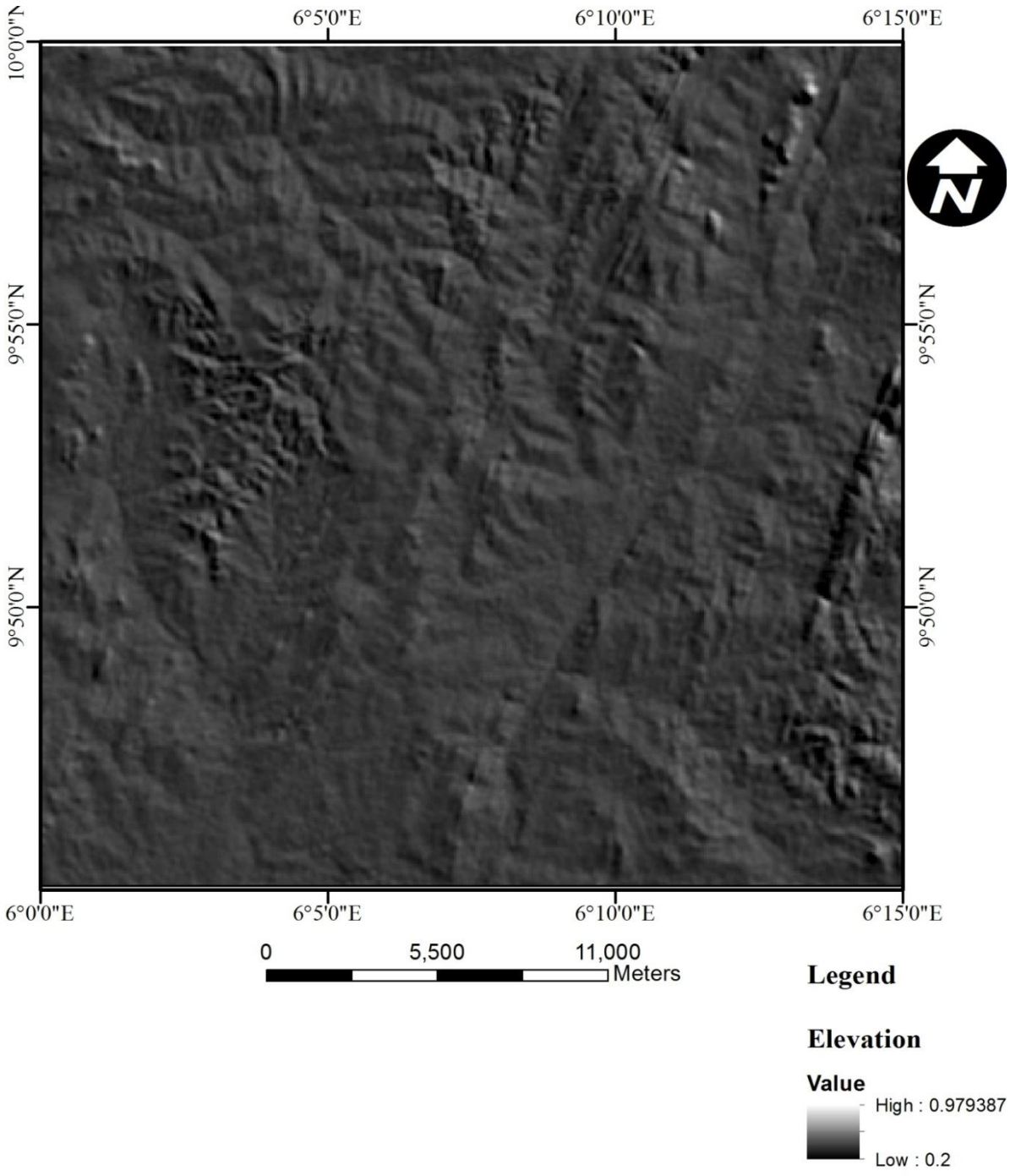


Figure 4.9:Shaded relief image derived from DEM with illumination direction (solar azimuth), 45^0 used in identifying lineaments in different reliefs and topography.

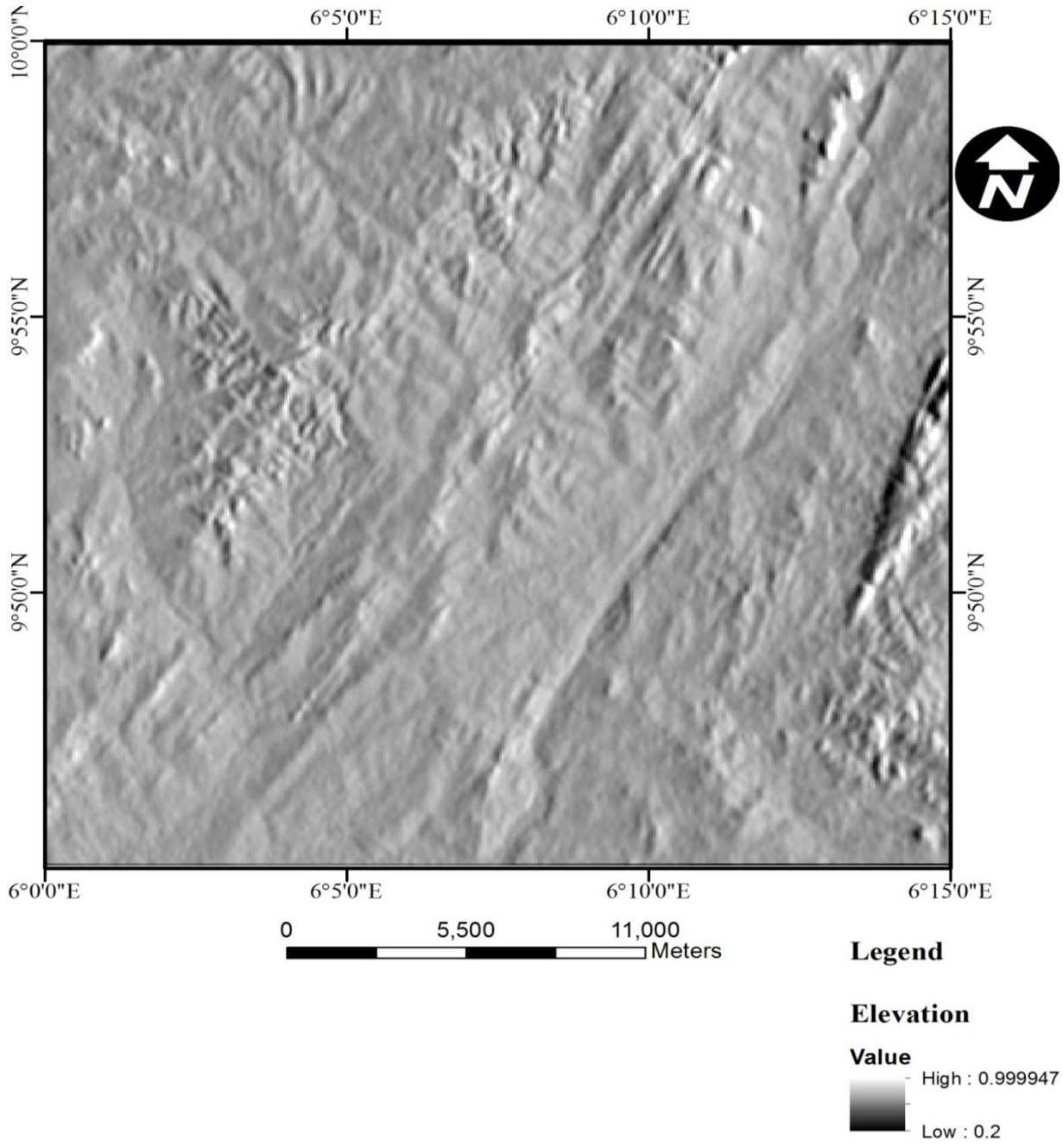


Figure 4.10: Shaded relief image derived from DEM with illumination direction (solar azimuth), 90^0, used in identifying lineaments in different reliefs and topography.

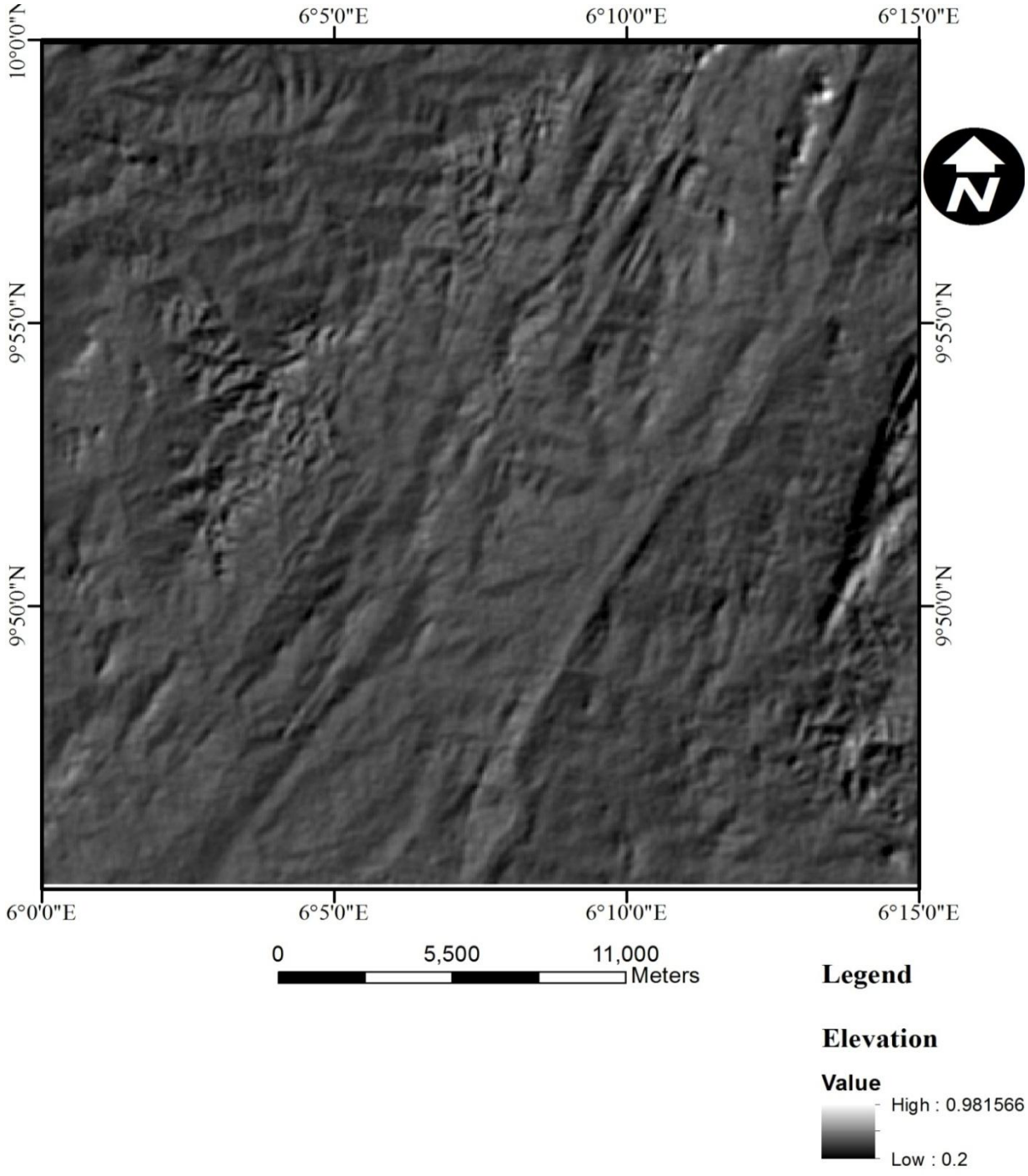


Figure 4.11:Shaded relief image derived from DEM with illumination direction (solar azimuth), 135^0, used in identifying lineaments in different reliefs and topography.

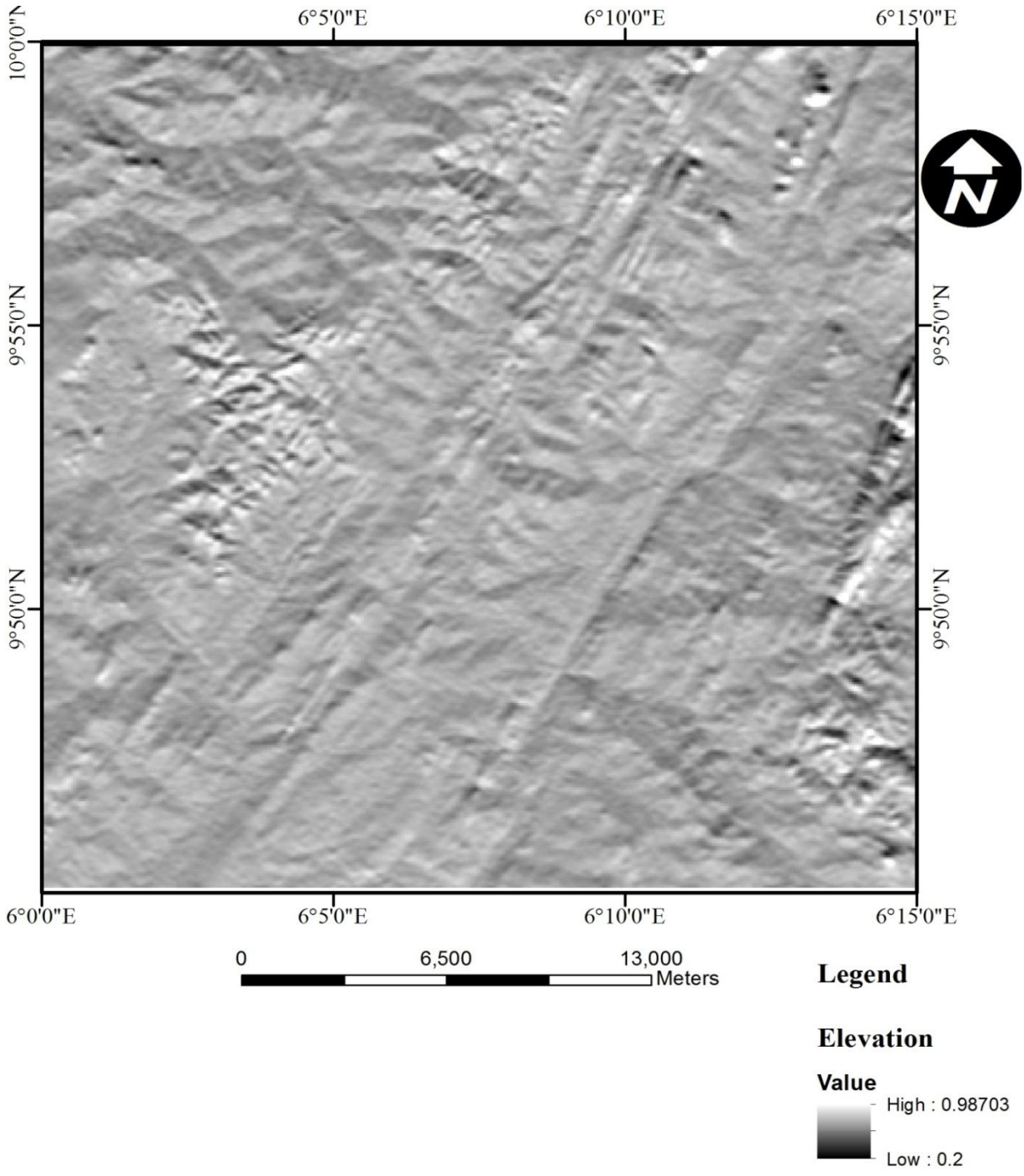


Figure 4.12:Shaded relief image derived from DEM with illumination direction (solar azimuth), 180^0, used in identifying lineaments in different reliefs and topography.

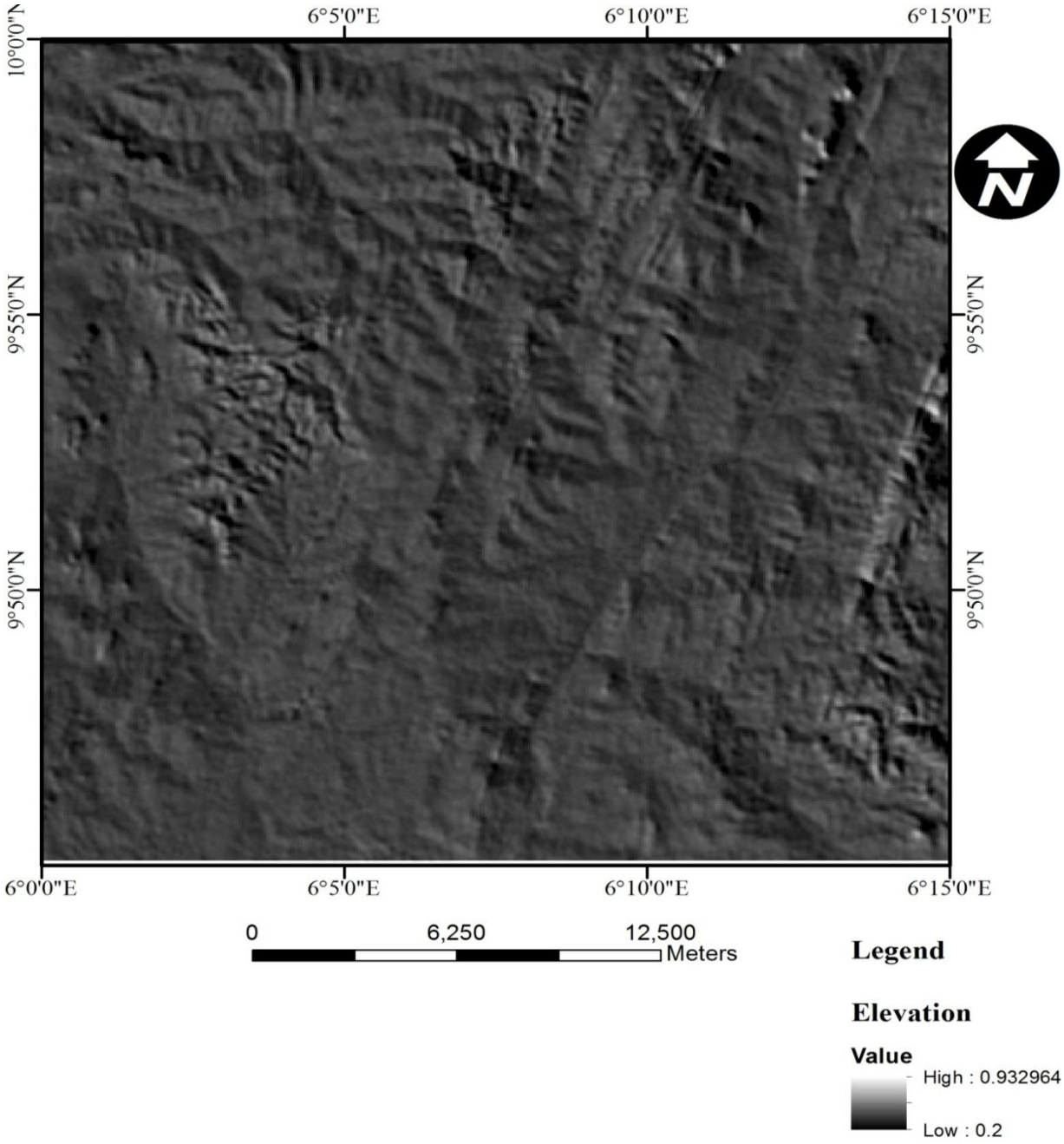


Figure 4.13:Shaded relief image derived from DEM with illumination direction (solar azimuth), 225^0, used in identifying lineaments in different reliefs and topography.

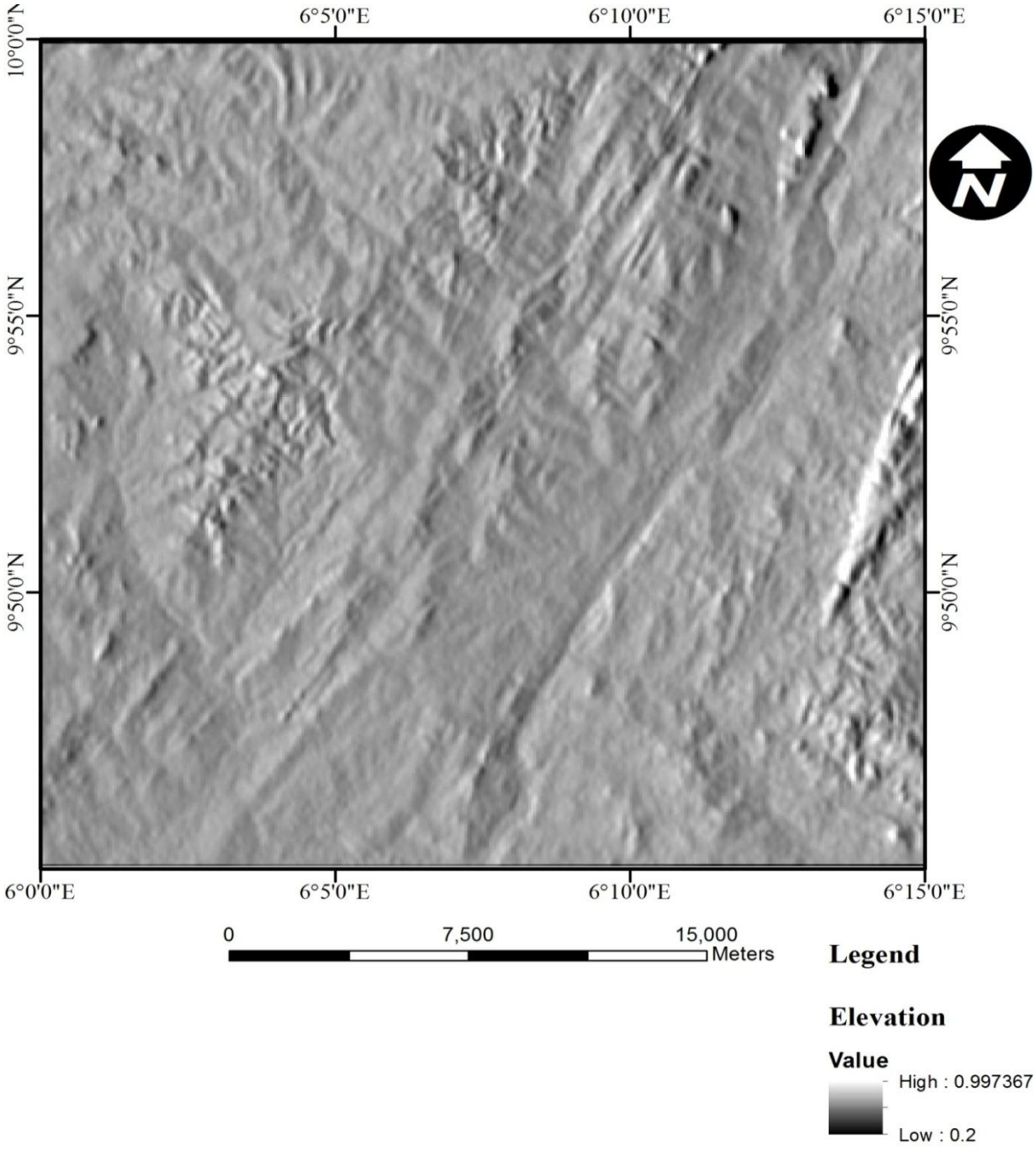


Figure 4.14: Shaded relief image derived from DEM with illumination direction (solar azimuth), 270^0, used in identifying lineaments in different reliefs and topography.

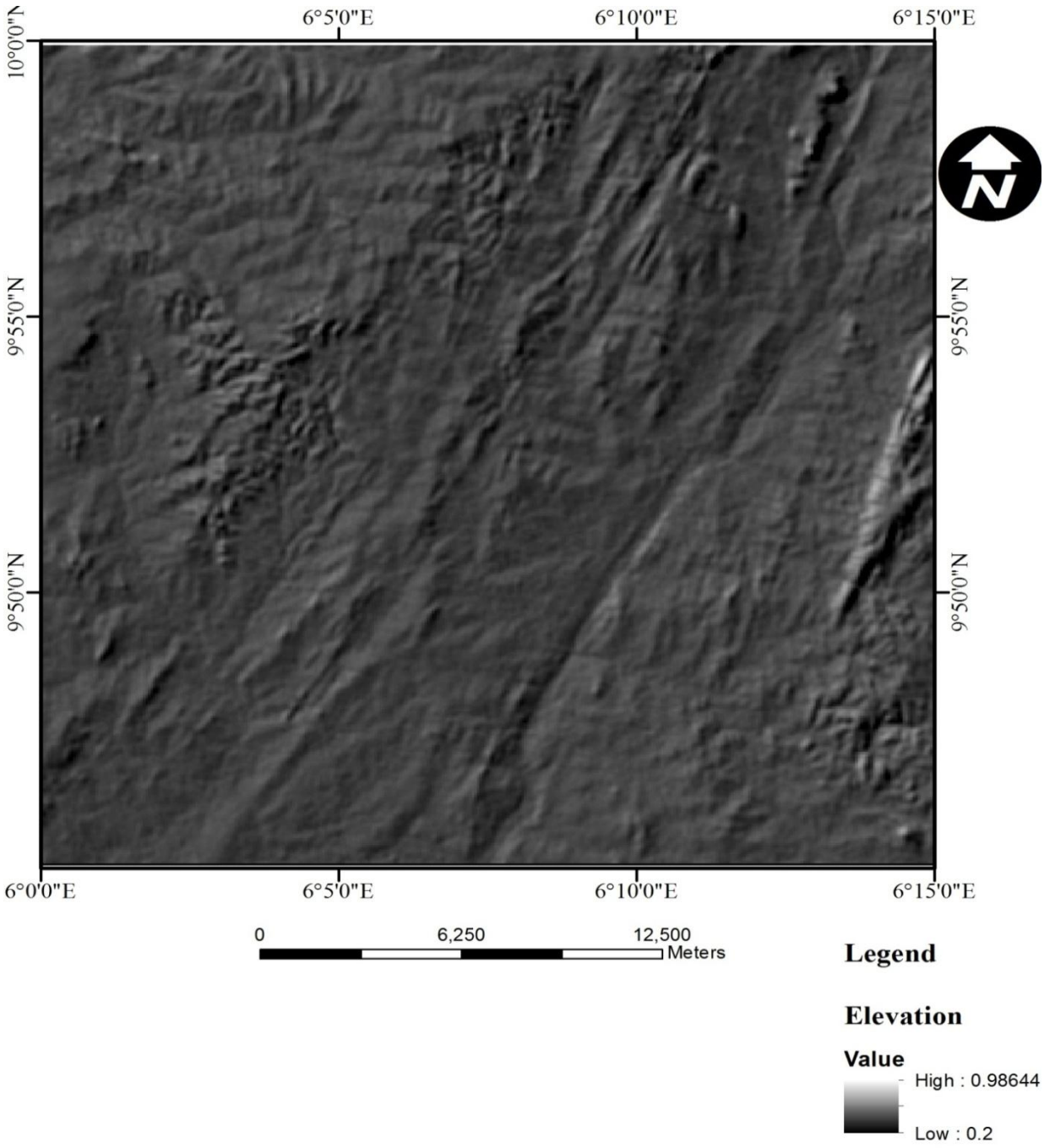


Figure 4.15:Shaded relief image derived from DEM with illumination direction (solar azimuth), 315^0, used in identifying lineaments in different reliefs and topography.

Production of shaded relief images was followed by the combination of shaded relief images to produce two combined shaded relief images. The first combined shaded relief was produced from combination of shaded relief images with azimuth directions 0^0,45^0,90^0 and 135^0 (Fig. 4.16). The second combined shaded relief images were produced from the shaded relief images with azimuth direction 180^0, 225^0, 270^0 and 315^0 (Fig. 4.17).

Production of first and second combined shaded relief images was followed by automatic generation of lineaments from both images using PCI Geomatica Software (Fig 4.18 and Fig. 4.19). Buffering of both lineaments images was carried out using ArcGis Software (Fig. 4.20 and Fig. 4.21). This was followed by adding the two buffered images to produce a thematic image that shows the similarities between both images (Fig. 4.22). Re-classification into two classes was then performed on the combined thematic image (Fig. 4.23) and lineaments were manually digitized to produce a final lineament map for the study area (Fig. 4.24).

The lineament map revealed a dominant N-S, NW-SE and to a lesser extent NE-SWorientations of lineaments (Fig. 4.24). The concentration of lineaments per unit area was determined through lineament density analysis of the study area (Fig. 4.25).The lineament density can be expressed in variable ways; in the present study it is expressed as the number of lineaments per grid unit area. The resulted lineament density was classified into three categories; low, moderate and high. The major part of Zunegru area is characterized by low to moderate lineament density. The lineament density increases toward the northern and northeastern sectors of the area.

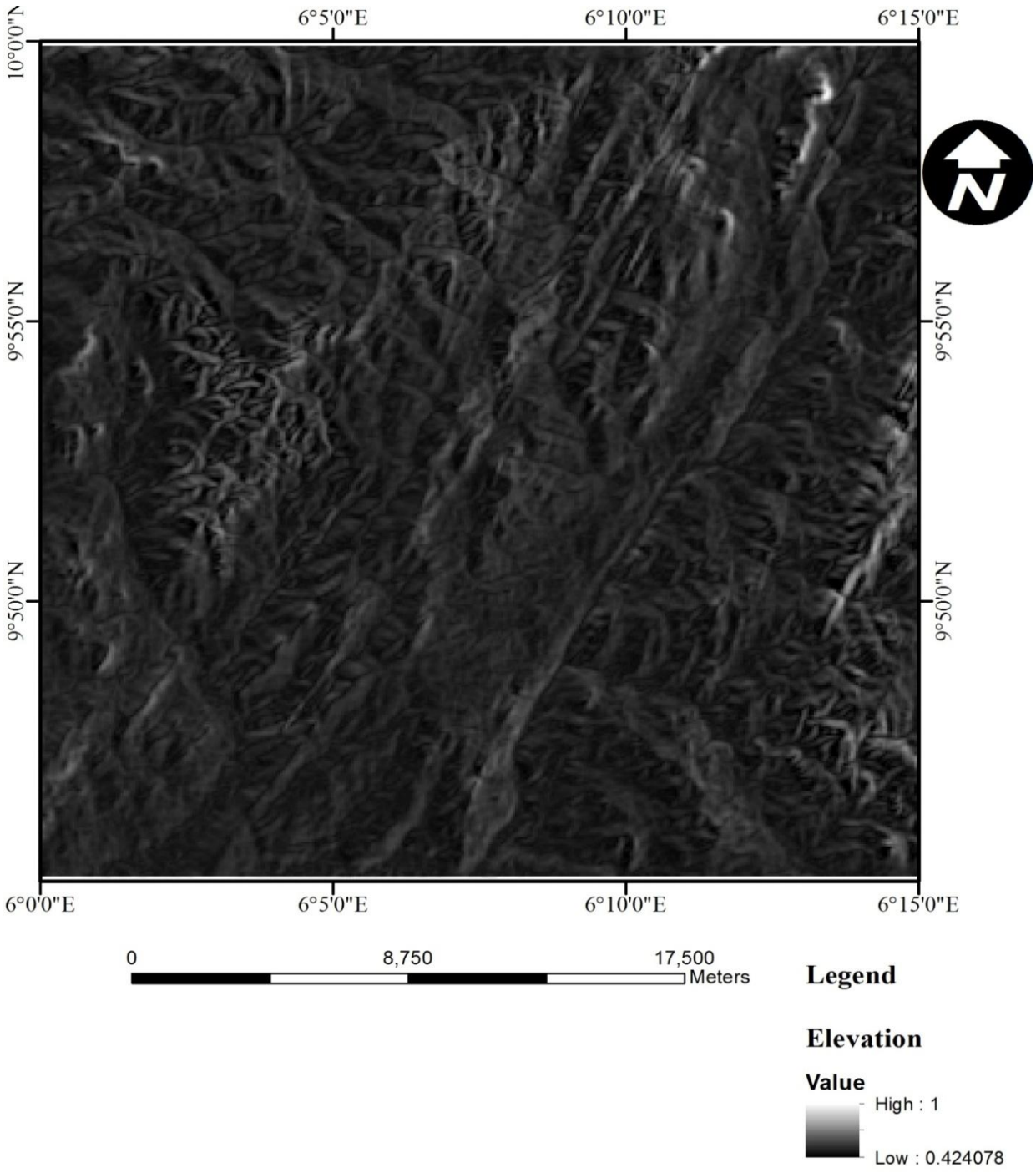


Figure 4.16: Shaded relief images derived by combining four other shaded relief images with azimuth directions 0^0,45^0,90^0 and 135^0

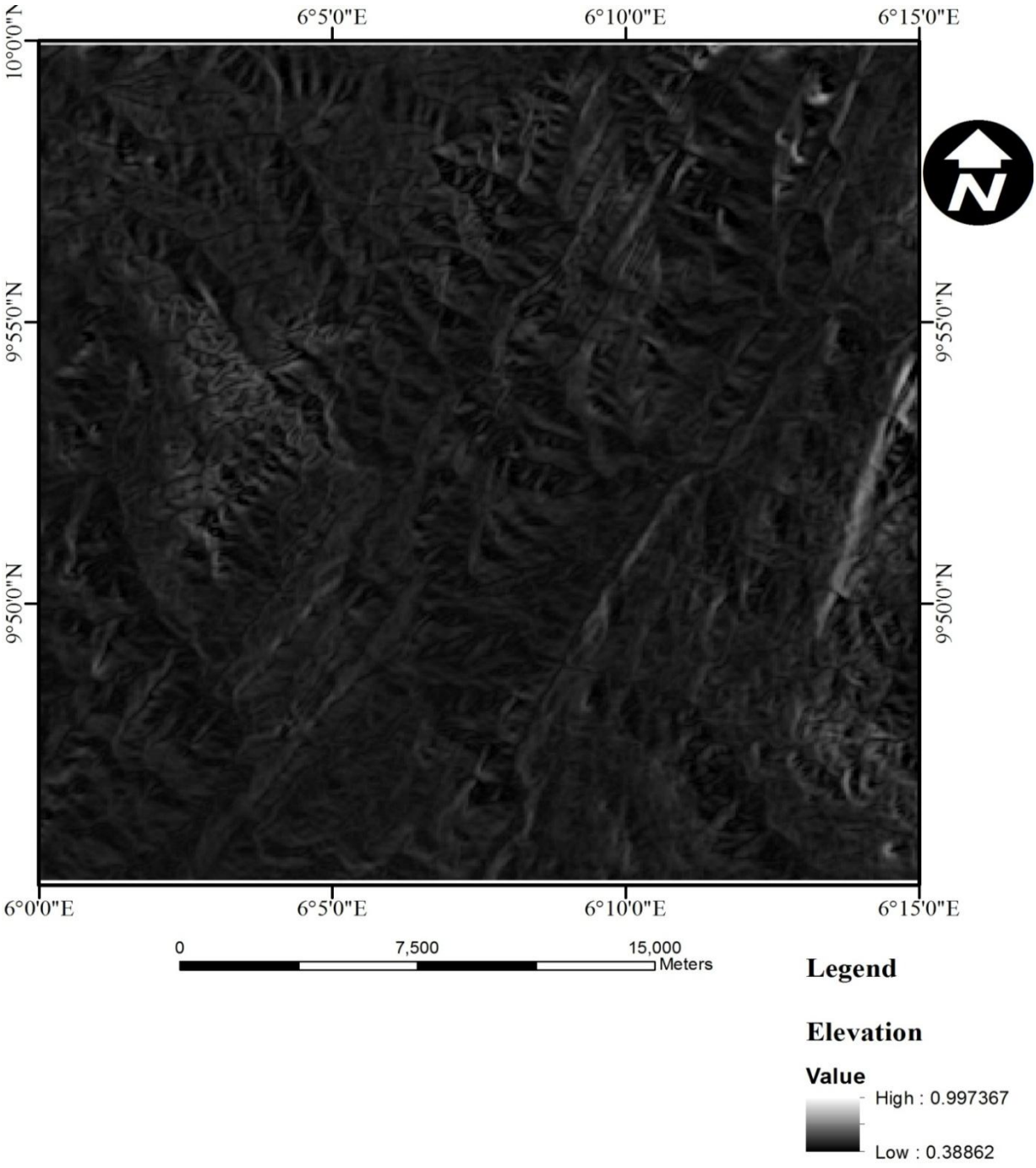


Figure 4.17: Shaded relief images derived by combining four other shaded relief images with azimuth directions 180^0, 225^0, $270^0$and 315^0

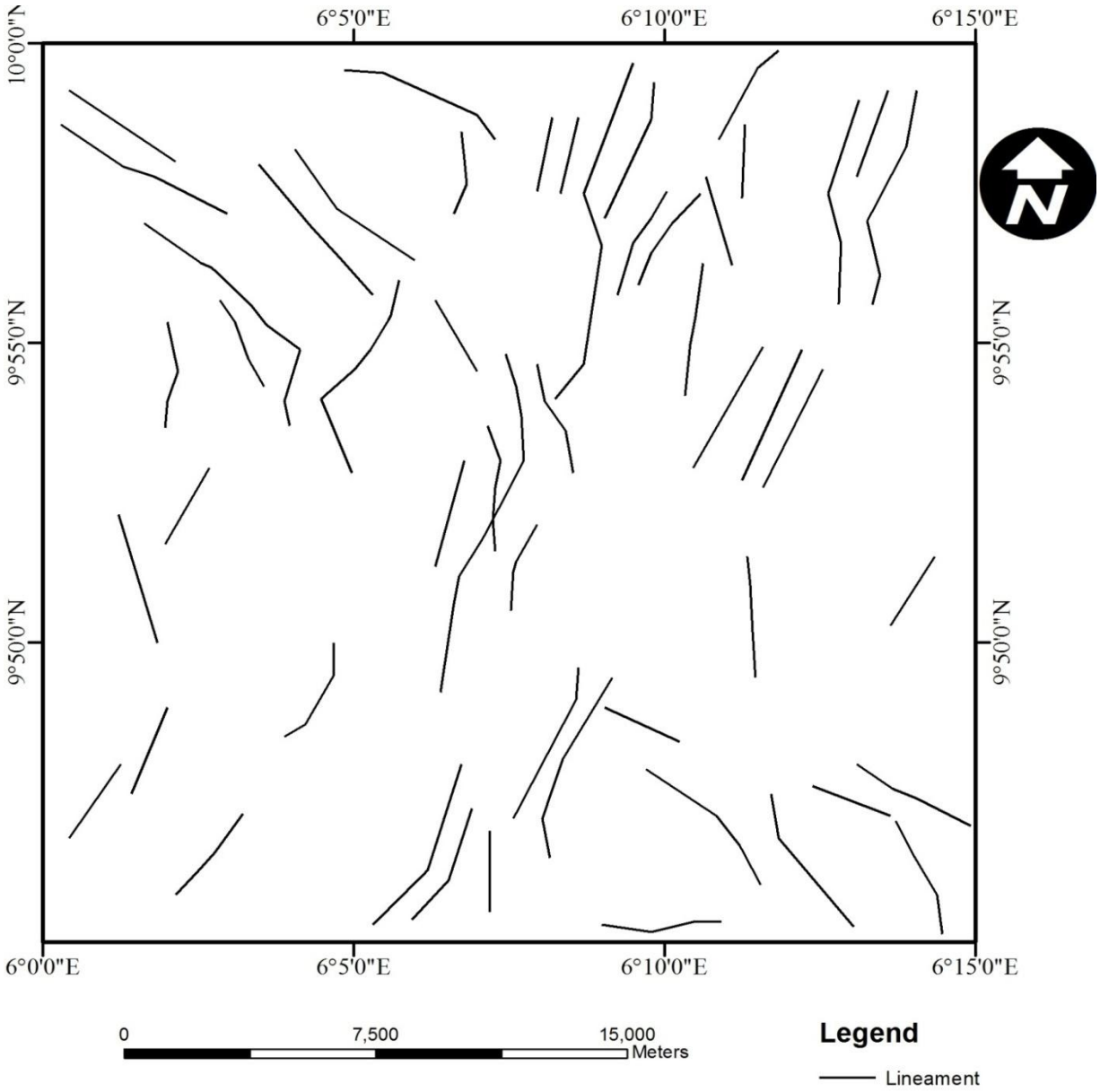


Figure 4.18: Lineaments from combined shaded relief images with azimuth direction 0^0,45^0,90^0 and 135^0 showing two main trend directions, with the predominance of NNE-SSW lineaments over the NNW-SSE direction.

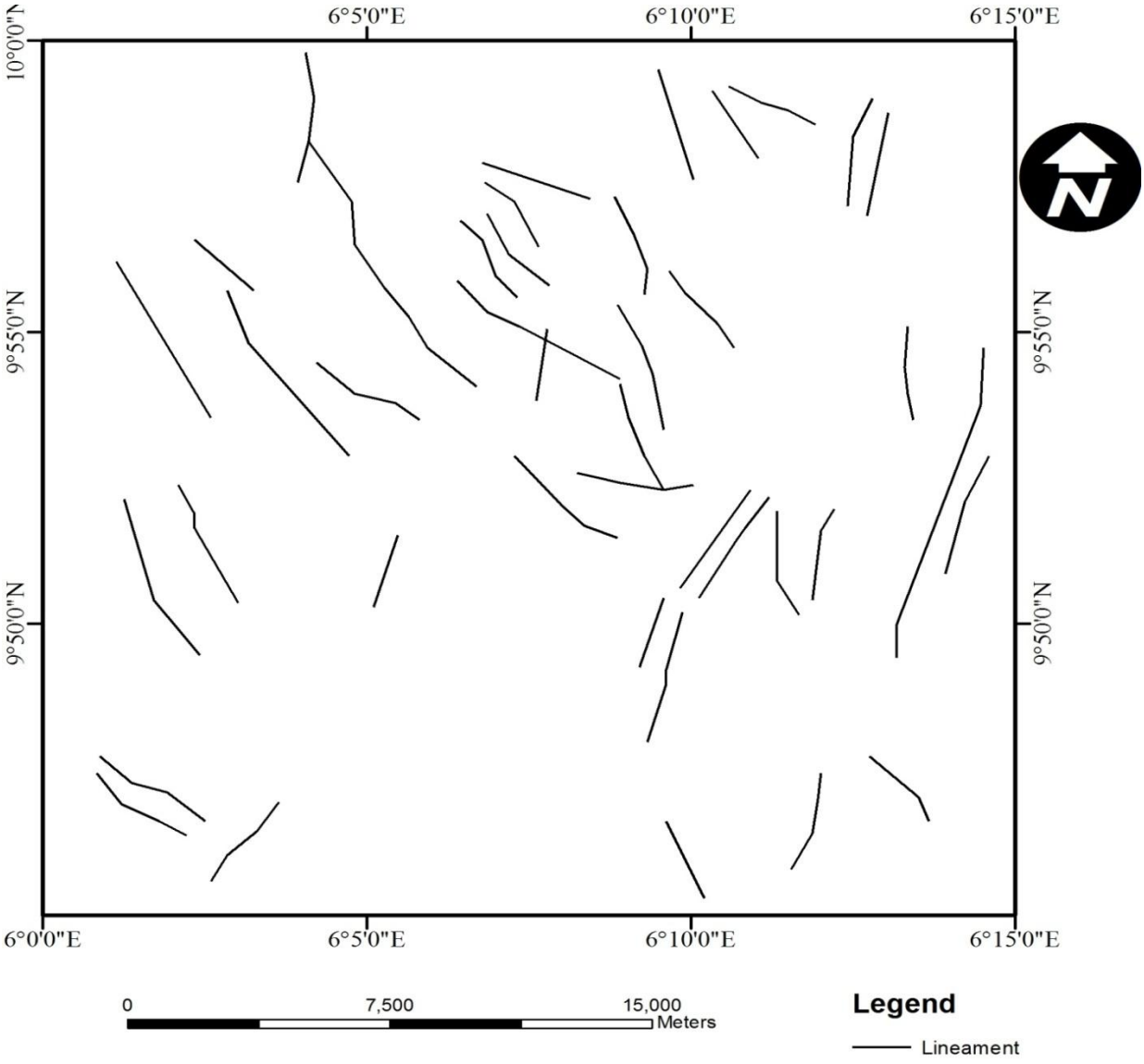


Figure 4.19: Lineaments from combined shaded relief images with azimuth direction 180^0, 225^0, 270^0 and 315^0showing two main trend directions, with the predominance of NNW-SSE lineaments over the NNE-SSW directions.

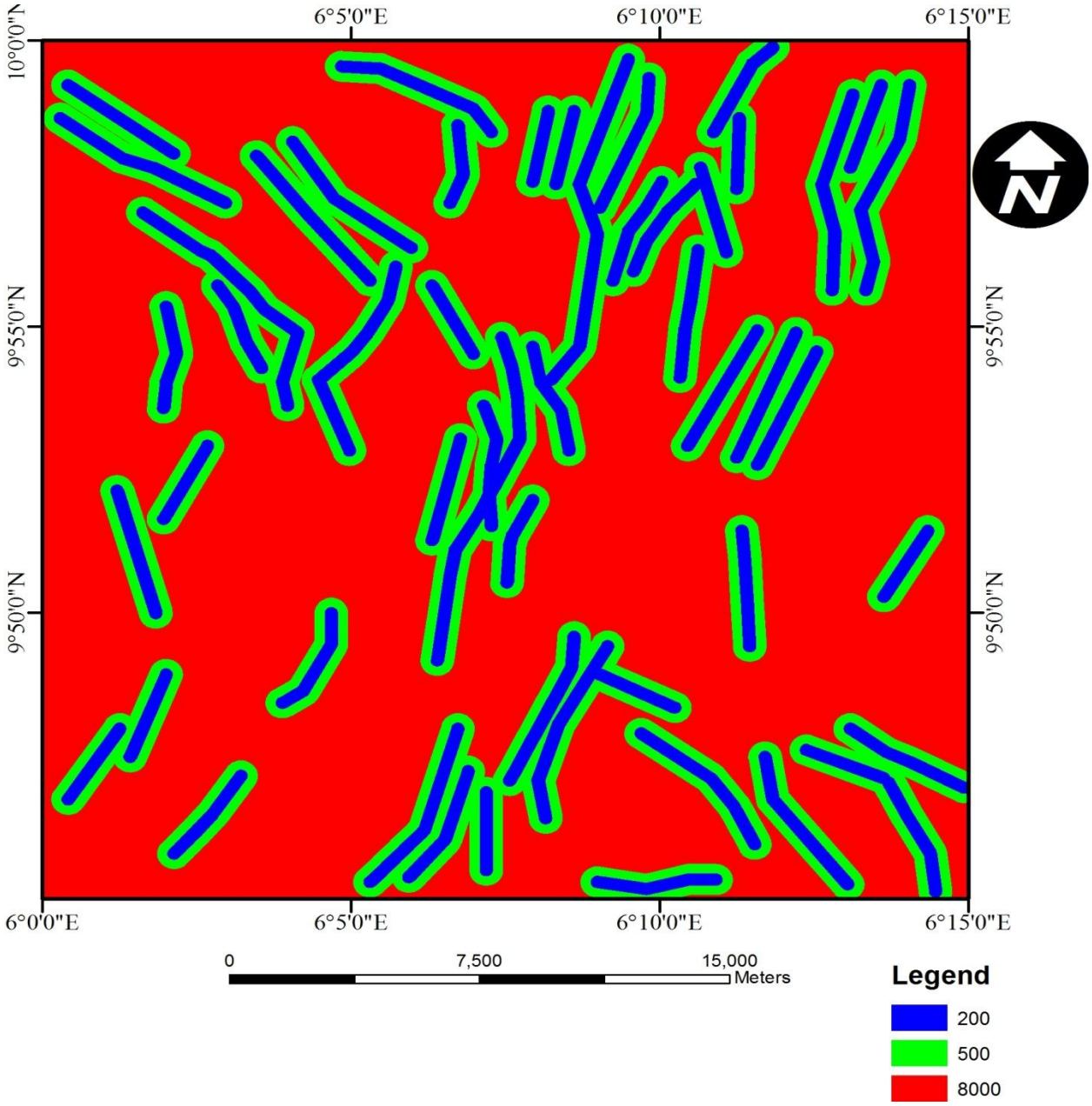


Figure 4.20: Buffered combined shaded relief image with azimuth directions 0^0, 45^0, 90^0, 135^0showing two main trend directions, with the predominance of NNE-SSW lineaments over the NNW-SSE directions.

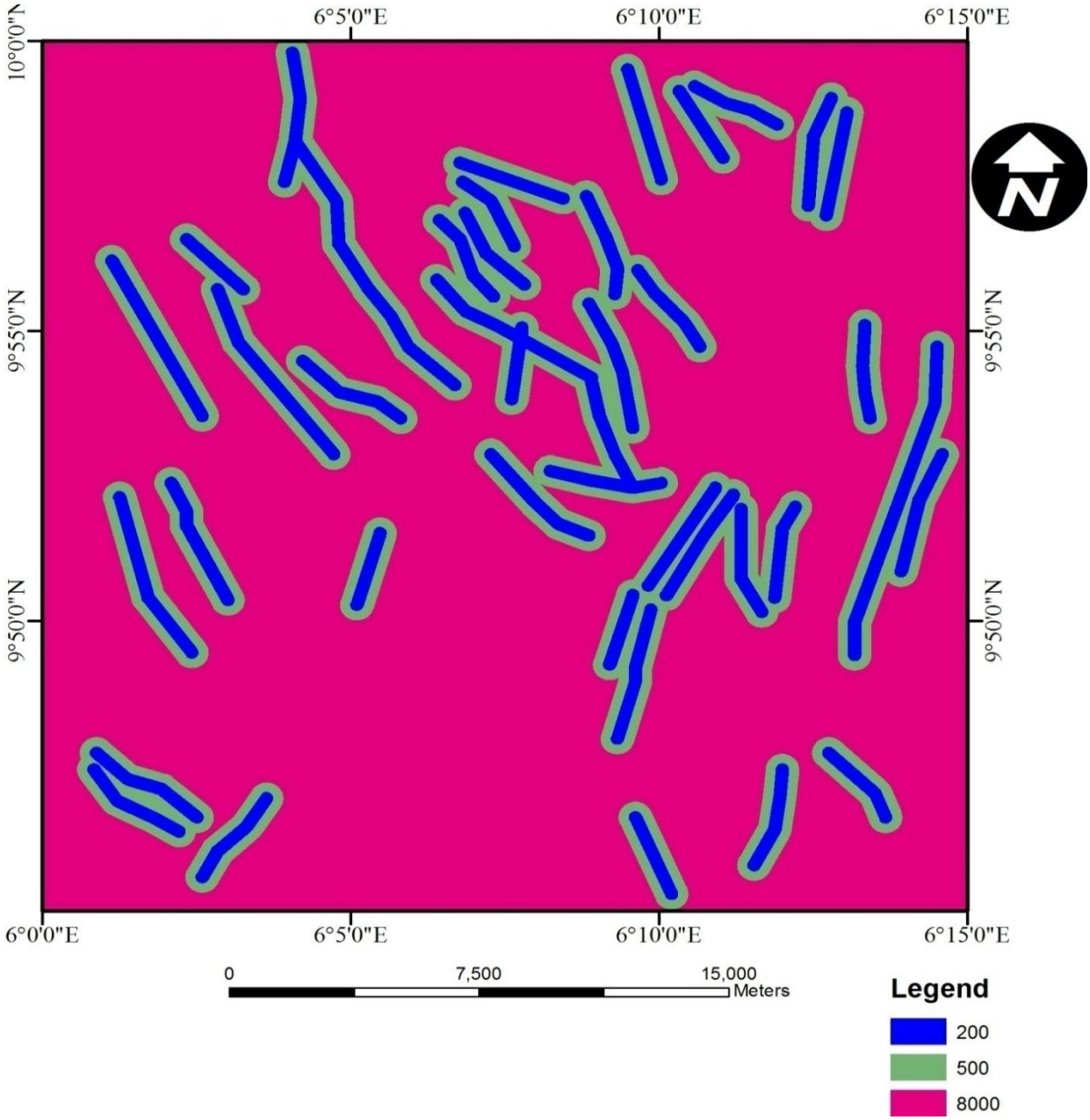


Figure 4.21: Buffered combined shaded relief image with azimuth directions 180^0, 225^0, 270^0, 315^0showing two main trend directions, with the predominance of NNW-SSE lineaments over the NNE-SSW directions.

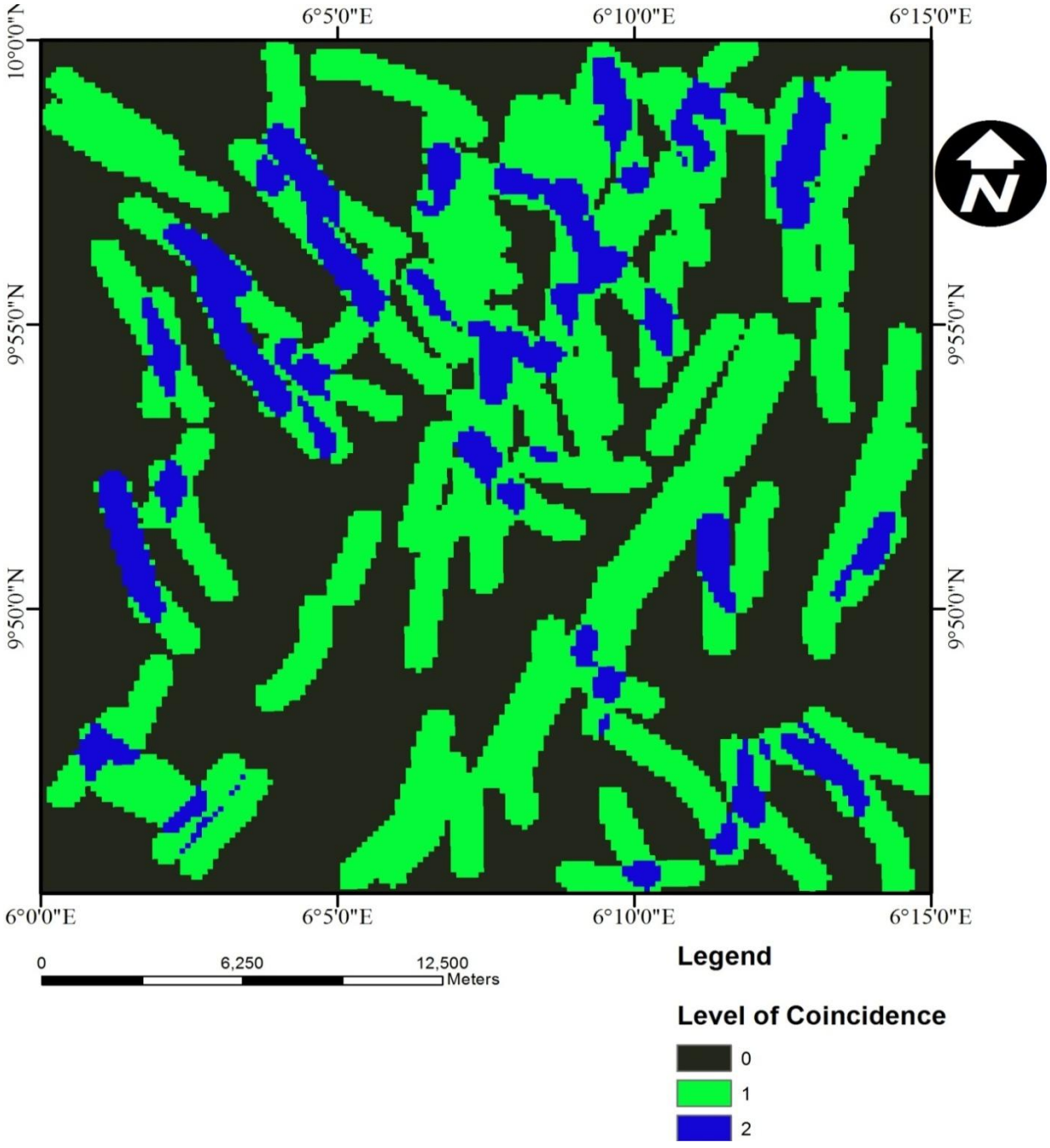


Figure 4.22: Level of coincidence for combined shaded relief images (0^0, 45^0, 90^0, 135^0) and (180^0, 225^0, 270^0, 315^0) showing the combination of lineaments from two shaded relief image to produce the general lineaments of the area.

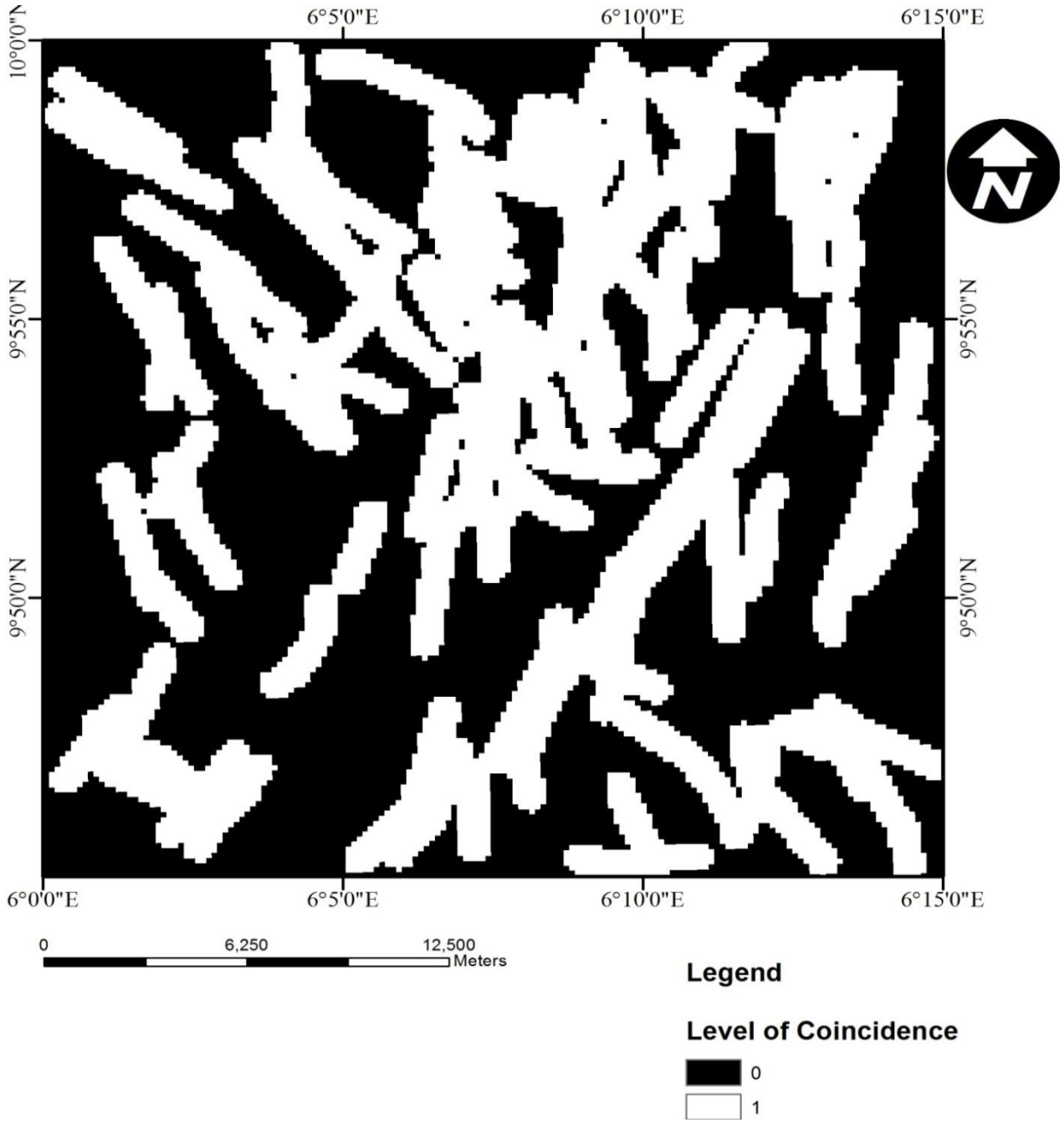


Figure4.23: Reclassified Level of coincidence for combined shaded relief images (0^0, 45^0, 90^0, 135^0) and (180^0, 225^0, 270^0, 315^0) displaying the all the lineaments in the study area in black and white colours for easy digitizing.

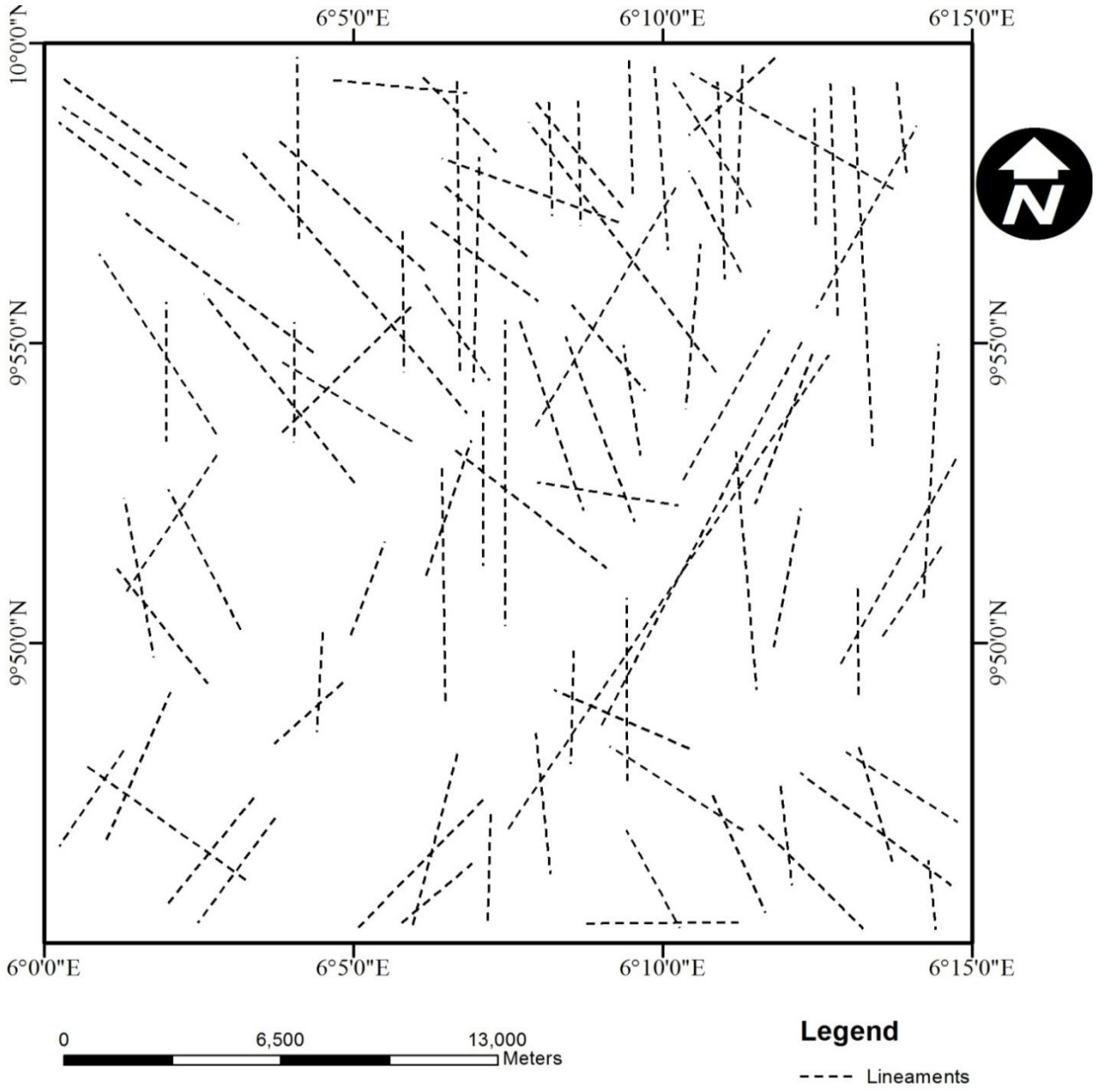


Figure 4.24:Final lineament map for the study area showing three major trends, with the predominance of N-S and NW-SE lineaments over the NE-SWlineaments.

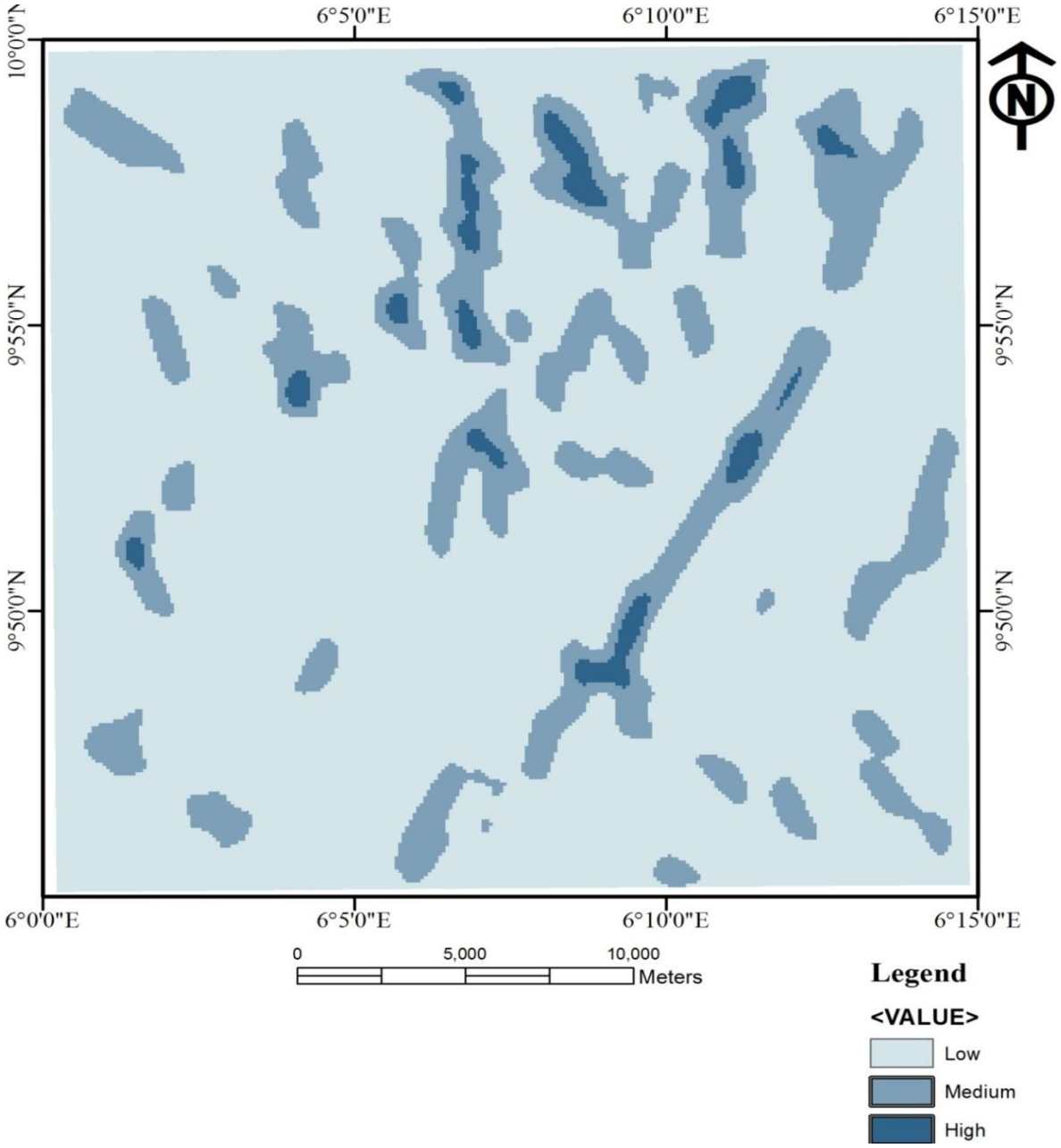


Figure 4.25: Lineament density map for the study area showing a high lineament density at the northern and central parts of the study area and a medium to low lineament density in other parts.

4.2 FIELD GEOLOGY AND PETROGRAPHY

4.2.1 PREAMBLE

The lithological units mapped during the field investigation comprise gneisses, migmatites, quartzites, phyllites, schists, amphibolites and mylonites (Fig. 4.26).Fresh rock samples were collected from the field and representative samples were selected for petrographic studies to determine their textural and mineralogical composition. In addition, oriented rock samples were also collected for strain analyses. JMicro vision Software v1.2.7 was used to estimate the modal composition of minerals in the slides prepared from representative rock samples (Table 4.1).

4.2.2 Gneiss

This rock covers about 25 to 30% of the area mapped. It is the main rock in places like Gulangi, Ushama, Jangaro and Kutuku. Gneiss in the study area has poor schistocity because of the preponderance of quartz and feldspars. It is well jointed and containsstructures like joints and several cross-cutting pegmatite veins. In some places, this rock is highly weathered and breaks easily utilizing foliation planes, while in other parts of the study area where itis in contact with the schists, it occurs as hilly, massive and low lying outcrop.

Generally, it is medium-to-coarse grained and usually grey (light) in colour, though the weathered varieties look grayish black on the surface. This rockhas high dips with dip angles ranging from 45 to 75^0.

Three varieties of gneiss are found in the study area. These are: (a) an augen gneiss (b) banded gneiss and (c) granitic gneiss.

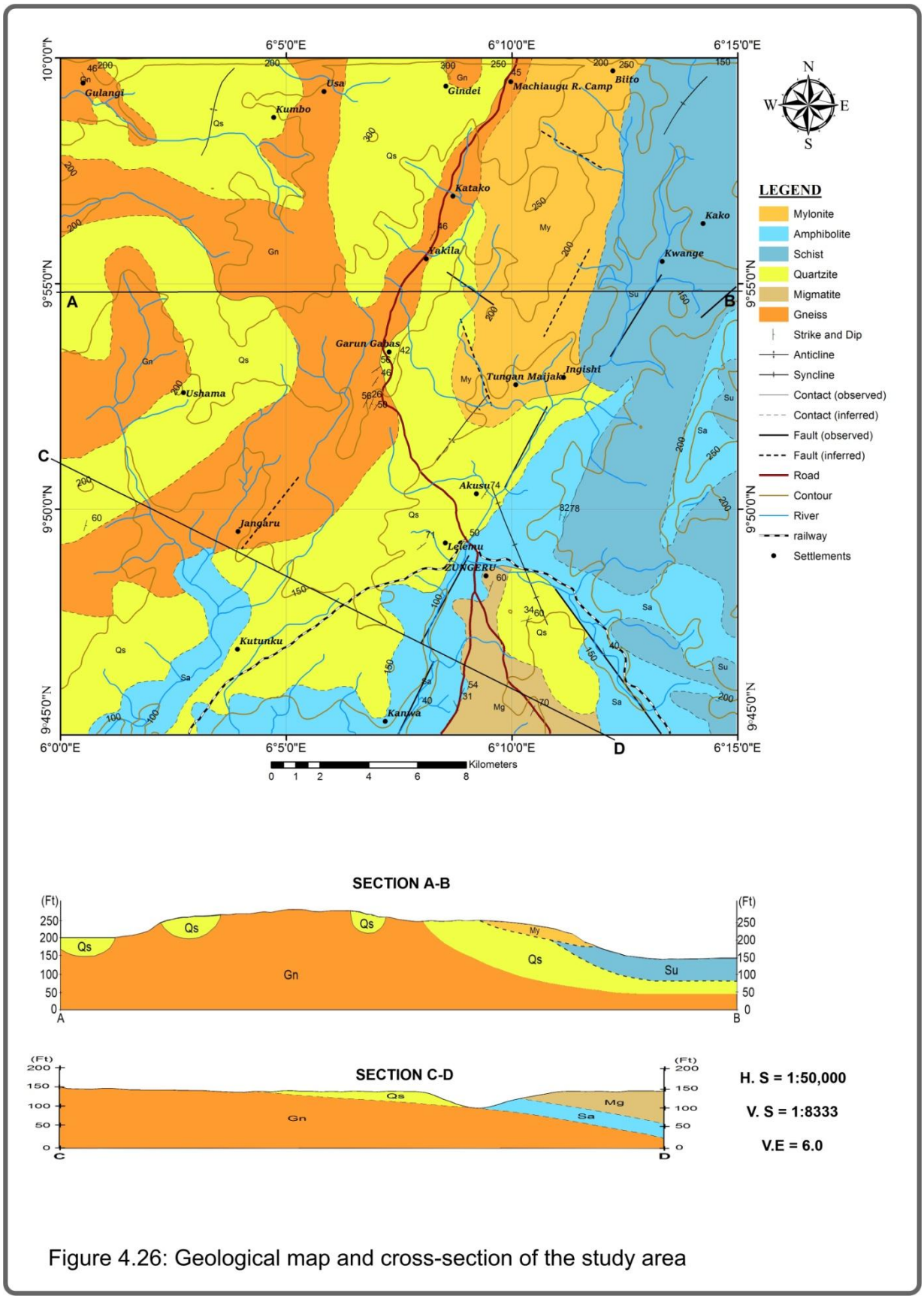


Figure 4.26: Geological map and cross-section of the study area

Table 4.1:Modal compositions in percentage (%) of the rocks from the study area (Based on JMicroVision Software v1.2.7)

Minerals	Rock Types							
	A	B	C	D	E	F	G	H
Quartz	30.00	42.86	14.71	26.27	99.99	16.05	39.09	44.87
K-feldspar	-	30.95	32.35	9.76	-	-	-	28.21
Plagioclase	41.00	-	8.82	15.20	-	10.53	-	-
Microcline	-	-	-	-	-	1.63	-	-
Biotite	12.60	4.77	36.00	12.20	-	5.58	-	17.95
Muscovite	6.38	9.52	5.88	-	-	17.26	50.57	8.97
Hornblende	-	-	-	19.51	-	-	-	-
Garnet	10.00	-	-	-	-	-	-	-
Augite	-	-	-	4.90	-	-	-	-
Chlorite	-	-	-	4.88	-	-	-	-
Epidote	-	4.76	-	2.44	-	-	-	-
Ilmenite	-	-	-	4.88	-	-	-	-
Opaque Mineral	-	7.14	2.24	-	0.01	3.95	10.34	-
Total	100	100	100	100	100	100	100	100

LEGEND:

A=Mylonitized Garnet Mica Schist

B=Augen Gneiss

C=Migmatite Gneiss

D=Amphibolite

E=Quartzite

F=Quartz-Feldspar-Mica Gneiss

G=Quartz-Muscovite-Phyllite

H=Garnet-Biotite Gneiss

I=Mylonitic Granite Gneiss

4.2.2.1 Augen Gneiss

This is a weakly mylonitized or sheared rock in which feldspar forms porphyroblasts or augen about which the rest of the rock has been deformed. Mineralsin this rock generally have large grain size.Feldspars form mineral sub-horizontal lineations in some places (Plate I). The dominantconstituent of this rock are quartz, biotite and orthoclase feldspar, while muscovite, epidote and opaque minerals occur as matrix as well as minor minerals in slide Stn 4 (Plate II).



Plate I: A photograph of augen gneiss showing feldspar mineral lineation around Garun Gabas. Location: (9° 52' 21.1" N, 6° 06' 46.3" E).

Under plane polarized light, orthoclase crystals in this rock are subhedral to euhedral in shape, with low relief while in XPL (Stn 4). It is heterogeneous, cloudy and some crystals even show simple twining. Epidote constitutes a small percentage of this rock, occurring at the southern portion of the slide with a high birefringence and an interference colour ranging from small patches of yellow to soapy green colour.

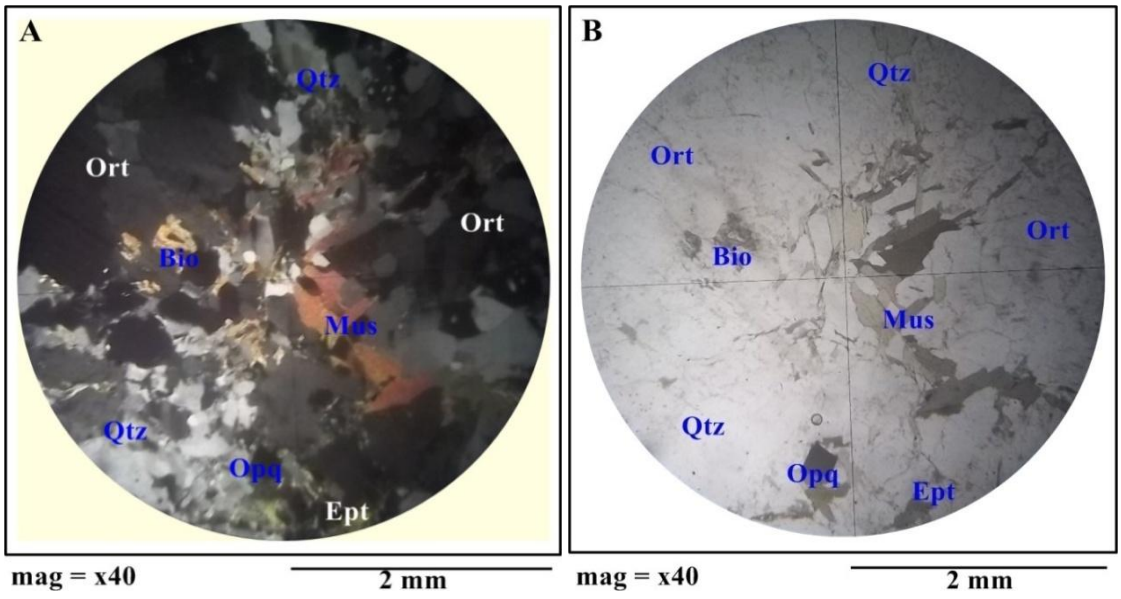


Plate II: Photomicrographs of augen gneiss. (A) View in XPL. (B) View in PPL. Qtz=quartz, Mus=muscovite, Bio=biotite, Opq=opaque mineral, Ort=orthoclase, Ept=epidote(Slide no: Stn4).

4.2.2.2 Banded Gneiss

The foliation in this rock is defined not only by the parallelism of the biotite crystals, but by the segregation of coarse leucosome of quartz and feldspars into separate layers (Plate III). The major minerals in this rock are quartz, muscovite and plagioclase while biotite, microcline and opaque minerals form the minor constituents.

Plagioclase in this rock is euhedral to subhedral, colourless with low relief and displays a distinct polysynthetic twining. Colourless to greyish, anhedral shape microcline displays cross-hatched twining in XPL (Plate IV).

Muscovite is abundant in this rock. It is colourless and has a moderate to high relief. The muscovites crystals are aligned in an N-S or E-W direction when the stage is rotated and goes into parallel extinction. Muscovites also form traces of micro folds in this rock in slide Stn 11 (Plate IV).



Plate III: A photograph of banded gneiss north of Zungeru town. Location: (9° 49' 57.9" N, 6° 10' 25.2" E).

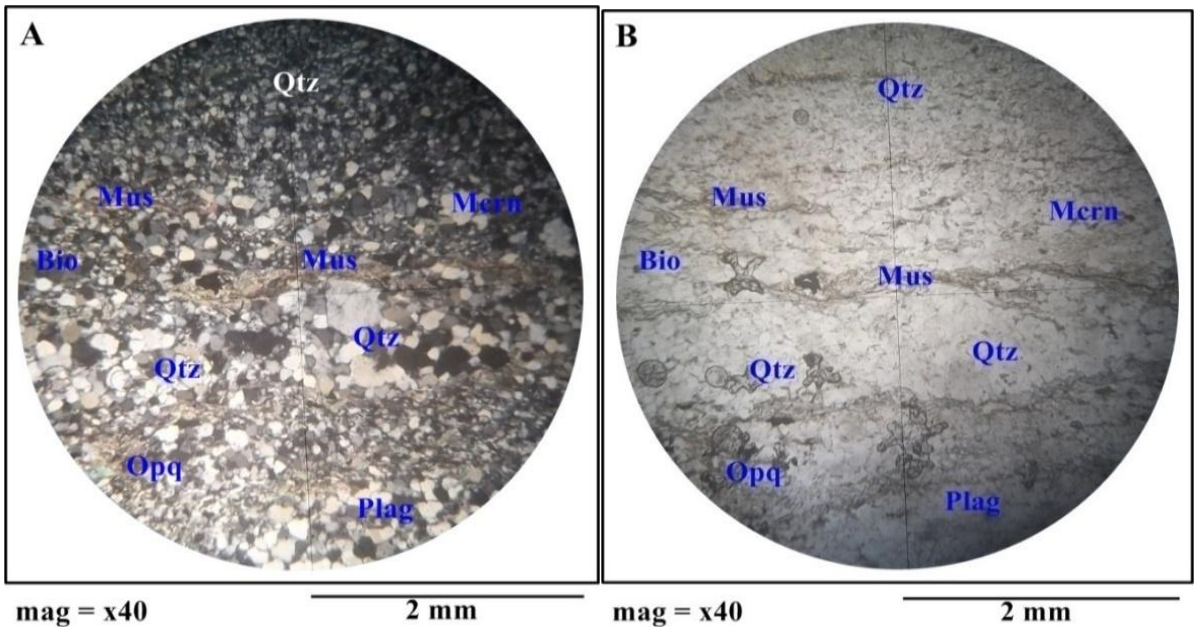


Plate IV: Photomicrographs of Banded Gneiss. (A) View in XPL. (B) View in PPL. Qtz=quartz, Mus=muscovite, Bio=biotite, Opq=opaque mineral, Plag=plagioclase, Mcrn=microcline(Slide no: Stn11).

4.2.2.3 Granite Gneiss

This rock type was observed in only one location within Zungeru town (Plate V) and could not be represented on the geologic map. It is a distinctive medium-to-coarse grained porphyroblastic rock. It is light grey in colour, with a NNE-SSW orientation and dips to the east. Analysis of photomicrograph (Plate VI) of this rock shows that intense deformation has disrupted original K-feldspar phenocrysts to produce porphyroclasts with patchy extinction and fracturing. Quartz occurs in recrystallized layers separated by segregations of biotite and muscovite. Smaller grains of quartz also form the groundmass of this rock.



Plate V: Photograph of a Granite Gneiss outcrop in Zungeru townwith a distinct quartz vein. . Location: (9° 48' 18.0" N, 6° 09' 31.5" E).

Quartz is the most abundant mineral in thin-section. It is light coloured and comprises of subhedral to anhedral crystals. Quartz crystals have a low relief and undergo extinction at 50^0.

Also observed within quartz grains are micro fractures which are intra granularas seen in slide Stn 24 (Plate VI).

Biotite appears pale to greenish brown. The crystals are subhedral in shape and have a moderate relief. They exhibit properties of pleochroism and a perfect cleavage. Biotite undergoes extinction at an angle of 60^0 (Plate VI).

In thin-section, Orthoclase is the second most abundant mineral. It is grey in colour, has a low relief and subhedral in shape. This mineral shows characteristic simple carlsbald twinning and zoning (Plate VI).

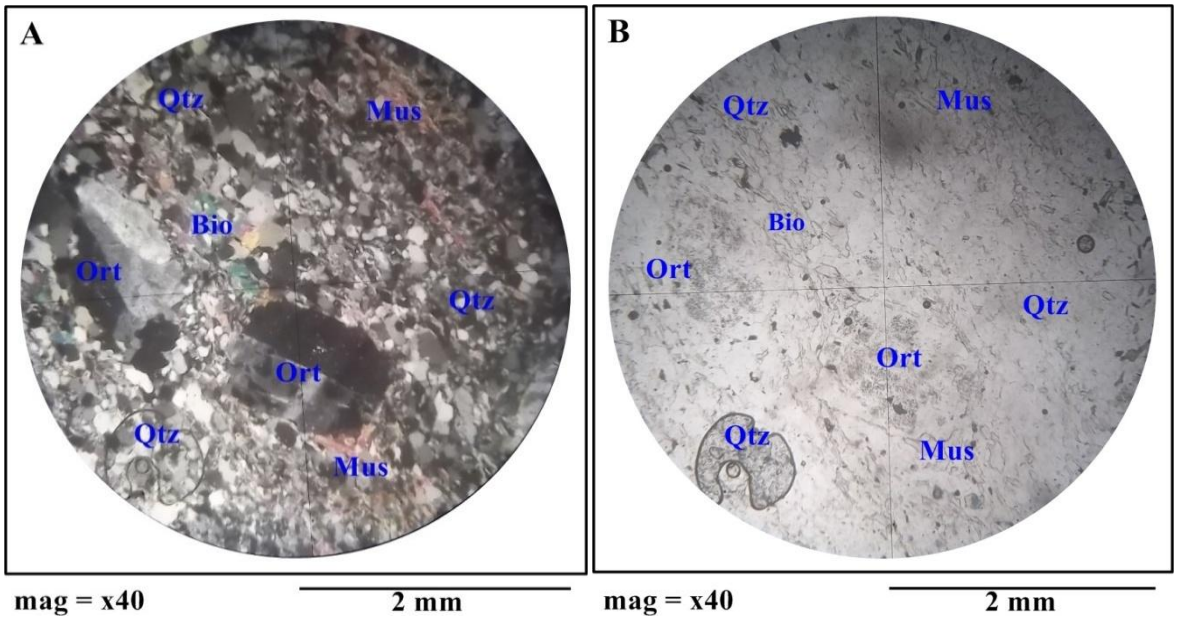


Plate VI: Photomicrographs of Granite Gneiss. (A) View in XPL. (B) View in PPL. Qtz=quartz, Mus=muscovite, Bio=biotite, Ort=orthoclase, Mcrn=microcline(Slide no: Stn24).

4.2.3 Migmatite

Migmatite is mapped only in few locations, mainly in the southeastern part of the study area(Fig. 4.26). They are not as extensive as the other rocks found within the study area. It is limited in occurrence and more concentrated in Jankwata and Dogon Ruwa areas.The migmatite is

adistinctively banded medium grained rock and grayish in colour (Plate VII). The migmatitic banding is regular in form and consists of two components – a palaesome and a neosome. Some exposures occur as flattish outcrops, inhomogeneous and consist of schistose, gneissose and granitic component.



Plate VII: Photograph of a flat-lying Migmatite-Gneiss outcrop around Dogon Ruwa with light and dark bands. Location: (9° 46' 48.0" N, 6° 12' 1.6" E).

Ptygmatitic folding occurs in vein-like structure with quartz-filled mineral composition. At some places, this rock dip at a very high angle, almost vertical.The migmatite consists of a coarse leucosomes of k-feldspar, plagioclase and quartz and melanosomes of biotite, muscovite and probably opaque oxide minerals as depicted in slide Stn 9 (Plate VIII).

In PPL view, the rock contains very abundant brown elongated biotite dispersed all over having preferred orientation. Biotite crystals have moderate relief, anhedral in shape, one perfect cleavage and are pleiochroic, ranging from light brown to dark. In XPL, it has a moderate birefringence and an interference colour of dark brown with patches of dark purple.

Muscovite, quartz and plagioclase feldspar form the matrix minerals in this rock while distinctively abundant, heterogeneous and cloudy orthoclase with very large grain size stands out in the ground mass. The plagioclase feldspars are well-formed, six-sided euhedral shaped, with well-defined albite twinning.

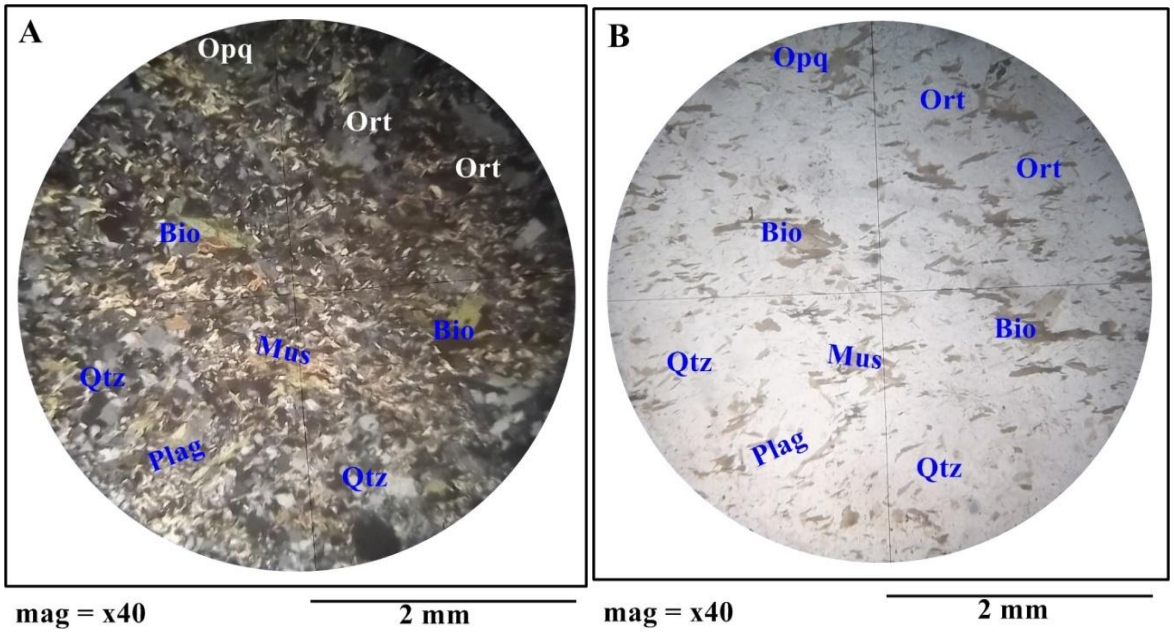


Plate VIII: Photomicrographs of migmatite sample. (A) View in XPL. (B) View in PPL. Qtz=quartz, Bio=biotite, Ort=orthoclase, Opq=opaque mineral, Mus=muscovite, Plag=plagioclase(Slide no: Stn9).

4.2.4 Quartzite

Quartzite is the most widespread and constitute about 40% of the rocks in the area of study. The dip angles on quartzite outcrops range from 35 to 65^0 to the East.The quartzite rarely occurs as a

single body of rock, but as pebbles and boulders of different shapes and sizes on most of the hills and surrounding areas.

Two types of quartzite were found in the study area, which are the whitish to light brown massive type(Plate IX) and the reddish brown, fine to medium grained schistose variety.Under River Kaduna Bridge at Kundu, there areoccurrences of reddish brown, fine to medium grained schistose meta-quarzite, which are highly deformed and sheared. Here, a sharp contact was observed between quartzite and amphibolite rocks.



Plate IX: A Photograph of whitish massive quartzite outcrop at Garun Gabas. Location: (9° 51' 25.5" N, 6° 07' 37.5" E).

Thin-section view of this rock shows (Stn 2) the tight packing and recrystallization of quartz grains characteristic of quartzite (Plate X). The brownish and purple colour of the quartz crystals

in Cross Polarized Light is probably due to the thickness of the thin-section slide which is a little bit higher than the normal thickness required.

Quartz is subhedral in shape; fine to medium grained and occurs as porphyroclasts. The quartz crystals are colourless, have a low relief and exhibits wavy, undulose extinction with extinction angles ranging from 50^0 – 60^0. Some of the quartz crystals formed grains that have sutured boundaries and are polycrystalline in nature.

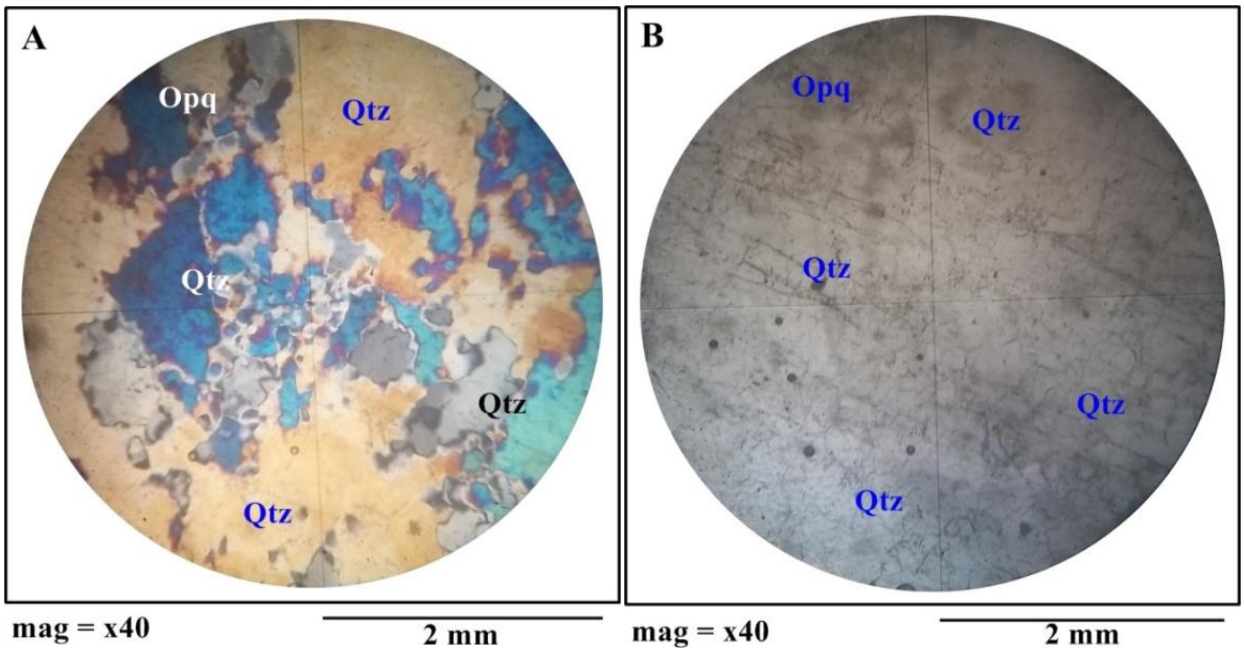


Plate X: Photomicrographs of Quartzite. (A) View in XPL. (B) View in PPL. Qtz=quartz and Opq=opaque mineral(Slide no: Stn2).

4.2.5Phyllite

Pyllite is not well exposed in the study area and cannot be represented on the map. It occurs generally as low lying rocks that is highly weathered, foliated and fractured so much that they could be broken with bare hands (Plate XI). The schistocity is defined by a very strong preferential alignment of phyllosilicate minerals. These platy and prismatic minerals are aligned

such that they form a weak compositional banding. The rock varies in colour from brown to dark grey. Fragments of phyllite and quartzite were observed within the vicinity of fault zones.



PlateXI: Photograph of phyllite with distint S_1 cleavage planes. Location: (9° 48' 18.8" N, 6° 09' 31.5" E).

Major minerals in this rock (Stn 25) are muscovite and quartz while the minor ones are the opaque minerals (Plate XII). There is an enormous amount of white mica (muscovite) constituting about 50% of this rock (Table 4.1). It has an interference colour ranging from green to pink; a perfect cleavage and a high birefringence.Quartz is anhedral in shape; fine to medium grained and occurs as porphyroclasts. The mineral is colourless, has low relief and exhibit wavy, undulose extinction with extinction angles ranging from $50 – 60^0$.

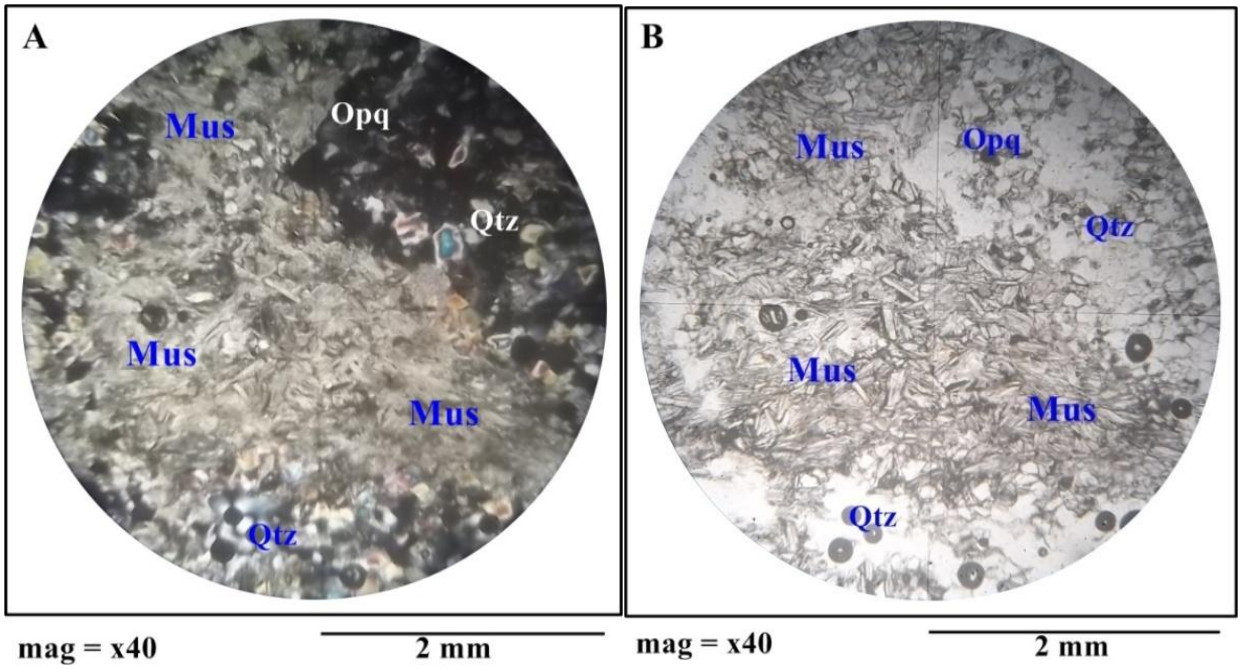


Plate XII: Photomicrographs of Quartz-Muscovite-Phyllite. (A) View in XPL. (B) View in PPL. Qtz=quartz, Mus=muscovite, Bio=biotite, Gnt=garnet, Opq=opaque mineral(Slide no: Stn25).

4.2.6Garnet Mica Schist

Garnet mica schist covers about 10-15% of the total area mapped (Fig. 4.26). It is a soft, highly weathered and friable rock. It is generally poorly exposed. In hand specimen, it is brown to light grayish in colour, and fine to medium grain in texture. The rock consists dominantly of plagioclase feldspar, quartz, garnet, biotite and muscovite. It has high dip angles with their entire foliation planes dipping from 30 to 74^0dominantly to the west (Plate XIII). Intense strain of the parental garnet mica schist has produced a mylonite from this rock in shear zones within the study area.

Garnet grains are small and anhedral with some minute opaque minerals which could be ilmenite embedded in it as evident in plane polarized light (PPL) view of slide Stn 1. In cross polarized light(XPL), the mica rich-layer and bands of quartz and feldspar show a pronounced diagonal segregation (Plate XIV).



Plate XIII: Outcrop of schist dipping to the west found around Tungan mai-jaki. Location: (9° 52' 45.4" N, 6° 10' 59.8" E).

Relatively rigid garnet survived as abraded relics or porphyroclasts while quartz, feldspar and the micas depict a tectonic foliation that is aligned roughly NE-SW, which resulted from compositional segregation, normally into leucocratic and melanocratic layers respectively.

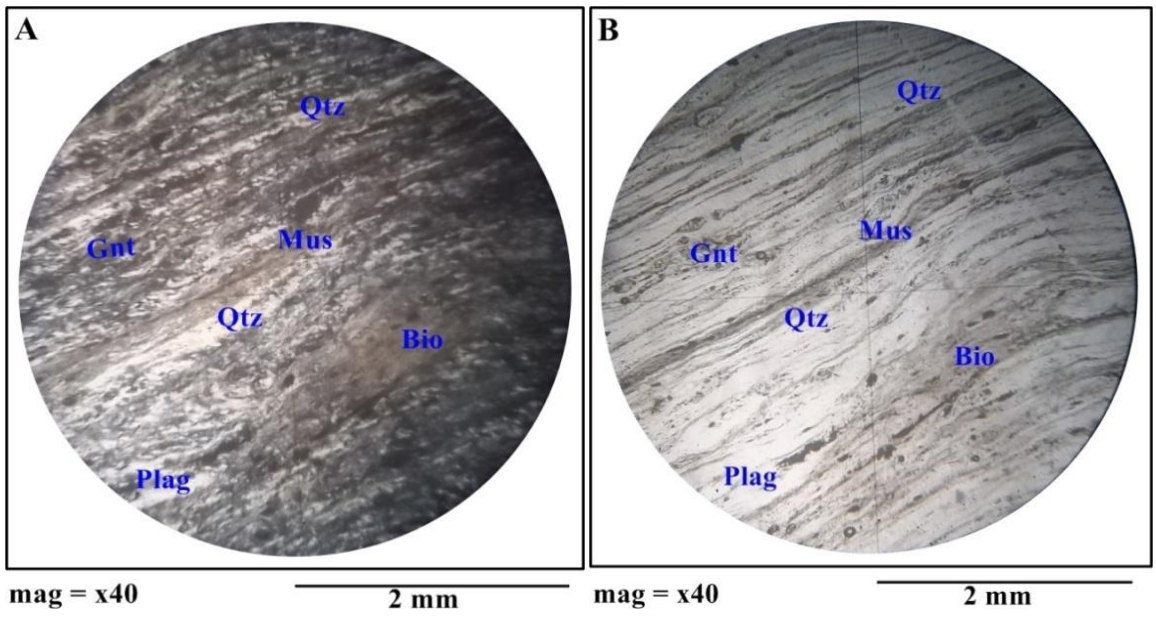


Plate XIV: Photomicrographs of garnet-mica schist. (A) View in XPL. (B) View in PPL. Qtz=quartz, Mus=muscovite, Plag=plagioclase, Bio=biotite, Gnt=garnet(Slide no: Stn1).

4.2.7Amphibolite

Good exposures of amphibolite are found in the channel of River Kaduna at Zungeru. It is black to dark-green in colour, fineto medium grained in texture and has distinct cleavage planes in some exposures. Quartz veins can be seen running sub-parallel to the strike line.In some places, the contact of the amphibolite with surrounding rocks, are often marked by development of cataclastics and mylonites as a consequence of a major fracture zone within the area and minor shear zones (Plate XV).In some places, there exist an interlayered contact between quartzite, phyllite, schist and amphibolites.



Plate XV: Photograph of an amphibolite outcrop east of zungeru found along a fault zone. Location: (9° 47' 31.2" N, 6° 10' 21.7" E).

The dominant mineral constituents of this metabasic rock are hornblende, plagioclase and quartz (Plate XVI). Plagioclase, biotite and augite occur as larger grains, while smaller grains of quartz

and plagioclase form the groundmass. Small grains of opaque ilmenite occur throughout the rock, and other minor phases present are chlorite and epidote.

Hornblende forms relatively small discrete prisms. It is pale geen in colour, has good cleavages (57^0-60^0) and low to moderate birefringence.

Plagioclase occurs in this rock as subhedral crystals with a broad and well-developed albite twinning. It has a higher relief than quartz and then tends to be equant and unzoned.

Augite has a dark-green interference colour and it is easily distinguished by its double cleavage characteristic at angle of about 87˚ and 93˚.

Biotite in this rock has the typical mica habit (001) cleavage, high birefringence and goes into parallel extinction. It has low to moderate relief and extreme pleichroism. Its dominant colour under XPL is yellowish-brown and its interference colour ranges from soapy-green to purple to yellow to brown.

Epidote is less abundant in this rock. It has a distinctive yellowish green colouration and a perfect cleavage. Some of these minerals form crystals elongated along the b axis.

4.3.8 Fault Rocks

The rocks of the study area are transverse by a major dextral transcurrent fault zone, the Kalangai-Zungeru-Ifewara fault system (KZI) and a number of other minor shear zones. This is shown on a regional scale as well as at outcrop scale. The KZI fault system has affected the rocks in the area through dynamic metamorphism marked by mylonites, sheared gneiss, and cataclasite quartzites (Plate XVII and Plate XVIII). These cataclastic rocks are considered to have been derived from earlier basement.

They are rocks of granitic or gneissic protolith. Some are formed from the changes in the physical properties of quarzites, amphibolites and schists. In some places, the mylonitic rocks are intercalations of amphibolites with quartzites. These rocks are medium to very fine grained and grey in colour. The rocks are fracturedwhile most of the joints are healed by quartz veins. They are not normally well exposed, and never form prominent topographic features. There are however good exposures in the gorge of River Kaduna.

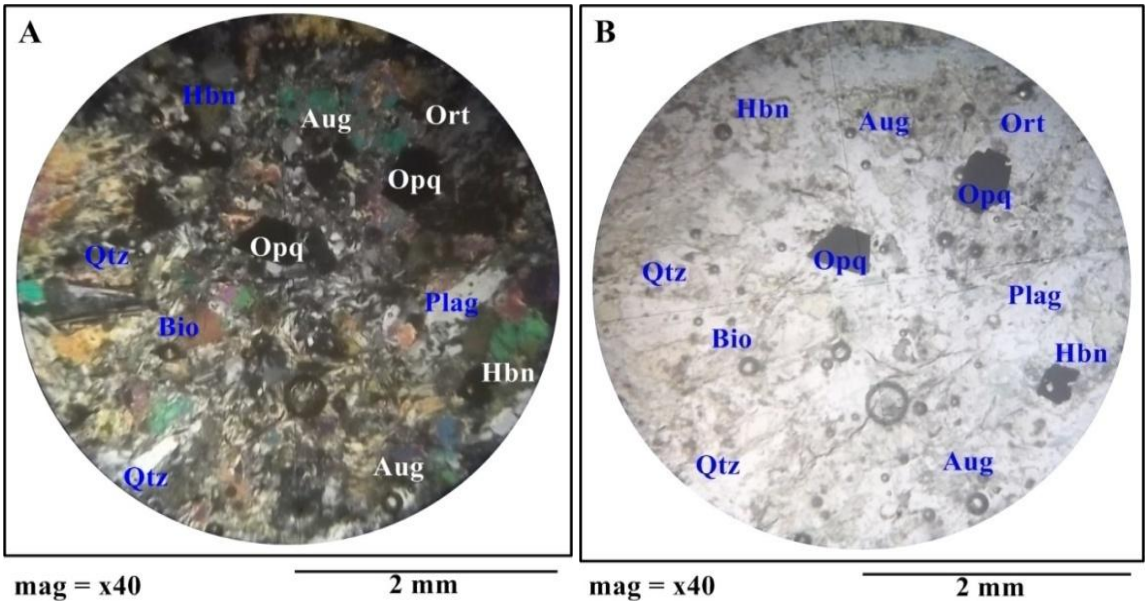


Plate XVI: Photomicrographs of amphibolite. (A) View in XPL. (B) View in PPL. Qtz=quartz, Bio=biotite, Ort=orthoclase, Aug=augite, Opq=opaque mineral, Hbn=hornblende, Plag=plagioclase (Slide no: stn8).

4.4 GEOLOGIC STRUCTURES

4.3.1 Preamble

The planar and linear structures resulting from both ductile and brittle deformation events have been identified and described in this section. This investigation covered megascopic, mesoscopic and microscopic structures.

In most cases, most of the ductile structures identified were deformed by folds. The style of folding, the difference in orientation in both planar and linear structures and overprinting relationships have allowed for the classification of these structures.

The symbols used for the structural classifications are: D for deformation events, F for folds, S for foliations and L for lineations. Relative ages of events are designated by subscript numbers, starting with the oldest. As such, all the ductile structures have either been classified into an earlier D_1 structure or a latter D_2 structure.



Plate XVII: Photograph of mylonitic garnet mica schists dipping to the westand scattered chuncks of cataclastic quartzite all within a shear zone in the study area. Location: (9° 52' 18.3" N, 6° 07' E).



Plate XVIII: Photograph of sheared gneiss within a shear zone in the study area trending NNE-SSW and dipping to the west. Location: (9° 53' 26.9" N, 6° 07' 17.2" E).

4.3.2 Folds

Even in the fairly well exposed areas, outcrops are few to enable the form of major folds to be traced. Some of the folds were deduced from opposing dips, therefore the tectonic analysis of the region is consequently based primarily on small-scale structures.

F_1 is the first generation of folding in the area. A well-developed axial plane cleavage is typically associated with these folds. F_2folds were generated due to the rotation andbending of the S_1 foliation along shear zones as depicted by folded quartz mineral vein in Plate XIX and Plate XX. These types of folds are distinguished from F_1 folds as they are associated with crenulation cleavages(Plate XXI). The F_2 folds were superposed over the F_1 folds and produced thefold interference patterns in migmatites.

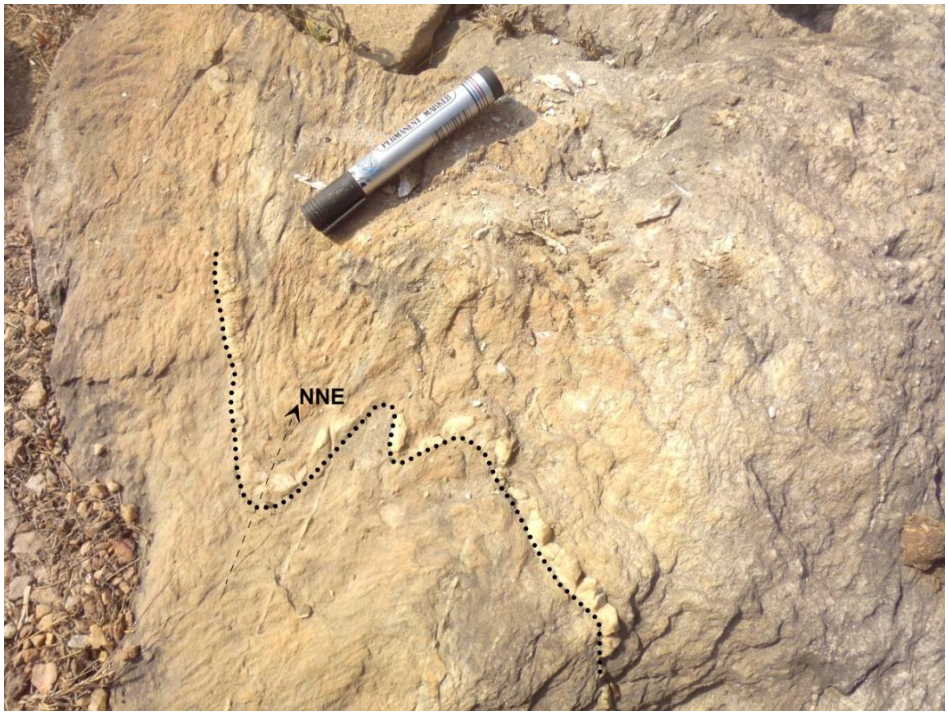


Plate XIX: Photograph of mica schist with refolded F_2 "S-fold" oriented NNE depicting the right-limb of a major F_2 fold. Location: (9° 48' 18.0" N, 6° 09' 31.5" E).



Plate XX: Photograph of amphibolite outcropwith quartz vein forming almost N-S open to isoclinal F_2 fold. Location: (9° 47' 23.0" N, 6° 09' 9.0" E).

4.3.3 Primary Foliations (S_0) and Cleavages

In many cases the primary foliation (S_0) is parallel to the first secondary foliation, S_1. Large parts of the primary foliations (S_0) have been affected by later deformations, but they are locally preservedin weakly deformed rocks.

The first recognized planar fabric in the gneisses, migmatites and associated metasediments is designated S_1. This cataclastic foliation is prevalent in the basement rocks like gniess and it is an axial planar foliation with a major orientation of (296/84)(Fig. 4.27A-B). The S_1 cleavage and the mineral content is related to the originof the deformed rocks, as a result in basic and ultrabasic rocks thisfoliation appears as a disjunctive cleavage and in metasedimentaryrocks as a schistosity.

The S_1 foliation was refolded by a later phase of progressivedeformation so that its traces remain as internal foliation in the external S_2 foliation.This S_2 foliation appears as amylonitic foliation in highly deformedmylonitic garnet mica schist. S_2 is a penetrative foliation which intenselyaffected the S_1 foliation (Plate XXI). It is normally inclined to S_1 but in highlydeformed basement rocks in the study area.These two foliations became parallel to produce anS_1–S_2 composite foliation.During D_2 deformation, S_1 foliation was folded by F_2 folds andS_2 developed parallel to the axial planes of the folds.

4.3.4Lineations

Lineations are identified by the line formed due to the intersection of cleavage on the bedding plane (Plate XXII) and in some cases, the parallelalignment of minerals such as quartz, biotite and feldspar porphyroclasts. L_1 linear fabric which is the first generation lineation is closely associated with the S_1 foliation. L_2 appears inthe form of a stretching lineation or sometimes mineral lineation.This lineation is generated parallel or sub-parallel to the axis ofthe F_2 folds.

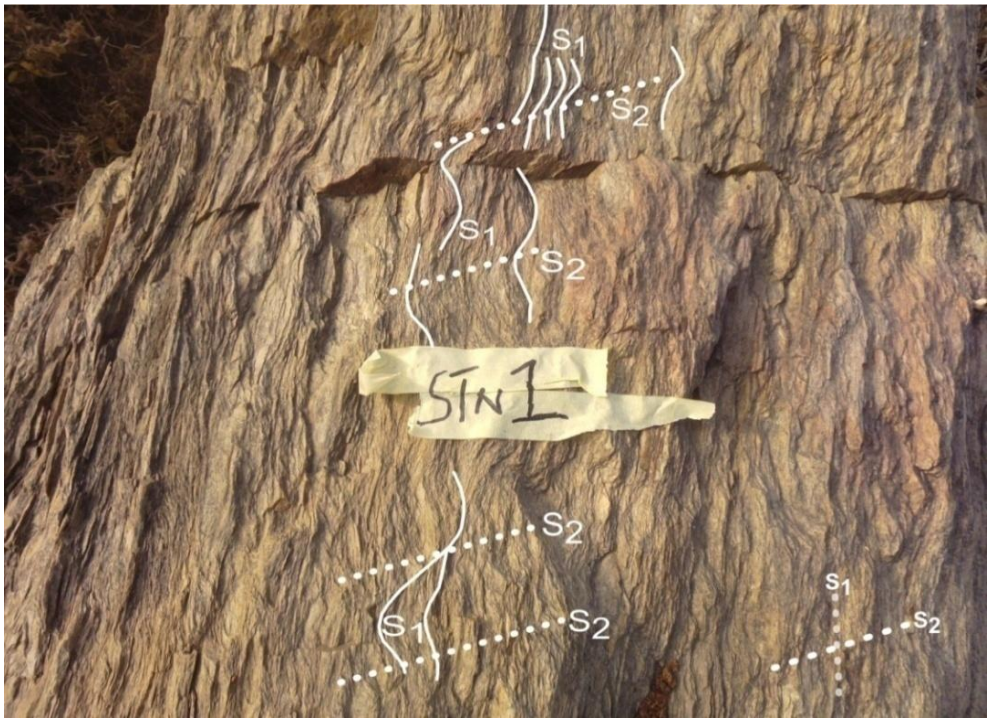


Plate XXI: Crenulation cleavages on garnet mica schist showing S_1 and S_2 foliations. Location: 9° 52' 18.3" N, 6° 07' E.

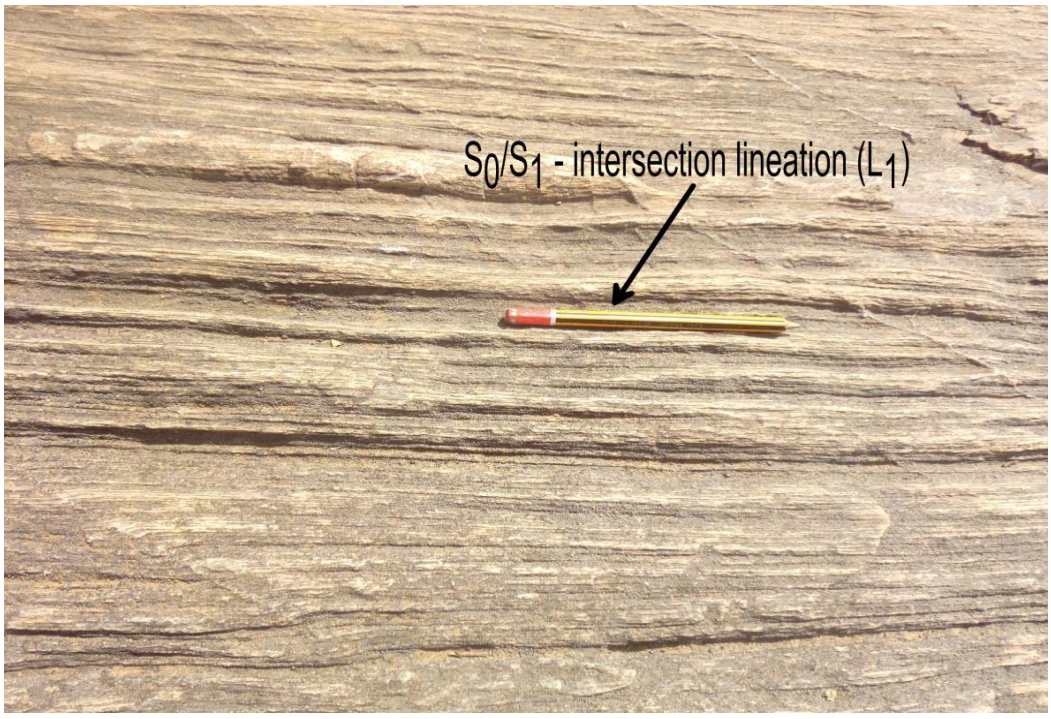


Plate XXII: Photograph ofL_1 intersection lineation on outcrop of gneiss at akusu. Location: 9° 49' 57.9" N, 6° 10' 25.2" E.

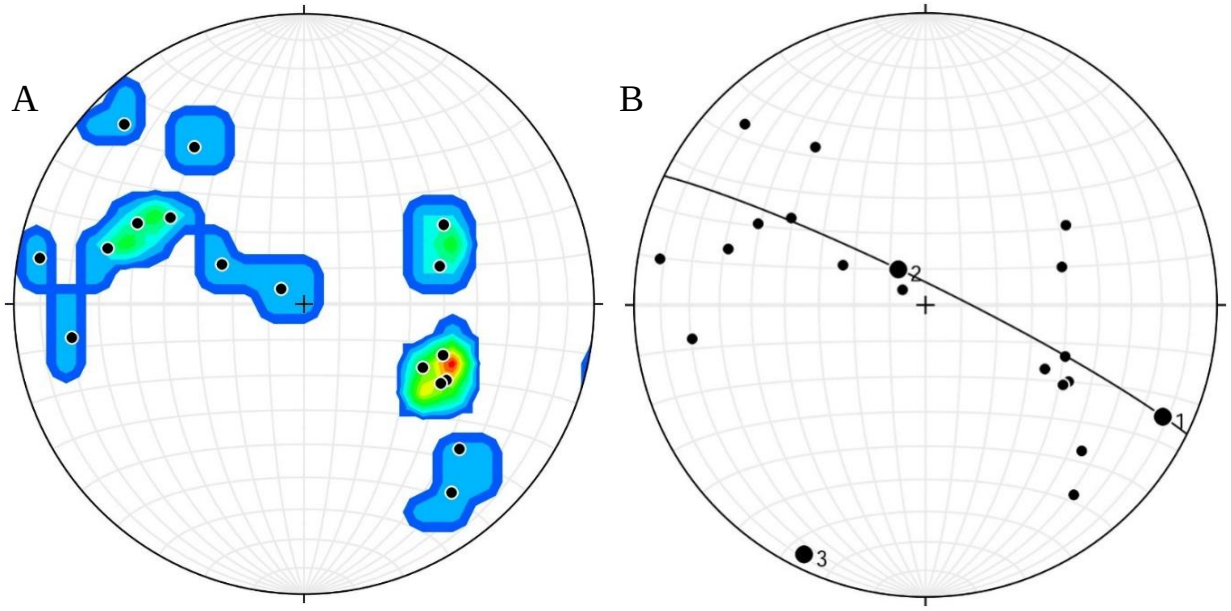


Figure 4.27: (A) Stereonet projection of S_1 cataclastic foliations represented on a lower hemisphere Schmidt net. (B) Poles to cataclastic foliation, S_1(lineation data) plotted on contoured Schmidt net.

4.3.5 Faults

A fracture becomes a fault when the rocks and constituent linear features are displaced. The sense of movements can be deduced from the displacement of structural markers, and/ or abrupt contacts of different rock units. The major type of fault seen in the field is the strike-slip fault, mostly at an outcrop scale (Plate XXIII). This type of transcurrent fault was also clearly seen and traceable on satellite images where they exhibit a dextral sense of movement (Fig. 4.32).

4.3.6 Joints and Veins

Lineaments not identified on Landsat images are assumed to be narrow in width and short in length. These are mapped as joints. The joints in the area fall into two categories of jointing systems which are the orthogonal system and the conjugate system (Plate XXIV).



Plate XXIII: (A) An outcrop scale strike-slip fault with sinistral sense of shear. Location: 9° 52' 45.4" N, 6° 07' 5.6" E.

Veins are simply fractures filled with mineral crystals that precipitated from watery solution. In the study area, quartz is the most common vein fill forming En echelon vein arrays in some places (Plate XXV).En echelon veins herein, seem to have formed as a result of shear within rock bodies associated with displacement across a fault/shear zone.

Joint orientation measurements were taken from different outcrops in the field in order to determine the dominant joint orientations and densities using rose diagram and statistical method known as the circle inventory method (Table 4.2-4.5).



Plate XXIV: Outcrop scale orthogonal joint system on granite gneiss at Zungeru town.Location: 9° 48' 18.0" N, 6° 09' 31.5" E.



Plate XXV: Photograph of gneisswithEn echelon sigmoidal quartz veins defining a dextral shear zone.Location: 9° 47' 58.9" N, 6° 04' 55.7" E.

Table 4.2: Circle-inventory for evaluating joint density in Augen Gneiss

Station #4, Augen Gneiss **Radius of Inventory Circle = 37cm;** **Area = 4301cm^2**	
Trend of Joint	**Length of Joints (cm)**
N42W	90
N84W	60
N54W	68
N38E	70
N70W	158
N52E	125
N30E	16.7
	587.7cm = Cumulative Fracture Length

Joint Density = $\frac{587.7cm}{4301cm2}$ = 0.14cm^{-1}

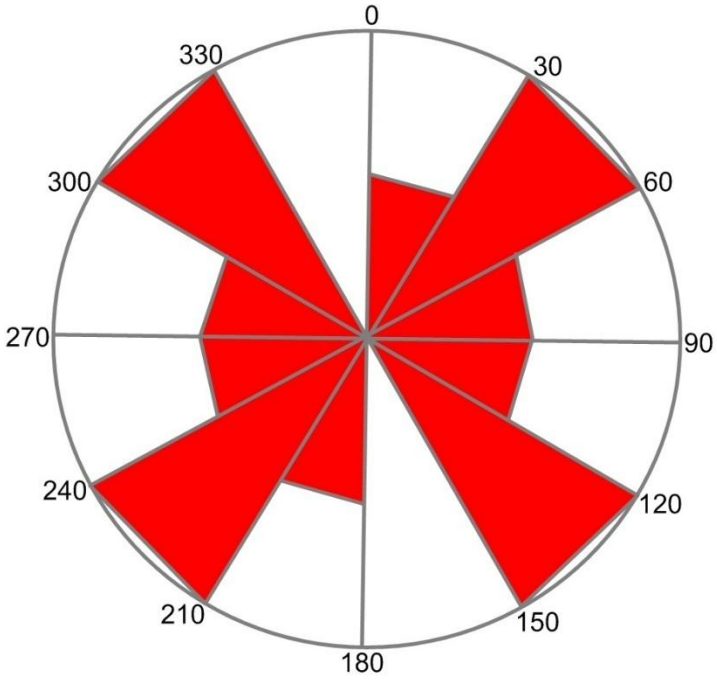


Figure 4.28: Rose diagram showing the dominant orientations of joint in augen gneiss

Table 4.3: Circle-inventory for evaluating joint density in quartzite

Station #7, Quartzite **Radius of Inventory Circle = 37cm;**	**Area = 4301cm^2**
Trend of Joint	**Length of Joint (cm)**
N38W	104
N44W	96
N23W	60
N35E	51
N8E	49
N56W	94
N35W	38
N39E	53
	545cm = Cumulative Fracture Length

Joint Density = $\frac{545cm}{4301cm2}$ = 0.13cm^{-1}

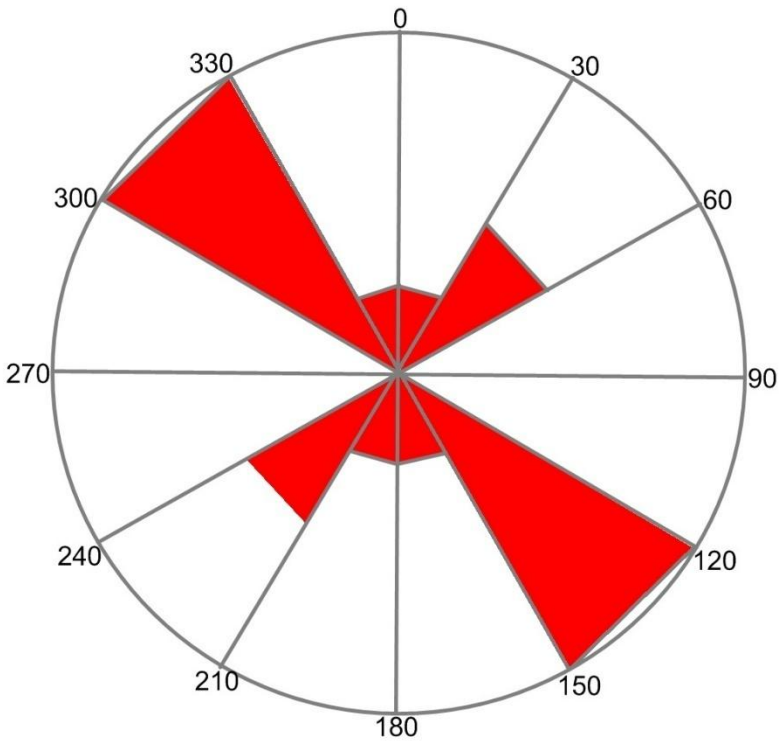


Figure 4.29: Rose diagram showing the dominant orientations of joint in quartzite

Table 4.4: Circle-inventory for evaluating joint density in migmatite

Station #10, Migmatite **Radius of Inventory Circle = 37cm;** **Area = 4301cm^2**	
Trend of Joint	**Length of Joint (cm)**
N40E	277
N38E	180
N51E	195
N50E	172
104E	23
NS	25
N27E	20
94E	27.3
	919.3cm = Cumulative Fracture Length

Joint Density = $\frac{919.3cm}{4301cm2}$ = 0.21cm^{-1}

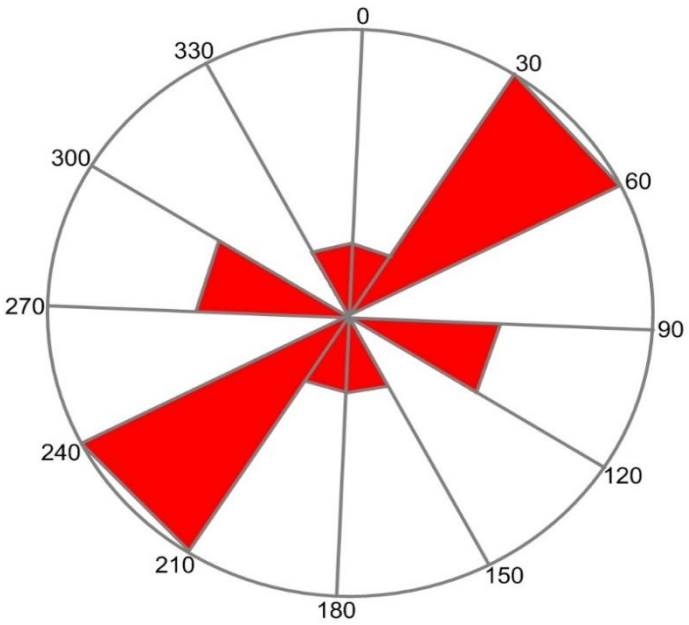


Figure 4.30: Rose diagram showing the dominant orientations of joint in migmatite gneiss

Table 4.5: Circle-inventory for evaluating joint density in granite gneiss

Station #24, Granite Gneiss **Radius of Inventory Circle = 37cm;**	**Area = 4301cm^2**
Trend of Joint	**Length of Joint (cm)**
N28E	63
N21E	25.7
109E	9
N27E	48
124	15
N27E	26
N54W	31
N49E	36
N47E	48
N28E	60
N54W	15.5
	377.2cm = Cumulative Fracture Length

Joint Density = $\frac{377.2cm}{4301cm2}$ = 0.088cm^{-1}

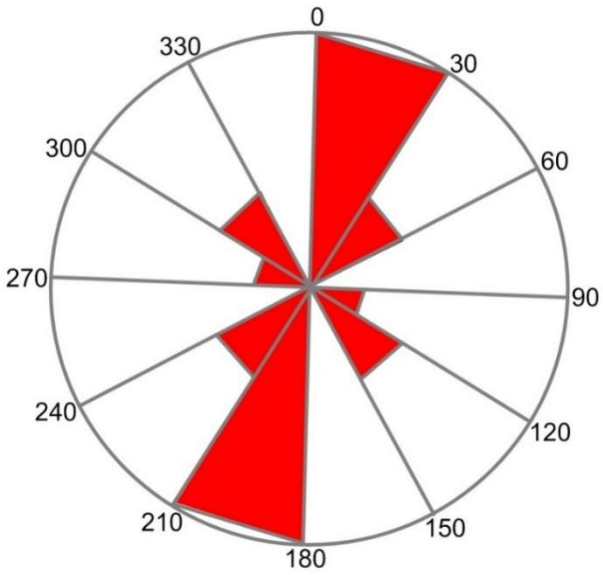


Figure 4.31: Rose diagram showing the dominant orientations of joint in granite gneiss

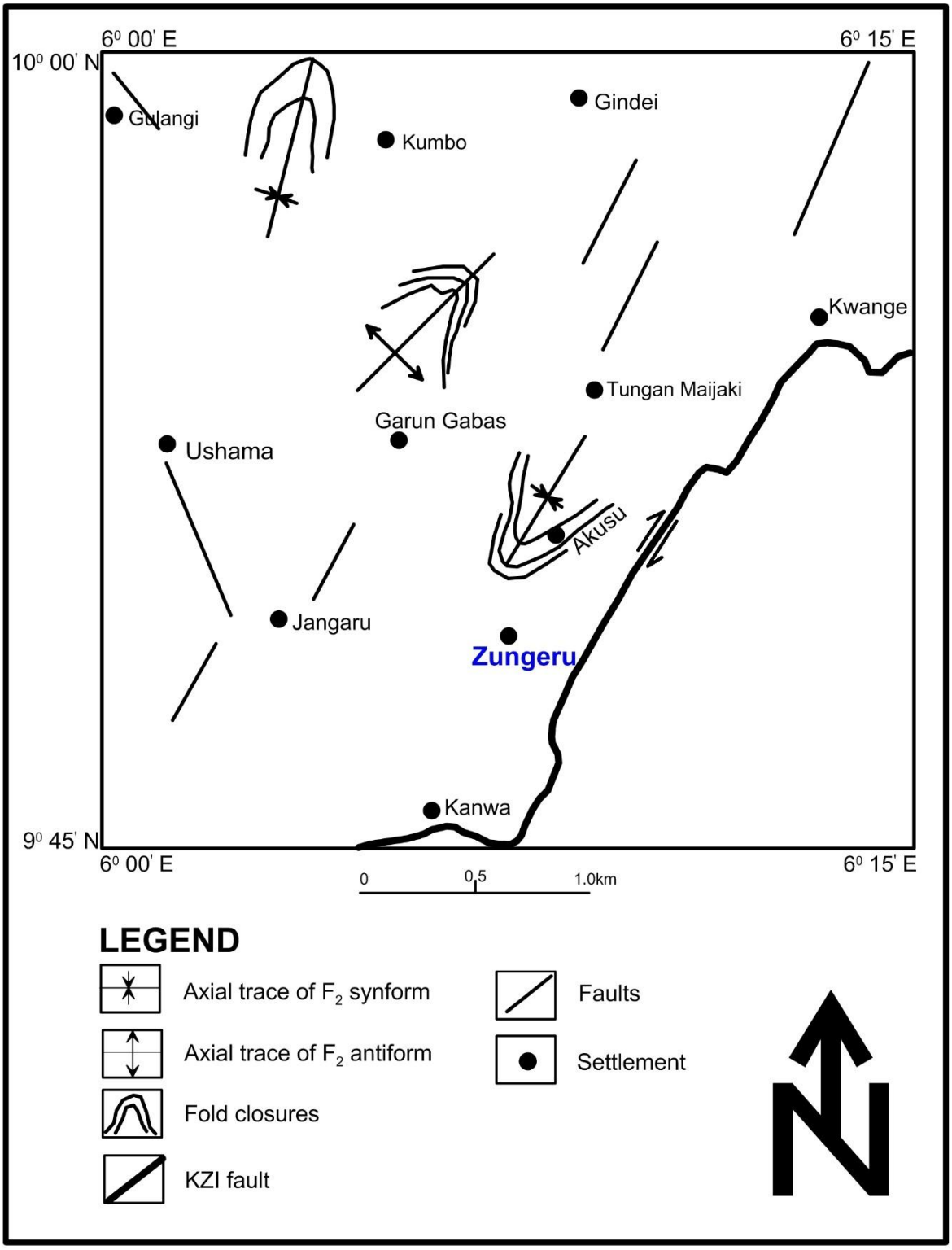


Figure 4.32: Locations of major structures in the Zungeru region manually extracted from Landsat images

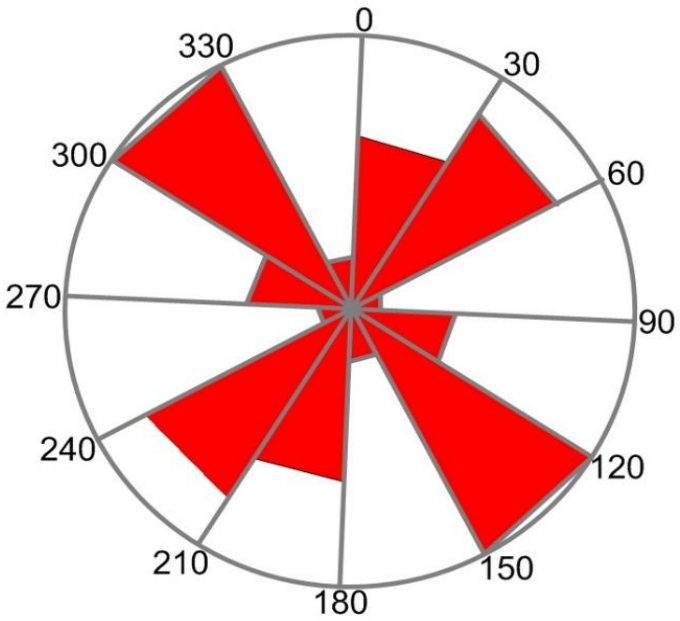


Figure 4.33:Rose diagram generated from combined joints orientations in all the rocks in the study area.

4.4 MICROTECTONICS

This deals with deformation structures on the scale of individual grains.Deformation in rocks is achieved by a large number of processeson the scale of individual grains. The actual processesinvolved depend on factors such as mineralogy, compositionof the intergranular fluid, grain size, lattice-preferredorientation, porosity and permeability; and on externalcontrols such as temperature, lithostatic pressure, differentialstress, fluid pressure and externally imposed strain rate.

4.4.1 Intracrystalline Deformation

Crystals can deform internally without brittle fracturingby movement of so-called lattice defects, a process knownas intracrystalline deformation. A crystal lattice which contains a large numberof similar dislocations can be slightly bent; as a result, the crystaldoes not extinguish homogeneously as observed with crossed polars;this effect is known as undulose extinction (Plate XXVI).

4.4.2 Twinning

Twinning can accommodate only a limitedamount of strain and always operates in specific crystallographic directions. Twinning is most common in plagioclase and calcite, but also occurs in dolomite, kyanite,microcline (Eggleton and Buseck 1980; White andBarnett 1990), biotite (Goodwin and Wenk 1990), quartz(Dauphiné twinning; Barber and Wenk 1991; Lloyd 2004),diopside (Raleigh 1965; Raleigh and Talbot 1967) andjadeite (Ferrill et al. 2001).

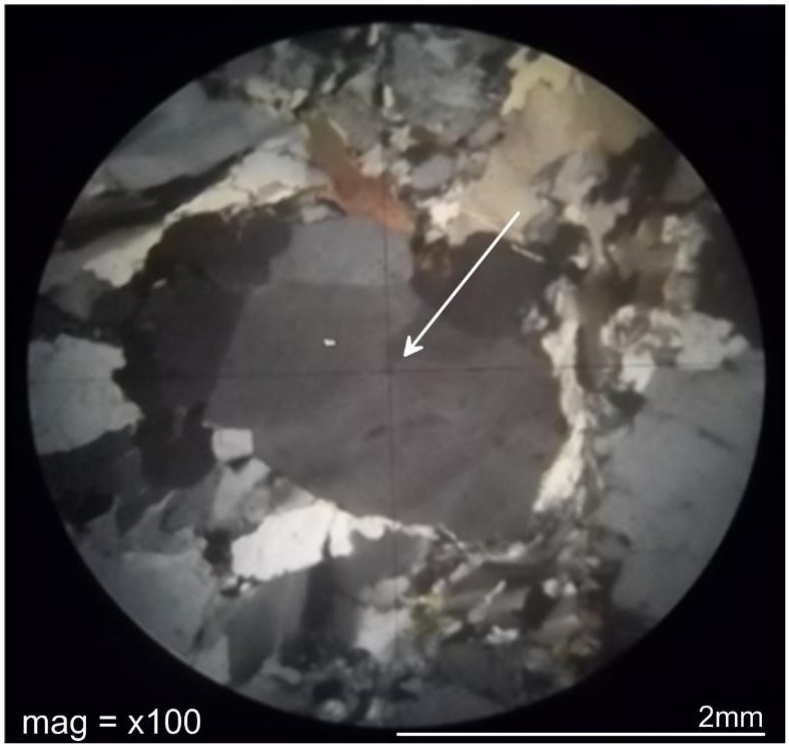


Plate XXVI: Photomicrograph ofgneiss with undulose extinction in quartz. Grain boundaries are irregular due to grain boundary migration (Slide no: stn4).

In the study area, both albite and cross-hatched twinning were observed in plagioclase and microcline respectively (Plate XXVII - Plate XXIX).

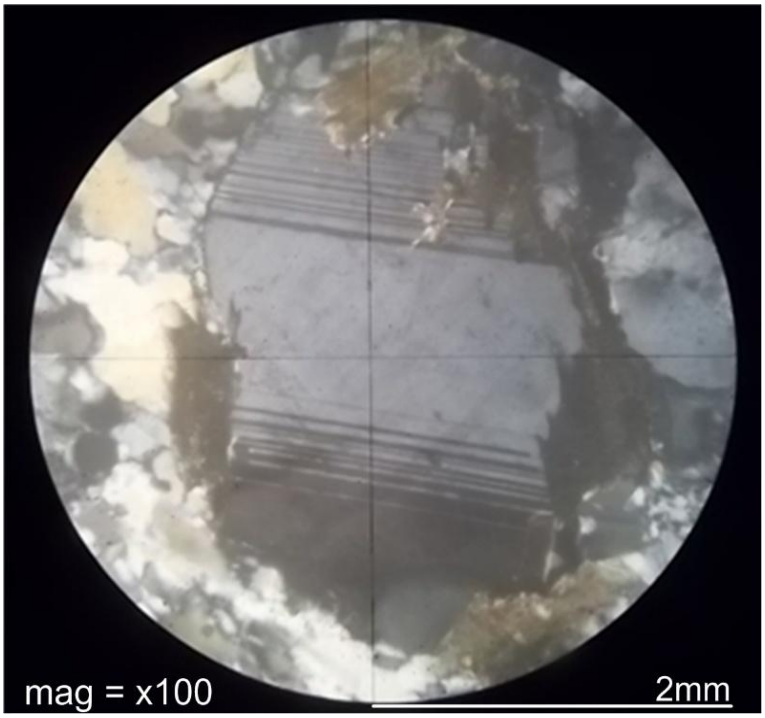


Plate XXVII: Photomicrograph of augen gneiss with albite twinning and multiple twin planes in plagioclase (Slide no: stn4).

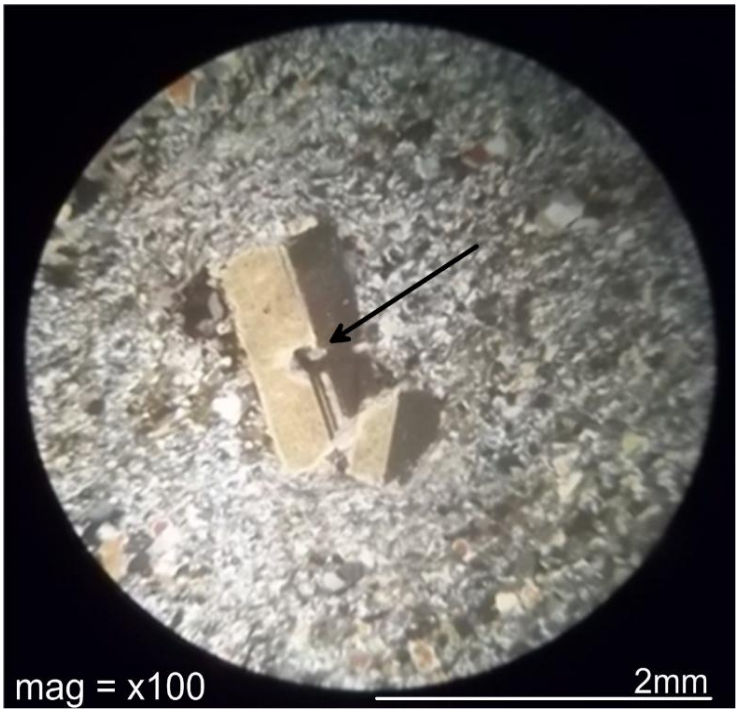


Plate XXVIII: Photomicrograph of migmatitewithalbite twinning and single twin plane in plagioclase (Slide no: stn10).

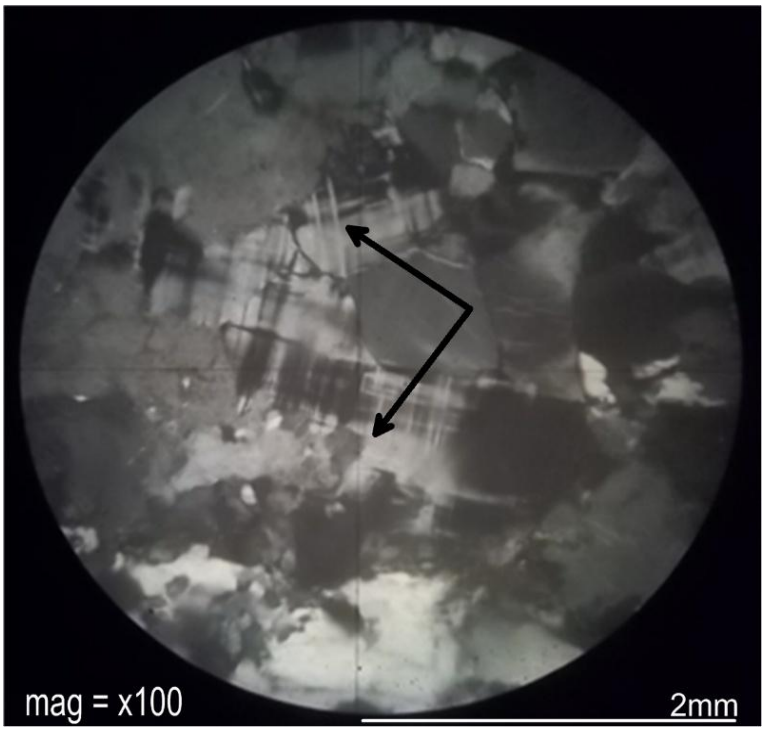


Plate XXIX: Photomicrograph of augen gneiss withcross-hatched twinning in microcline(Slide no: stn4).

4.4.3 Dynamic Recrystallisation

The reorganisation of material with a change in grain size, shape and orientation within the same mineral is known as recrystallisation (Poirier and Guillopé 1979; Urai et al. 1986; Hirth and Tullis 1992).In partially recrystallised fabrics bimodal grain size distribution is characteristic, with aggregates of small new grains ofapproximately uniform size between large old grains with undulose extinction (Plate XXX). The uniform size of new grains is due to deformationand recrystallisation at a specific differential stress.

4.4.4 Microfolding and Microfaulting

When an older planar fabric is present in a rock, the associatedmechanical anisotropy may give rise to a harmonic,regularly spaced folding which produces some of the mostintriguing structures in rocks, such as crenulation cleavage (Plate XXXI).

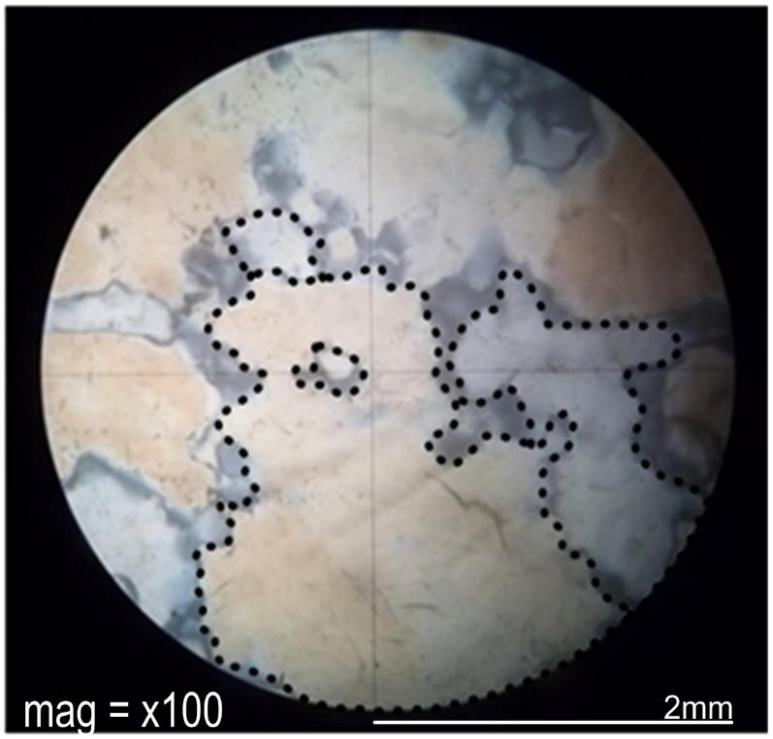


Plate XXX: Photomicrograph of quartzite showing polycrystalline quartz with irregular grain boundaries formed in response to grain boundary migration (GBM) recrystallization (Slide no: stn2).

Thelimbs of the folds may line up to form a crude foliation,but in many cases solution transfer or oriented crystallization or recrystallisation of new grains (Gray and Durney 1979a), become important after the folds have reacheda certain amplitude, and develop a spaced foliation alonglimbs of microfolds.

At the eastern portion of Plate XXXI, there is an N-S trending strike-slip micro fault. Evidence of this dextral strike-slip faulting is the lateral displacement of the diagonal mica, feldspar and quartz marker bands.

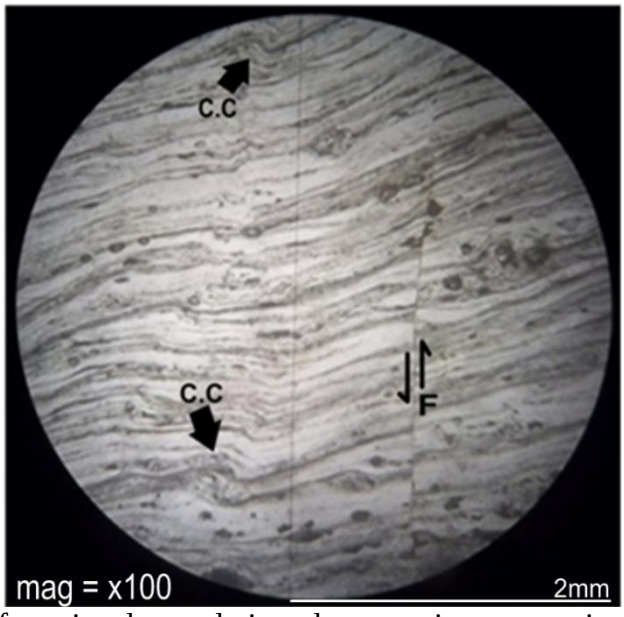


Plate XXXI: Differentiated crenulation cleavages in garnet mica schist with asymmetric microfolds(Slide no: stn1).

4.4.5 Shear Zones and Sense of Shear:

The kinematics of the shear zones related to the $D_1$and D_2 deformation was considered at the microscopic and outcrop scales.Mylonites are produced predominantly by ductile deformation and usuallyshow significant recrystallisation of the matrix.

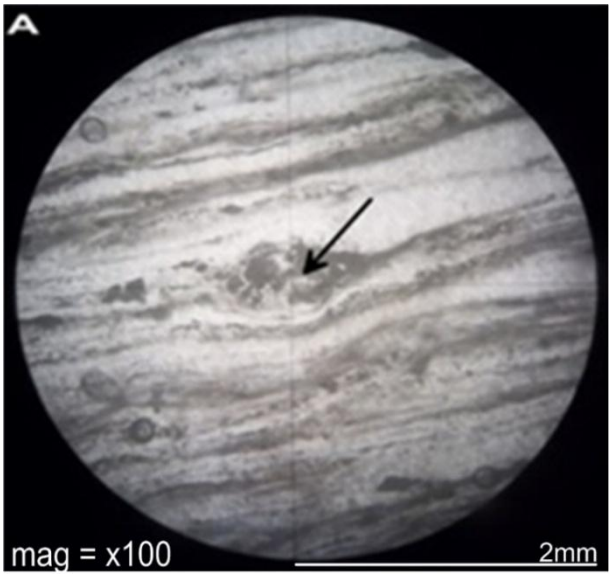


Plate XXXII: (A) Photomicrograph of garnet mica schist showing σ-type K-feldspar porphyroclast with a weak stair-stepping(Slide no: stn1).

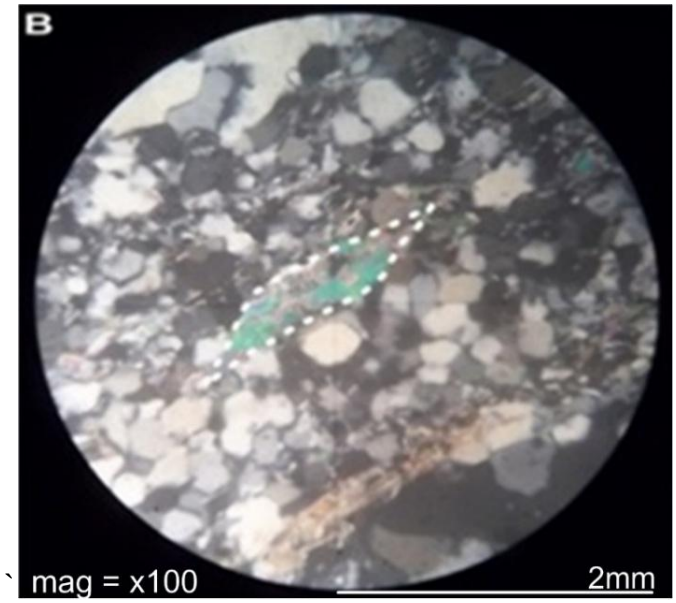


Plate XXXII: (B) Photomicrograph of augen gneiss showinglenticular Muscovite mica fish. Both porphyroclasts exhibit a dextral shear sense(Slide no: stn4).

4.5 STRAIN ANALYSIS

Strain ellipse orientations, phi and axial ratios, Rs (Table 4.6), were obtained from photomicrographs of all seven samples through the normalized Fry plots (Fig. 4.34) generated by *EllipseFit*software.

Table 4.6: Phi and Rs values for samples cut parallel to foliation (XY)

Samples	Phi	Rs
LOC 1	102	1.4
LOC 2	56	9.9
LOC 3	15	1.3
LOC 4	17	3.5
LOC 5	130	1.4
LOC 6	102	3.7
LOC 7	104	2.9

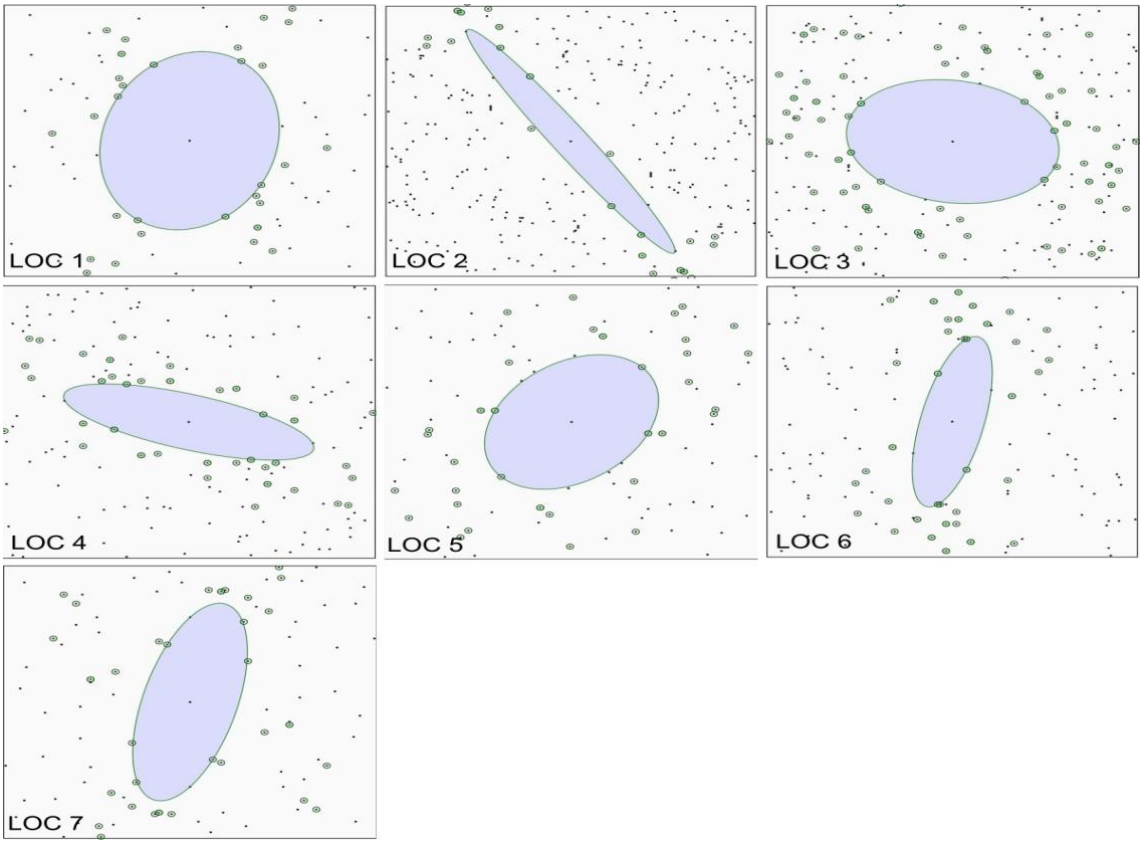


Figure 4.34: Fry plots for two dimensional strain analysis of samples cut parallel to foliation (XY).

CHAPTER FIVE

DISCUSSION

5.1 GENERAL GEOLOGY

Remote sensing is commonly used nowadaysin mineral explorations.Landsat Thematic Mapper (TM) and Advanced Space borne ThermalEmission and Reflection Radiometer(ASTER) images are some of the remote sensing data that are frequently used ingeological exploration and mapping of hydrothermal alteration zones (Buckinghamand Sommer, 1983; Kaufmann, 1988; Drury and Hunt, 1989; Carranza and Hale, 1999;Crosta and Filho, 2003; Assiri *et al.*,2008;Warner and Farmer, 2008).Moore *et al.* (2007) have used remote sensingdata (Landsat-5) to quantify basaltic rock outcrops during the Clark Area Soil Survey.

Some rocks of the region are poorly exposed. These rocks were observed in the field during exposure mapping as small isolated outcrops, hence remote sensing lithological mapping technique was employed to compliment field geological mapping.

Satellite data used for remote sensing analysis of the study area are digital elevation model (DEM) and Landsat images. The DEM was downloaded from the United States Geological Survey website (http://srtm.usgs.gov/). Landsat data was obtained from Global Land Cover Facility, University of Maryland (http://glcfapp.glcf.umd.edu/data/).

For lithological discrimination of the study area, false colour composite technique and principal component analysis were employed. The false colour composite analysis is very effect in discriminating areas covered by vegetation from areas that are not. Vegetation cover displays as green for bands 7, 4, 1 (Fig. 4.1) and blue for bands 7, 5, 4 (Fig. 4.2).

Principal Component Analysis was used to further discriminate the various lithologies in the study area after applying the false colour composite technique. PCA bands produce more distinct color composite images than spectral color composite imagesbecause the data are uncorrelated (Richards, 1999). PCA is applied to the fused image, and the resulting image has high spatial resolution and a wide range of color that make the different lithological units easily discriminated.

Using these two techniques together and correlating with field data, the approximate boundary of the gneiss, amphibolites, quartzites, schists and mylonites was deduced. The geological map of the study area was produced based on field data and the images produced from these two analyses are presented in Figures 4.1-4.6.

Due to the rock discriminationpower of the colour composite images for bands 7:4:1 (Fig. 4.1), 7:5:4 (Fig. 4.2), 1/3:5/7:3/5 (Fig. 4.3) and 5/1:5/7:4 (Fig. 4.4), they were used for preliminary identification of the different rock types in the study area.

In Fig. 4.1, the red and green colours are indicating different rock types and vegetation, while the blue colour delineates the major river in the southeastern quadrant of the map. The very dark reddish-purple colour at the eastern portion of the map is area occupied by both amphibolites and schist. Gneiss is represented at the central and northeastern portion of the map bylight reddish-purple colour. The remaining rock types and vegetation in the area are represented by green colour. Fig 4.2 depicts areas covered by gneiss, amphibolite, migmatite and mylonite by yellow colour while vegetation appears as blue.

False colour composite in R.G.B of band ratio 1/3:5/7:3/5 (Fig. 4.3) displays amphibolite and gneiss as blue while quartzite generally exhibits a greenish-yellow coloration. The major water

body in the southeastern portion of the area is displayed as black while areas occupied by gneiss and amphibolite are light purple (Fig. 4.4).

The major drainage system is indicated by purple colour in the principal component analysis of bands 1, 2 and 3 (Fig. 4.5), but the different lithologies and drainage systems exhibit an almost uniform colour (Fig. 4.6).

5.2 STRUCTURAL GEOLOGY

Deformation patterns on the basementrocks of Nigeria are so complex (Rahaman, 1988; Ogezi, 1977; Ajibade and Wright, 1989; McCurry, 1976) andhence require a detailed study to understand their strainhistory. Additionally, the homogeneity of deformation onthe rocks which is dependent on the degree of responseto the prevailing stress fields is important in elucidatingthe tectono-metamorphic conditions that affected therocks.

The study area was affected by several successive deformations with deformational phase accompanied by generation of structures on different scales. Field observations, measurements and micro-structural study of these structures and their overprinting relationships have led to the establishment of the structural patterns of different deformational phases and succession. The characteristics and effects of these deformational phases strongly depend on the rock type and metamorphic conditions.

5.2.1 Superimposition of Structures and Strain Patterns

Both ductile and brittle deformational structures were mapped and these include folds, cleavages, lineations, joints and veins. The major type of fault observed in the study area is the strike-slip fault. Thrust faults were not identified in the study area because of the prevalence of steep dips

and tight folding. Joints and veins were encountered in the field and almost all the rocks in the study area are jointed.

The rose diagram plots on all the rock types in the area show that the joints have a dominant NW-SE, NE-SW and NNE-SSW trends (Fig. 4.33). From the circle inventory analysis, the joint density in augen gneiss is $0.14cm^{-1}$with major (NW-SE) and (NE-SW) orientations (Fig .4.28). Quartzite and granite gneiss have fracture densities of $0.13cm^{-1}$ and $0.088cm^{-1}$ respectively and NW-SE, NE-SW and NNE-SSW orientations (Fig .4.29 and Fig. 4.31). Joints in migmatite gneiss have dominant NE-SW, ESE-WNW trends and also N-S to a lesser extent (Fig. 4.30). The circle inventory method of joint density determination shows that granite gneiss is the most jointed, having the highest joint density while migmatite is least jointed due to it plastic nature.

The sequence of structures has been established using orientation of fold axial planes, style of folding, attitude of planar and linear fabrics, and overprinting of one fabric by another.

D_1 deformationis associated with thedevelopment of F_1folds, axial planar S_1 foliations and L_1 lineation.These fabrics have been largely overprinted by the D_2 deformationand can be recognized on macroscopic andmicroscopic scales. Both S_1 and L_1 fabrics originated during the earliest phase of deformation, D_1. The D_1 event led to the cataclastic deformation of the basement and the development of cataclastic foliation, S_1. In most cases, the foliation is parallel to lithological layering.

After D_1 deformation, some rock bodies of the studied area wereprogressively affected by a second deformation episode (D_2) which produced structures with a general NNE-SSW orientation. Satellite imagery trends show that the study area has been folded into major antiformal and synformal structures (Fig. 4.32). The larger parts of D_2 fabrics are mylonitic,

consistingof mylonitic foliations, L_2 lineations and a steeply dipping open to isoclinal NNE trending F_2 folds. During D_2 deformation, S_1 foliations were folded by F_2 folds andS_2cleavages developed parallel to the axial planes of the folds.

Major D_1 structures found in the study area have been re-oriented by subsequent structures, so only the approximate initial orientation of F_1 folds could be determined. Stereographic plots of poles to cataclastic foliation (S_1) gives orientation of F_1 axial plane as (296/84) (Fig. 4.27-A). Two concentrations of lineation data depicted on the stereogram are: one characterized by gentle NW plunges and the other with gentle SE plunges (Fig. 4.27-B).

5.2.2 Microtectonics

The rocks in the study area have been deformed by ductile flow through a range of mechanisms of ductile grain scale deformation such as intracrystalline deformation, twinning and recrystalization which reduces the damage imposed during the deformation processes.

At themicroscopic scale, a number of oriented thin-sectionscut parallel to the accompanying lineations and foliations were examined to determine thesense of shearing. Most of these thin-sections have been selected from mylonitic rocks containing asymmetric feldspar, and garnet porphyroblasts. At the microscopic scale the shear sense criteria consist of porphyroclasts, mica fish, shear band cleavageand asymmetric microfolds (Plate XXXII-A) and (Plate XXXII-B). Most of the shear sense indicatorsdefine a predominantly dextral strike-slip and some show reversesense of shear.

5.2.3 Strain Analysis

The ellipsoidal shape of the grains generated usingthe Fry method on the photomicrograph of rocks from the study area revealsheterogenous and varying grain deformation as well asvarying orientations corresponding also to the marginal NE-SW, NW-SE, E-W, and NNE-SSW (Fig. 4.34).

The shapes range from near circular to the flattening type(Fig. 4.34).Quartzite, migmatite gneiss and granite gneiss on the western and central portion of the study area exhibit the circular type,which is indicative of low degree of deformation. The flattening type was observed in augen gneiss, quartz-muscovite-phyllite and banded gneiss. It shows grain elongation in the directions of the marginal NW-SE and NNE-SSW and E-W, indicative of a high degree of deformation (Genier and Epard, 2004).

5.3 TECTONIC EVOLUTION

The rocks in the study area have undergone minimum of two major deformational events and these resulted in two recognizable phases of deformation, D_1 and D_2.

The earlier clearly recognizable event is the D_1 deformation which affected all the rocks in the study area. This led to the development of L_1S_1 fabric and the folding of S_0 fabric into F_1 fold, and S_1 axial trace. The second deformation event led to the formation of L_2S_2 fabric as a result of the folding of S_1 into isoclinal NNE-SSW trending upright folds. Evidently, primary foliations and lineations have largely been affected by later deformations which resulted to the superposition of F_2 folds over the F_1 folds thereby producing an interference pattern.

D_1 event led to the cataclastic deformation of the basement and the development of cataclastic foliation (S_1) following the accumulation of sediments. After the first deformational episode, the

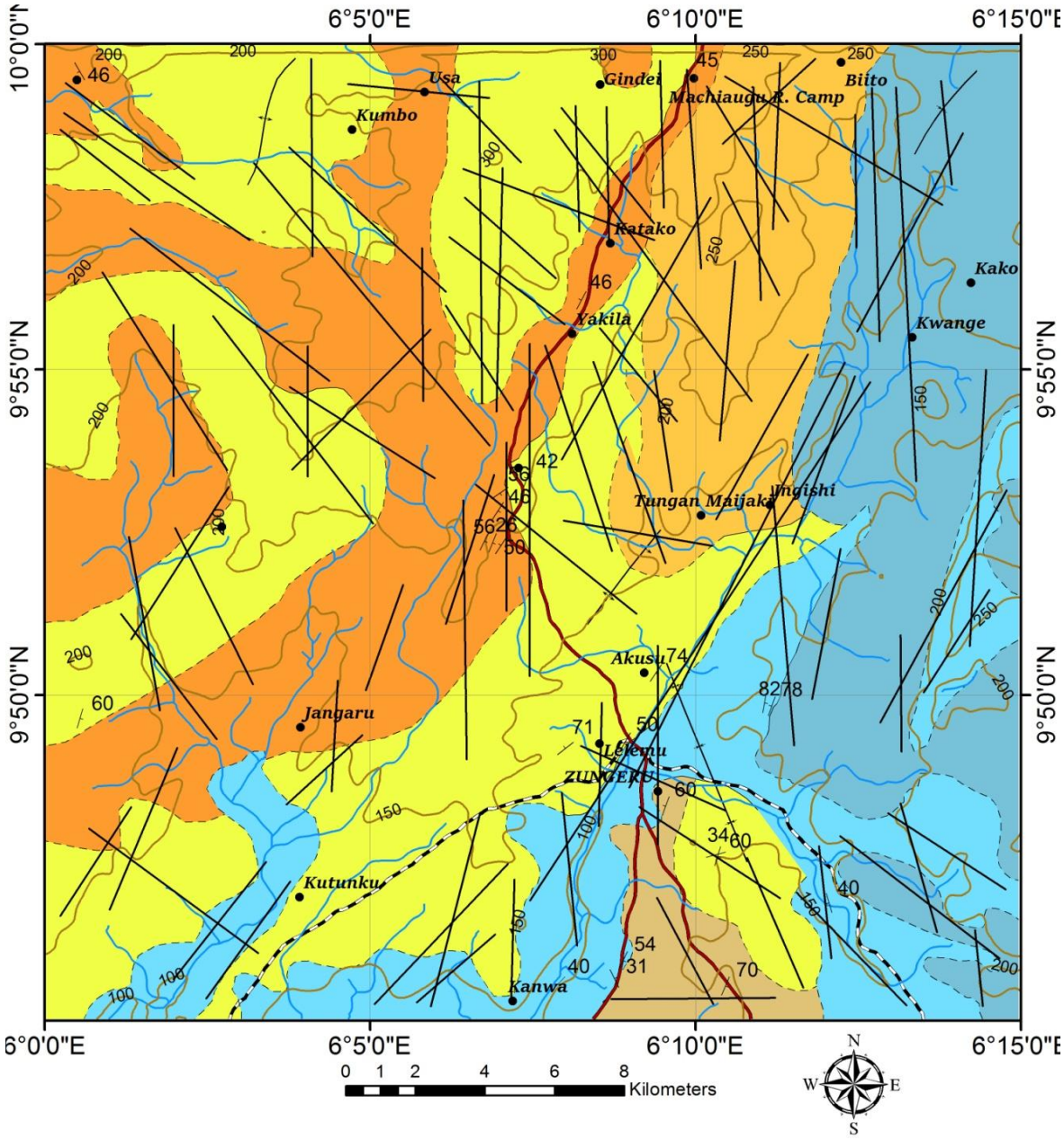
rocks in the study area were congruently deformed and folded during subsequent D_2 movements, producing small scale structures.

The D_2 event which produced upright NNE-SSW folds and axial planar cleavages is the last major deformation that affected the schist belts in NW Nigeria. The last stage of the Pan-African Orogeny is represented by a NE-SW and NW-SE conjugate fracture system. These brittle conjugate fault systems can be related to a single late Pan-African tectonic event on a continental scale which resulted from a horizontal E-W maximum stress. The major N-S trend as revealed in the rose diagram of lineaments orientation (Fig. 4.36)depicts the orientation of major Pan-African structures. In the study area, this faults have offset the N-S trending Pan-African mylonitic shear zones.

The effects of Pan-African orogeny are widespread and well documented (e.g., Odeyemi, 1981; Oyawoye, 1964; Ajibade et al., 1979; Rahaman, 1988; Elueze, 1988; Danbatta, 2002). Structures in the study area compared with those observed in some of the northwestern Nigerian schist belts indicates similar structural trends.

One of the strongest litho-structural controls observed in thestudy area is the one imposed on theRiver Kaduna as indicated by NE-SWtrending mylonitic rocks formed by shearing of pre-existing rocks (Fig. 4.35).The river, as it flows through Zungerualso appears to be controlled by a majorfracture which is the Kalangai-Zuneru-Ifewara fault. Such large scale transcurrent fault zones are visible on satellite imageries exhibiting a dextral sense of shear (Fig. 4.32).

The study area is a shear zone which evolved through a transpressional deformation. Evidence in support of this claim include: the displacement of marker beds observed both in the field and satellite imageries; the N-S and NE-SW alignments of lineaments and joints observed in satellite



LEGEND

Mylonite	Strike and Dip	Road
Amphibolite	Lineament	Contour
Schsit	Anticline	River
Quartzite	Syncline	railway
Migmatite	Contact (observed)	Settlement
Gneiss	Contact (inferred)	

Figure 4.35: Geological and lineaments map of the Zungeru area. Note the alignment of the NE-SW lineaments and the major drainage system in the area which suggest that this river is fault controlled.

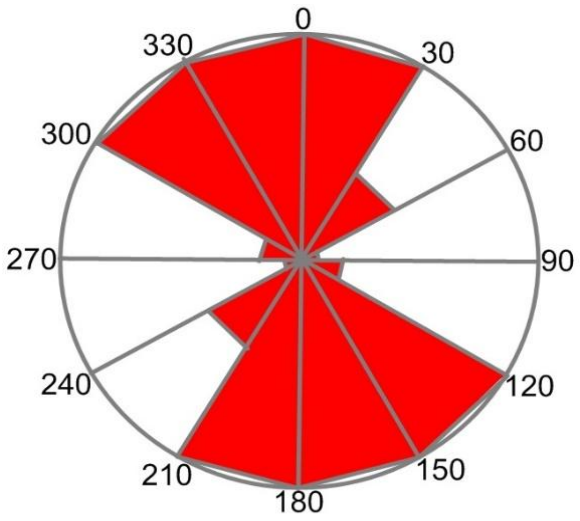


Figure 4.36: Dominant direction of lineaments from final lineament map plotted on a rose diagram

imageries and in the field respectively; the N-E and NNE-SSW orientation of fold axis and porphyroclasts (K-feldspar and mica fish) exhibiting a dextral shear sense as observed during microstructural analyses.

This type of deformation involves strike-slip movements and also a component of shortening, east-west, orthogonal to the deformation zone (Fig.4.37). Evidence of compression and shortening was observed within the NE-SW trending River Kaduna. Here, the very dark brown quartzite exposures were found superimposed on amphibolite outcrops (Plate XXXIII).

The kinematic analysis of the rocks of the study area indicates that the strain is due to the pervading E-W stress which resulted in an E-W direction shortening. Thus, this research suggests that the mylonites within the study area were produced as a result of Pan-African shearing along the Ifewara-Zungeru fault and may also be associated with some compressional thrust tectonics.

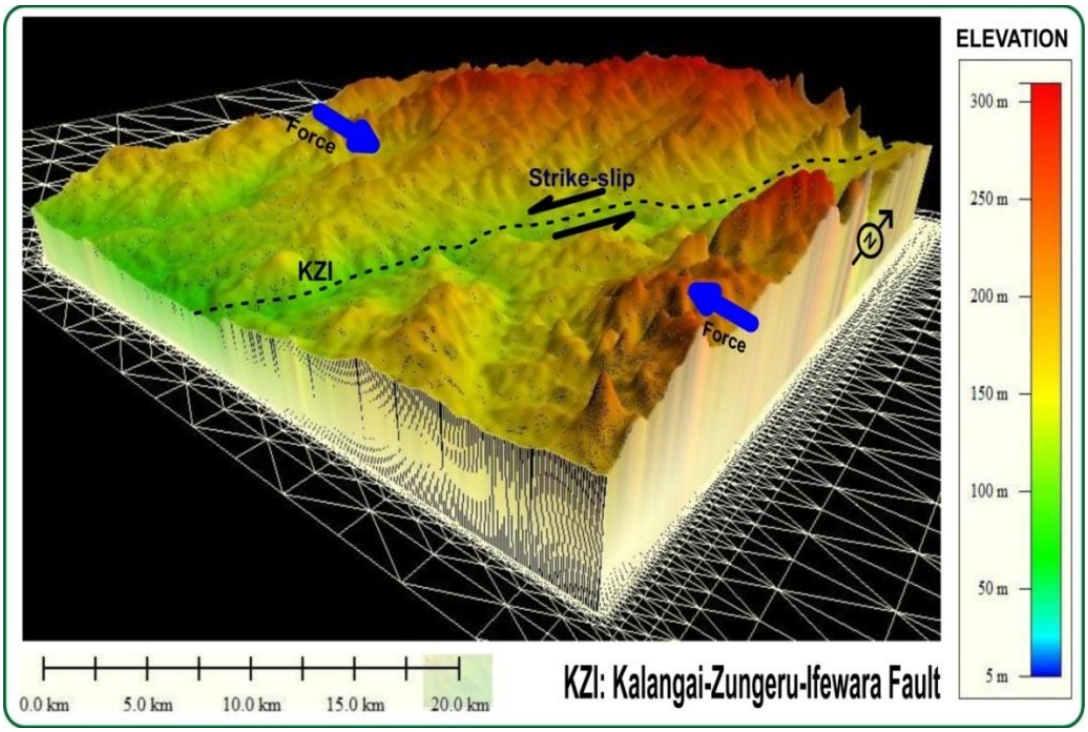


Figure 4.37: A 3-D schematic diagram depicting the transpressional deformation pattern of the study area.



Plate XXXIII: Photograph of quartzite and amphibolite in thrust relationship with one another at Kundu. Location: (9° 49' 16.8" N, 6° 08' 56.3" E).

CHAPTER SIX

SUMMARY, CONCLUSION AND RECOMMENDATIONS

6.1 SUMMARY AND CONCLUSION

The study area comprise gneiss, migmatite-gneiss, schist, amphibolite, quartziteand mylonite.Contact relationships between the various rocks are commonly sharp, although gradational and interlayered contacts were also encountered in some places. A comprehensive and up-to-date geological map showing clearly the variousrock types and their contact relationships have been produced.Remote sensing has proven useful for lithological discrimination and delineation of structural lineaments within the study area.

The rocks in the area studied have been deformed by at least two intense phases of deformation (D_1 and D_2). The cataclastic deformation of the basement is believed to have taken place during the first deformational episode, producing cataclastic S_1 cleavages while the second deformational event led to the folding of both the basement and metasedimentary rocks in the area into series of antiforms and synforms and also producing NNE-SSW trending small scale structures.

Present day NE-SW and NW-SE orientation of major and minor fractures and the N-S trending mylonitic shear zones and lineaments imply that the area was affected by late stage Pan-African orogeny which has largely over-printed and re-oriented structures produced by earlier orogenic events.

Field evidences including wide zones of mylonite, displacement of lithologies and/or marker horizons have been noted both in the field and on landsat images. At microscopic scale, sense of shear indicators like porphyroclasts, mica fish and asymmetric microfolds define a predominant

dextral strike-slip movement consistent with Pan-African shortening.Strain analysis reveals that the ellipsoidal shapes of the grains generated usingthe Fry method on the photomicrograph of thin-sections of rocks from the study area haveheterogenous and varying grain deformation as well asvarying orientations corresponding to the marginal NE-SW, NW-SE, E-W, and NNE-SSW. This also reveals that the augen gneiss, banded gneiss and phyllites have undergone higher strain as compared to other rocks in the study area.

Thrust faults and fault-propagation folds were not found within the study area as the area is basically dominated by dextral strike-slip faults and shear zones. Evidence of thrust tectonics was observed within the NE-SW trending faults controlled River Kaduna.

6.2 RECOMMENDATIONS

Mylonitic rocks showing evidence of thrust tectonics could not be studied fully because they are poorly exposed and lack distinctive geometry. Detailed mapping should be carried out elsewhere along the Zungeru-Ifewara fault in order to find clearer evidence of thrust tectonics and also study properly the style of deformation therein.

The present study examines two-dimensional penetrative strain. However, it is possible to calculate three-dimensional strain ellipsoids from axial ratios and strain ellipse orientations for three mutually perpendicular sections for each sample. Three-dimensional data generated from photomicrographs otained by cutting each sample into three mutually perpendicular surfaces will give a more comprehensive strain analysis of the Zungeru study area.

6.3CONTRIBUTION TO KNOWLEDGE

The following have been achieved through this research:

i) The geological and structural maps of the area on a scale of 1:50000 have been produced;

ii) The dominant stress direction and the amount of strain in the rocks of the study area have been determined.

iii) The orientations and densities of joints and shear fractures have been determined using various statistical techniques.

iv) The tectonic evolution of the study area has been established through megascopic, mesoscopic and microscopic analysis of geologic structures found within the study area.

REFERENCES

Adekoya, J. A. (1996). The Nigerian schist belts: age and depositional environment: implications from associated banded iron-formations. *Journal Mining and Geology*, Nigeria **32**, 35-46.

Affaton, P., Rahaman, M.A., Trompette, R. & Sougy, J. (1991). The Dahomeyide Orogen: Tectonothermal Evolution and relationships with the Volta Basin. In: *The West African Orogens and Circum-Atlantic Correlatives*, Dallmeyer, R.D. & Lécorché, J.P. (Eds), pp. 107-122, Springer-Verlag.

Ajibade A.C. (1971). The Geology of Zungeru area, Unpublished M.Sc Thesis, University of Ibadan, 240pp.

Ajibade A.C. (1987). Proterozoic crustal development in the Pan African regime of Nigeria. In; C.A. Kogbe (Editor) *Geology of Nigeria published by Rock View (Nigeria) Ltd*, p 57-63.

Ajibade, A. C. (1976). Provisional classification of the Schists Belts of North Western Nigeria In: C. A. Kogbe "Geology of Nigeria" 2nd revised edition.*Rock View Nigeria limited, jos,*85-90.

Ajibade, A. C. (1982). The cataclastic rocks of the Zungeru region and their tectonic significance. *Journal Mining and Geology* (Nigeria), **18**, 29-41.

Ajibade, A. C. (1988). Structural and tectonic evolution of the Nigerian basement with special reference to NW Nigeria. In*:*(*International Conference on Proterozoic Geology Tectonics High-Grade Terrains (Ife, Nigeria*), 42-129

Ajibade, A. C. and Wright, J. B. (1989). The Togo-Benin-Nigerian shield: evidence of crustal aggregation in the Pan-African belt. *Tectonophys*,**165**, 125-129.

Ajibade, A. C., Fitches, W. R., and Wright J. B.(1979). The Zungeru mylonites, Nigeria: recognition of a major tectonic unit. *Review Geology Dynamics & Geography Physics*, **21**, 359-363.

Ajibade, A. C., Woakes, M., and Rahaman, M.A. (1987). Proterozoic Crustal Development in the Pan-African Regime of Nigeria. In: C. A. Kogbe (edition) "Geology of Nigeria" 2nd revised edition,*Rock View Nigeria limited, jos*,57-69.

Annor, A. E. (1995). U-Pb zircon age for the Kabba-Okene granodiorite gneiss: implication for the Nigeria's basement chronology, *Africa Geoscience Review*, **2** (1), 101-105.

Annor, A. E. (1998). Structural and chronological relationship between the low grade Igarra schist and its adjoining Okere migmatite-gneiss terrain in the Precambrian exposure of southwestern Nigeria.*Journal Mining Geology,***34** (2), 187-196.

Annor, A.E. and Freeth, S.J. (1985). Thermotectonic evolution of the basement complex around Okene, Nigeria, with special reference to deformation mechanism. *Precambrian Resourse*, **28**, 269-281.

Annor, A.E., Olasehinde, P.I., and Pal, P.C. (1990). Basement fracture patterns in the control of water channels – An example from central Nigeria. *Journal Mining and Geology*, **26**(1), 5-12.

Assiri, A., Alsaleh, A., and Mousa, H. (2008). Exploration of Hydrothermal Alteration Zones Using ASTER Imagery: A case study on Nuqrah Area, Saudi Arabia. *Asian Journal of Earth Science,***2**, 1819-1886.

Baba, S., Abba, S.I., and Dada, S.S. (2006). Preliminary Petrogenetic Study of some Rocks from Gwoza Area, NE. Nigeria. *Global Journal of Geological Sciences*,**4**(2), 147-155

Ball, E. 1980. An example of very consistent brittle deformation over a wide intracontinental area: the late Pan-African Fracture system of the Tuareq and Nigerian Shields. *Tectonophysics*,**61** (4), 363-379.

Barber, D.J. and Wenk, H.R. (1991). Dauphiné twinning in deformed quartzites: implications of an in-situ TEM study of the α-β-phase transformation. Physical Chemistry and Mineralogy,**17,** pp. 492–502

Black, R. (1980). Precambrian of West Africa. *Episodes***4**, 3-8

Black, R., Caby R., and Moussine-Pouchkine, A. (1979). Evidence for Late Precambrian PlateTectonics in West Africa. *Nature*,**278**, 223–226.

Black, R., Latouche, L., Liegeois, J.P., Caby, R., and Betrand, J.M. (1994). Pan-African displacement terranes in Tuareg Shield (Central Sahara). *Journal of Geology*,**22**, 641-644

Buckingham, W.F. and Sommer, S.E.(1983). Mineralogical characterization of rock surfaces formed by hydrothermal alteration and weathering- application to remote sensing. *Economic Geology*,**78**, 664-674.

Burke, K. C., Freeth, S. J., and Grant, N. K. (1976). The structure and sequence of geological events in the basement complex of the Ibadan area western Nigeria. *Precambrian Research*,**3**, 537-545.

Burke, K.C. and Dewey, J.F., (1972): Orogeny in Africa. In: African Geology, T.F.J. Dessauvagie and A.J. Whiteman (eds.), *University of Ibadan Press*, pp. 583-608.

Caby, R. (1989). Precambrian terranes of the Benin-Nigeria and Northeast Brazil and the late Proterozoic SouthAtlantic fit. *Geological Society of America Special Paper*, ***230,*** 145-158.

Caby, R. and Boesse, M. (2001). Pan African nappe system in southwest Nigeria: The Ife -Ilesha schist belt. *Journal of African Earth Sciences*, **33**, 211–225.

Caby, R., Betrand, J.M.I., and Black, R., (1981). Pan-African Ocean Closure and Continental Collision in the Hoggar-Iforas Segment, Central Sahara.In: A Kronaer edition, "Precambrian PlateTectonics" *Elsavier, Amsterdam*, 407-434

Caby, R., Sial, A., Arthaud, M. H. and Vauchez, A. (1990). Crustal evolution and the Brasiliano orogeny in northeast Brazil. In: DALLMEYER, R. D. & LECORCHE, J. P. (eds) The West African orogens and circum-Atlantic correlatives. *Springer Verlag*, New York, 373–397.

Cahen, L., Snelling, N. J., Delhal, J. and Vail, J. R. (1984). The geochronology and evolution of Africa. *Oxford, Clarendon*, 486- 512

Carranza, E.J.M. and Hale, M.(1999). Image processing and GIS for hydrothermal alteration mapping, Baguio district, Philippines. Proceedings of the 1999 IEEE International Geoscience and Remote Sensing Symposium, Hamburg, Germany, 28 June-2 July (on CDROM).

Characteristics of Pan African Granite Batholiths in the Basement Complex of Parts

Chukwu-Ike, I.M. (1978). Regional tectonic setting of the Northwestern Nigeria low-grade metasedimentary belt. *Journal of mining and geology, Nigeria***15**, 19-22

Cooper, M. (2007). Structural style and hydrocarbon prospectivity in fold and thrust belts: a global review. In: Ries, A. C., Butler, R.W.H. & Graham, R. H. (eds) Deformation of the Continental Crust: The Legacy of Mike Coward. *Geological Society, London, Special Publications*, **272**, 447-472.

Crespi, J.M.(1986). Some guidelines for the practical application of Fry's method of strain analysis: *Journal of Structural Geology*, **8**(7), 799-808.

Crosta, A.P., De Souza Filho, C.R., Azevedo, F. and Brodie, C.(2003). Targeting key alteration minerals in epithermal deposits in Patagonia, Argentina, using ASTER imergery and principal component analysis. *International Journal of Remote Sensing***24**, 4233-4240.

Dada, S.S. (1998). Crust-forming ages and Proterozoic crustal evolution in Nigeria: a reappraisal of currentinterpretations. *Precambrian Research*, **87**, 65-74.

Dada, S.S. (1999). Geochemistry and petrogenesis of the reworked Archaean gneissic complex of north-central Nigeria: major and trace element studies on Kaduna amphibolites and migmatitic gneisses. *Global Journal ofPure and Applied Science*, **5**, 535–543.

Dada, S.S. (2006). Proterozoic Evolution of Nigeria. In: The Basement Complex of Nigeria and Its Mineral Resources (Oshin O. edition.). A Symposium organized to mark the 60th birthday ofProf. M. A. O. Rahaman held at the Conference Centre, Obafemi Awolowo University, Ile – Ife, Nigeria, **6**, 29-44

Dada, S.S. (2008). Proterozoic Evolution of the Nigeria-Borborema Province," In: R. J. Pankhurst, R. A. Trouw, B. B. Brito Neves and M. J. De Wit, Eds., *West Gondwana*: *Pre-Cenozoic Correlations across the South Atlantic Region*, *Geological Society of London Special Publication, London*, 121-136

Dada, S.S. and Rahaman, M. A. (1995). Archaean–Lower Proterozoic crustal evolution in Nigeria. African Geoscience Reviews, **2,** 219–225.

Dada, S.S., Birck, J. L., Lancelot, J. R. and Rahaman, M. A. (1993). Archean migmatite-gnesis complex of North Central Nigeria: its geochemistry, Petrogenesis and crustal evolution. In: 16th International Colloquium on African Geology, Mbabane, Swaziland, Extended Abstracts, **1**, 97–102.

Dada, S.S., Birck, J. L., Lancelot, J. R., and Rahaman, M. A. (1993). Archean migmatite-gnesis complex of North Central Nigeria: its geochemistry, Petrogenesis and crustal evolution.

In: 16th International Colloquium on African Geology, Mbabane, Swaziland, Extended Abstracts, **1**, 97–102.

Dada, S.S., Briqueu L., Lancelot J.R, Harms U., Matheis G, (1995). Charnockitit and monzonitic Pan-African Series from north-central Nigeria: trace elements and Nd,Sr, Pb isotope constraints on petrogenesis. *Journal of Chemical Geology,* 124: pp. 233-252

Danbatta, U. A. (1991). Geologic investigation of the SW portion of the Zuru schist belt, NW Nigeria. *Unpubl. M.Sc. Thesis, A.B.U. Zaria*, 150 p.

Danbatta, U. A. (2002). Rb-Sr Isochron Dating of Granitoids from the Kazaure Schist Belt, NW Nigeria. *Global Journal of Pure and Applied Sciences*,**8** (3), 319-322.

Danbatta, U.A. (1998). Geotectonic evolution of the Kazaure schist belt in the Precambrain basement of NW Nigeria,*Unpublished PhD Thesis A.B.U Zaria*. 286pp.

Danbatta, U.A. (1999). Geotectonic evolution of the Kazaure Sciest Belt in the Precambrian Basement of NW Nigeria. Unpublished PhD Thesis, Ahmadu Bello University Zaria, 279-286

Danbatta, U.A. (2001). Tectono-Metamorphic evolution of the Kazaure Schist Belt, NW Nigeria. Paper presented at the-37" Annual Conference of Nigerian Mininig and Geoscience Society. NMGS Abtract, **33**, 56-109

Danbatta, U.A. (2003). The lithogeochemical framework underlying the geotectonic evolution of the Kazaure Schist Belt, NW Nigeria. *The Nigerian Journal of Scientific Research*, **4**(1), 1-13.

Danbatta, U.A. (2008). A Review of the Evolution and Tectonic Framework of the Schist Belts of Western Nigeria, West Africa. *Africa geoscience review,* **15 (**2**),** 145-158.

Drury, S. A.(1993). Image interpretation in Geology, **2**, 145 – 149, 225 – 231.

Drury, S. A., and Hunt, G.A.(1989). Geological uses of remotely-sensed reflected and emitted data of lateralized Archaean terrain in Western Australia. *International Journal ofRemote Sensing,***10**, 475-497.

Dunne, W.M., Onasch, C.M., and Williams, R.T.(1990). The problem of strain-marker centers and the Fry method: *Journal of Structural Geology,* **12(**7), 933-938.

Egbuniwe, I.G. (1982). Geotectonic evolution of the Maru Belt, NW Nigeria. *Unpublished Ph.D. Thesis, University of Wales,* Aberystwyth, 411p.

Eggleton, R. A., Buseck, P.R. (1980). The orthoclase-microcline inversion: a high-resolution transmission electron microscope study and strain analysis. *Contribution for Mineral and Petroleum,***74,**123–133

Ekwere, S.J., Ekwueme, B.N., (1991). Geochemistry of Precambrian gneisses in the eastern part of the Oban massif, southeastern Nigeria. *Geologie Mijnbouw,***70**, 105–114.

Ekwueme, B.N. (1987). Structural orientation and Precambrian deformational episode of Uwet area, Oban Massif, S. E. Nigeria. *Precambrian Resource***. 34**, 269-289.

Ekwueme, B.N. (1990). Rb-Sr age and petrologic features of Precambrian rocks from the Oban Massif southeastern Nigeria. *Precambrian Research,***47**, 271-286

Ekwueme, B.N. (1991). Geology of the area around Obudu Cattle Ranch, Southeastern Nigeria. *Journal of Mining and Geology.* **27**(1), 129-134.

Elueze, A. A. (1988). Geology of the Precambrian schist belt in Ilesha area, southwestern Nigeria. In: Precambrian Geology of Nigeria, (Eds. Oluyide et al.), *a publication of the Geological survey of Nigeria*, 77-82.

Elueze, A. A. (1992). Rift system for Proterozoic schist belts in Nigeria. *Tectonophysics,***209**, 167-169.

Erslev, E.A. (1988). Normalized center-to-center strain analysis of packed aggregates.*Journal of Structural Geology*, **10**(2), 201-209.

Ferre, E.C, Deleris, J, Bouchez, J.L., Lar, A.U., and Peucat, J.J (1996). The Pan-African Reactivation of Eburnean and Archaen Provinces in Nigeria: Structural and Isotopic Data. In: *Journal of the Geological Society, London*, **153,**719-728.

Ferre, E.C., Caby, R., Peucat, J. J., Capdevila, I. R., & Monie, P. (1998). Pan-African post-collisional ferro-potassic granite and quartz-monzonite plutons of Eastern Nigeria. *Lithostratigraphy*, ***45***, 255-278.

Ferrill, D. A., Morris, A.P., Evans, M.A., Burkhard, M., Groshong, Jr R.H., Onasch, C.M, Trepmann, C.A., Stöckhert, B. (2001). Mechanical twinning of jadeite – an indication of synseismic loading beneath the brittle-ductile transition. *Intern J Earth Sci*.**90**, 4–13

Fitches, W.R., Ajibade A. C., Egbuniwe I.G., Holt R. W., and Wright J.B. (1985). Late Proterozoic Schist Belts and Plutonism in NW Nigeria, *Geological Society of London*, **142**, 319- 337.

Fossen, H. (2010). Structural Geology. Cambridge University Press, New York, pp.1-417.

Freeth, S.J., (1971). Geochemical and related studies of West African igneous and metamorphic rocks. Doctoral dissertation, University of Ibadan unpublished pp. 228-231

Fry, N.(1979). Random point distributions and strain measurement in rocks: *Tectonophysics*, **60**, 89-105.

Garba, I. (1992). Rare earth element study of Bin Yauri gold deposit, Nigeria', *Appl. Earth Sci. (Transsection Institute Mining and Metallurgy Bulletin)*, **101**, 158–161.

Garba, I. (2002). Late Pan-African Tectonics and Origin of Gold Mineralization and Rare Metals Pegmatites in the Kushaku Schist Belt, *North Western Nigeria.Journal of Mineralogy and Geology.* 3*(*1**),**1-12.

Garba, I. (2003). Geochemical Discrimination of Newly Discovered Rare Metal Bearing and Barren Pegmatites in the Pan-African (600 +150 Ma) Basement of Northern Nigeria. *Applied Earth Science Transaction Institute of Mining and Mettallurgy,***112** (13**)**, 287-291.

Genier, F. and Epard, J.L. (2004). The Fry method applied to an augen orthogneiss; problems and results. Paper Presented at 2nd Swiss Symposium on Geosciences' Conference, Lausanne Swizerland.

Gibson, P. J. and Power, C. H.(2000). Introductory Remote Sensing: Digital Image Processing and Applications, *Taylor & Francis*, Inc., pp.58-63.

Goodwin, L. B, Wenk, H.R. (1990). Intracrystalline folding and cataclasis in biotite of the Santa Rosa mylonite zone – HVEM and TEM observations. *Tectonophysics*,**172**, 201–214

Grant, N.K. (1970). Geochronology of Precambrian Basement Rocks from Ibadan, southwestern Nigeria. *Earth and Planetary ScienceLetters*,**10,** 29-38

Grant, N.K. (1978). Structural distinction between a metasedimentary cover and an underlaying basement in the 600-m.y.-old Pan-African domain of northwestern Nigeria, West Africa. *Geological Society* of *America Berlletin,* **89,***50-58.*

Gray, D. R. and Durney, D.W. (1979a) Crenulation cleavage differentiation: implication of solution-deposition processes. *Journal of Structural Geology*,**1,** 73–80

Gray, D. R. and Durney, D.W. (1979b). Investigation on the mechanical significance of crenulation cleavage. *Tectonophysics*,**58**, 35–79.

Hirth, G.and Tullis, J. (1992). Dislocation creep regimes in quartz aggregates. *Journal of Structural Geology*,**14**, 145–159.

Hockey, R.D., Sacchi R., De-Graaff, W.P., Moutouh, E.O.G (1986). The geology of Lokoja-Auchi area, *Nigerian Geological Survey bulletin,***39**, 62-71.

Holland, J.G. and Lambert, R.S.T.J. (1969). Structural regimes and metamorphic facies: *Tectono Physics*,**7**, 197-217.

Holt, R. (1982). Geotectonic evolution of the Anka belt in the Precambrian basement complex of Northwestern Nigeria. Unpublished Ph.D. Thesis. Open University, England, 254 p.

Holt, R., Egbuniwe, I. G., Fitches, W. R. and Wright, J. B.(1978). The Relationship between low-grade metasedimentary belts, Calc-alkaline volcanism and the Pan-African Orogeny in NW Nigeria. Geol. Rundsch, **67**, 631-646.

Hubbard, F. H. (1975). Precambrian crustal development in Western Nigeria; indications from the two regions. *Geological SocietyAmerican Bulletin,***86**, 548-554.

Jensen, J. R. (1996). Introductory Digital Image Processing: A Remote Sensing Perspective. *2d ed*., Englewood Cliffs, New Jersey: Prentice-Hall.

Jones, H. A. and Hockey, R. D. (1964). The geology of part of Southwestern Nigeria Geological Survey of Nigeria, Bulletin, **31**: 1–101.

Kaufman, H.(1988). Mineral exploration along the Agaba-Levant structure by use of TM-data concepts, processing and results. *International Journal of Remote Sensing* **9**, 1630-1658.

Kröner, A., Ekwueme, B.N. and Pidgeon, R.T. (2001). The Oldest Rocks in West Africa: SHRIMP Zircon Age for Early Achean Migmatitic Orthogneiss at Kaduna, Northern Nigeria. *Journal of Geology,* university of Chicago, **19,** 399-406.

Leblanc, M. (1981). The late Proterozoic ophiolites of BouAzzer (Morocco): evidence for Pan-African plate tectonics. In: Kroner, A., (ed.) Precambrian plate tectonics, *Elsevier Amsterdam*, 435 -451.

Lloyd, G.E. (2004). Microstructural evolution in a mylonitic quartz simple shear zone: the significant roles of dauphine twinning and misorientation. In: Alsop GI, Holdsworth RE, McCaffrey K, Hand M (eds) Transports and flow processes in shear zones. GSL Special Pub **224**, 39–61

McCurry, P. (1971). Pan-African orogeny in northern Nigeria. *Geological Society of America Bulletin*, **82**, 3251–3263.

McCurry, P. (1976). Pan-African Orogeny in Northern Nigeria. *Geological Society of America Bulletin* **82**, 3251-3263.

McCurry, P. and Wright, J. B., (1977). Geochemistry of calc-alkaline volcanic in northwestern Nigeria and a possible Pan-African suture zone,*Earth Planetary Science Letter*, **37**, 90-96.

Miyashiro, A. (1973). Metamorphism and metamorphic belts. *Allen and Unwin*, London, 492pp.

Moore, C.A., Hoffmann, G.A. and Glenn, N.A.(2007). Quantifying basaltic rock outcrops in NRCS Soil Map Units Using Landsat-5 Data. *Soil Survev Horizon,* **48**, 59-63.

Mullan, H. S. (1979). Structural distinction between a metasedimentary cover and an under lying basement in the 600 m.y. old Pan African domain of northwestern Nigeria, West Africa: discussion. *Geological Society of America Bulletin* 90, 983–984

Nemcok, M., Schamel, S. & Gayer, R. 2005. Thrustbelts. Structural Architecture, Thermal Regimes and Petroleum Systems. *Cambridge University Press*, Cambridge.

Nwabufo, K.E. and Mbonu, M.C. (1988). Metasedimentary Belts of the Nigerian Basement Complex: Facts, Fallacies and New Fronties. *Geological Survey Edition Precambrian Geology*, 55-68.

Odeyemi, I. B. (1988). Lithostratigraphy and structural relationships of the upper Precambrian metasediments in Igarra area, southwestern Nigeria. In: *Precambrian Geology of Nigeria*, (Eds. Oluyide *et al*.) a publication of the Geological Survey Nigeria, 111-125.

Odeyemi, I. E. (1981). A review of the orogenic events in the Precambrian basement of Nigeria, West Africa. *Geologishe Rundschau,***70** (3), 879-909.

Odeyemi, I.B., Anifowose, A.Y.B. and Asiwaju-Bello, Y.A. (1999). Remote Sensing Fracture of South Western Nigeria. *The Journal of Technoscience*, Vol. 3. pp 56-60.

Ogezi, A. E. O. (1977). Geochemistry and Geochronology of the basement rocks from northwestern Nigeria. Unpublished Ph.D. thesis University Leeds England, 295 p.

Olabaniyi, S. B. (1997). Geological and geochemical studies of the Basement rocks and associated Iron Formation of Isanlu area in the Egbe-Isanlu schist, SW Nigeria. *Unpublished. Ph.D. Thesis* University Ilorin, Nigeria.

Olade, M. A. and Elueze, A. A. (1979). Petrochemistry of the Ilesha amphibolites and Precambrian crustal evolution in the Pan-African domain of southwestern Nigeria. *Precambrian Research*,**8**, 303-318.

Olasehinde, P. I, Pal, P. C, Annor, A.E. (1990). Aeromagnetic anomalies and structural lineaments in the Nigerian Basemen Complex. *Journal African Earth Science*, **11**(3 and 4), 351-355.

Onyeagocha, A. C. (1986). Geochemistry of basement granitic rocks from northcentral Nigeria. *Journal of African Earth Science*,**5**(2), 651-657.

Onyeagocha, A. C. and Ekwueme B. N. (1990). Temperature-Pressure Distribution Patterns in Metamorphosed Rocks of the Nigerian Basement Complex - a preliminary analysis. *Journal of African Earth Sciences,* **11**,83-93.

Onyedim, G.C. and Ocan, O.O. (2001). Correlation of SPOTimagery lineaments with geological fractures in part of Ilesha area, Southwestern Nigeria. *Journal Mining Geology*. **37**(1), 15-22.

Oyawoye, M. O. (1964). The Geology of the Nigerian Basement Complex - a Survey of our Present Knowledge of them. *Journal of Metallurgy*,**1**(2), 87-102.

Oyawoye, M. O. (1964). The petrology of a potassic syenite at Shaki, Western Nigeria. *Coniributions Mineralogy Petrology*,**16**, 123-129.

Oyawoye, M. O. (1972). The basement complex of Nigeria. *In* Dessauvagie, T. F., and Whiteman, A. J., eds. African geology. Ibadan, Geology Department, University of Ibadan, 42-98.

Passchier, C.W. and Trouw, R.A.J. (2005). *Microtectonics (2nd Ed)*. Springer-verlag Berlin Heidelberg, Germany, pp. 25-158.

Poirier, J. P. and Guillope, M. (1979). Deformation induced recrystallisation of minerals. B Mineral 102, 67–74

Rahaman, M. A. (1988). Recent advances in the study of the basement complex of Nigeria. In: Precambrian Geology of Nigeria, (Eds. Oluyide et al.) *a publication of the Geological Survey of Nigeria*, 71-43.

Rahaman, M. A. 1976. Review of the basement geology of southwestern Nigeria. In: Geology of Nigeria (edited by C. A Kogbe). *Elizabethan publishing Company Lagos*, 41-58.

Rahaman, M. A., Ekwere, S. J., Azmatullah, M. and Ukpong, E. E. (1988): Petrology and geochemistry of granitic intrusive rocks from the western part of the Oban Massif, southeastern Nigeria. *Journal African Earth Science* .**7**(1): pp.149-157.

Raines, G. L, Offield, T.W. and Santos, E.S. (1978). Remote sensing and subsurface definition of facies and structure related to uranium deposits Powder River Basin, Wyoming. *Economic Geology,* **75**, 1706-1725.

Raleigh, C. B, Talbot, J. L (1967). Mechanical twinning in naturally and experimentally deformed diopside. *American Journal of Science*,**265**,151–165

Raleigh, C. B. (1965). Glide mechanisms in experimentally deformed minerals. Science **150**, 739–741

Ramsay, J.G. and Huber, M.I. (1983). The Techniques of Modern Structural Geology – Volume 1: Strain Analysis, *Academic Press*, London, 307p.

Richards, J.A.(1999). Remote Sensing Digital Image Analysis: An Introduction, *Springer-Verlag*, Berlin, Germany, 240 p.

Rilley, D.N., Barton, M. and Dalton-Sorrell, C.(2006). Fusion of Landsat-5 thematic mapper and shuttle imaging RADAR-C data for geological mapping in Eastern Maine,USA.Availableat:www.gis.usu.edu/docs/protected/procs/asps/asprs2000/pdffiles/papers/222.pdf (accessed November 2006, verified July 2007).

Rowan, L.C., Wetlaufer, P.H., Goetz, A.F.H., Billingsley, F.C., Stewart, J.H., (1974). Discrimination of rock types and detection of hydrothermally altered areas in south central Nevada by the use of computer-enhanced ERTS images. *U.S. Geological Survev*. Prof. Pap. 883, 35.

Russ, W. (1957). The Geology of parts of Niger, Zaria and Sokoto provinces with reference to the occurrence of gold. *Geoloical Survey of Nigeria Bulletin*,**29**(2): 54-86

Sabins, F. (1997). Remote Sensing: Principles and Interpretation, *(3rd Ed)*, 494 p.

Truswell, J. F. and Cope, R. N. (1963). The geology of parts of Niger and Zaria provinces, northern Nigeria. *Geological Survey of Nigeria Bulletin*,**29**, 26- 53

Turner, D. C. (1983). Upper Proterozoic Schist Belts in the Nigerian Sector of the Pan-African Province of West-Africa. In: *C. A. Kogbe "Geology of Nigeria" 2nd Revised Edition*, Rock View Publication Company, Jos, Nigeria. 93-109.

Ukwang, E. and Ekwueme, B. N. (2009). Geochemistry and geotectonic study of granitic rocks of southwest Obudu Plateau, southeastern Nigeria. *Journal of Mining and Geology*, **45**, 73-82.

Urai, J., Means, W. D., and Lister, G. S. (1986). Dynamic recrystallization of minerals. In: Heard HC, Hobbs BE (eds) Mineral and rock deformation: laboratory studies, the Paterson volume. Geophys Monogr, **36**,161–200, *American Geophysics Union*, Washington DC

Utke, A. W. (1987). New aspects on the evolution of the late Proterozoic crust in NW Nigeria. In: Matiheis, G. and Schandelmeier, H. (Eds). Current Research in African Earth Sciences, Balkema, Rotterdam.

Van der Pluijm, B.A. and Marshak, M. (2004). Earth Structure: an introduction to structural geology and tectonics(2nd Ed). W.W. Norton and Company, New York, pp. 138-164.

Vaniman, D.T. (1976). The Godani granodiorite plutons, Nigeria Petrology and Regional setting. Unpublished Ph.D Thesis, University of California, Santa Cruz 286p

Warner, N. H. and Farmer, J. D.(2008). Laboratory and Remote Identification of Hydrothermal Alteration Materials Associated with Subglacial Outflood Surfaces in Iceland. Lunar and Planetary Science, p. 1477.

White, J. C.and Barnett, R. L. (1990). Microstructural signatures and glide twins in microcline, Hemlo, Ontario. *Canadian Minerology*,**28**, 757–769

Winkler, H.G.F. (1974). Petrogenesis of metamorphic rock 3rd ed. *Springer,* Berlin, 320pp.

Woakes, M., Rahaman, M. A., and Ajibade, A. C. (1987). Some metallogenic features of the Nigerian basement. *Journal of African Earth Sciences*, **6**, 655–664.

Wright, J. B. and Ogezi A. E. O. (1977). Serpentinites in the Basement of NW Nigeria. Nigeria *Journal Mining Geology*,**14**, 34-37.